Collective flows and alpha-clustering effects in heavy ion collisions:

from nucleonic to partonic degree of freedom

Yu-Gang Ma (马余刚)
Shanghai Institute of Applied Physics, CAS
and
Fudan University

NUSYS; 15th Aug 2019 @IMP-CAS

Collective flows

Azimuthal Distributions

Fourier Analysis of azimuthal particle distribution

$$\frac{dN}{p_t dp_t dy d\varphi} = \frac{1}{2\pi}\frac{dN}{p_t dp_t dy}\left[1+\sum_{i=1} 2v_i \cos(i\varphi)\right]$$

Systematic measurements as a function of particle mass and taking into account time scale

- **v_0 Radial flow** — **integrated over evolution**
- **v_1 Directed flow** — **early**
- **v_2 Elliptic flow** — **early**
- **v_n ……..**

v_1, v_2, v_n largest at intermediate impact parameters, zero at b = 0 and b = 2R

Flow (radial, directed and elliptic)

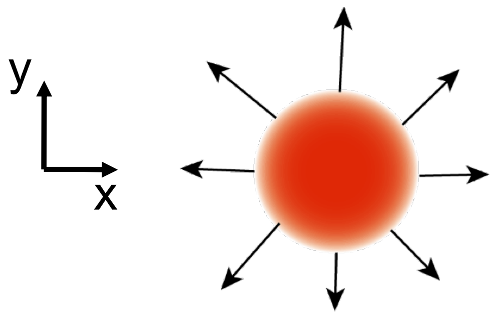

- Only type of transverse flow in central collision (b=0) is radial flow.
- Integrates pressure history over complete expansion phase

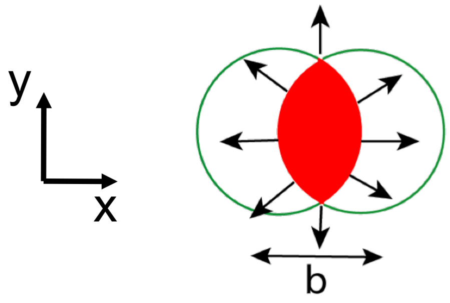

- Elliptic flow, caused by anisotropic initial overlap region (b > 0).
- More weight towards early stage of expansion.

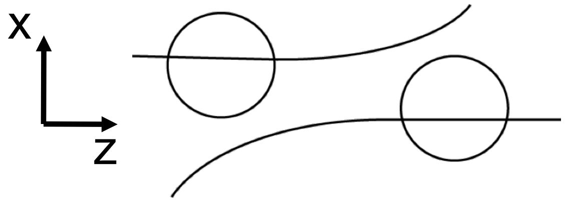

- Directed flow, sensitive to earliest collision stage (pre-equilibrium, b > 0)

Y.G.Ma

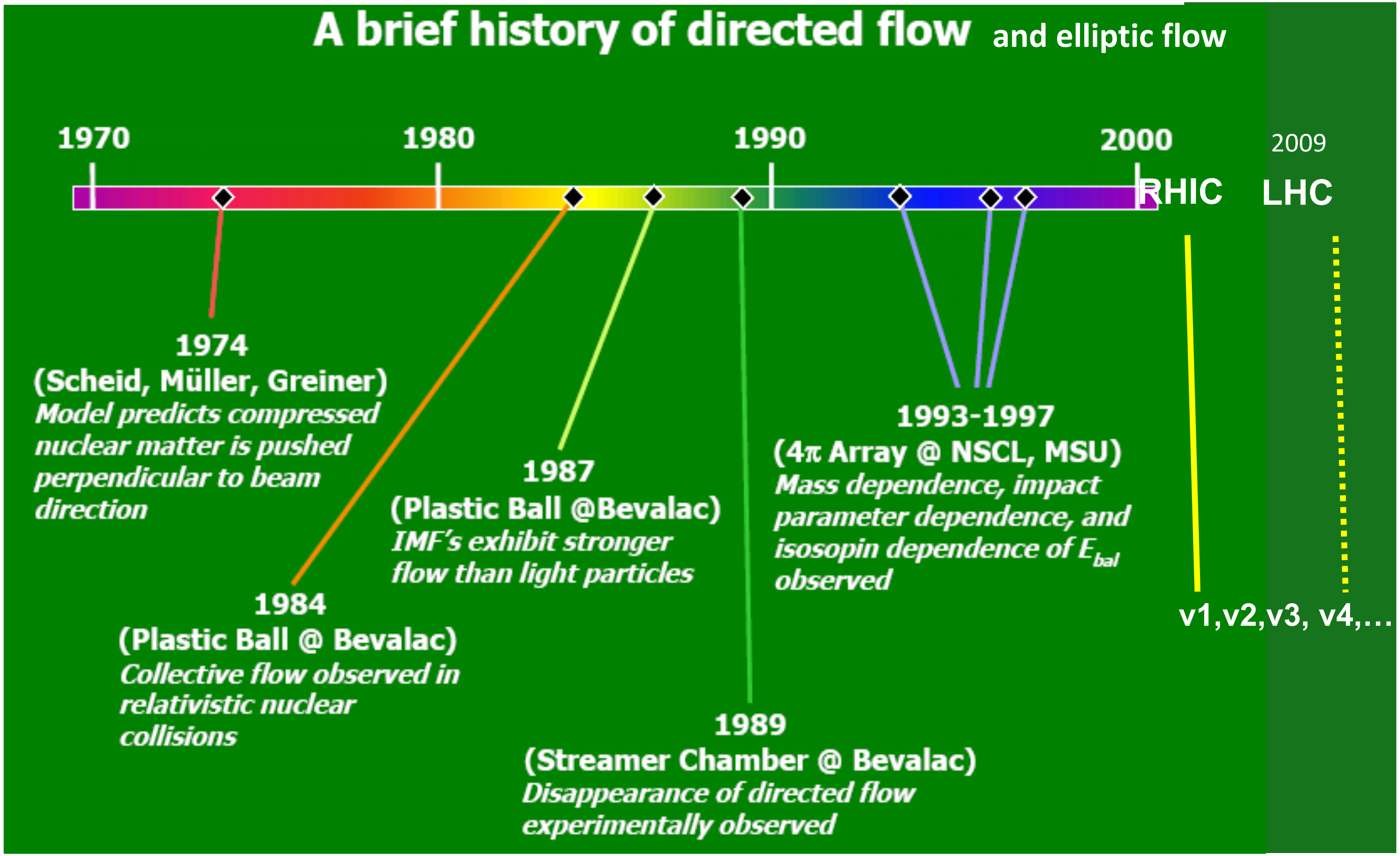
A brief history of directed flow and elliptic flow
1970
1980
1990
2000
2009
RHIC
LHC
1974
(Scheid, Müller, Greiner)
Model predicts compressed nuclear matter is pushed perpendicular to beam direction
1984
(Plastic Ball @ Bevalac)
Collective flow observed in relativistic nuclear collisions
1987
(Plastic Ball @Bevalac)
IMF's exhibit stronger flow than light particles
1989
(Streamer Chamber @ Bevalac)
Disappearance of directed flow experimentally observed
1993-1997
(4π Array @ NSCL, MSU)
Mass dependence, impact parameter dependence, and isosopin dependence of E_{bal} observed
v1,v2,v3, v4,…

Collective motion – the big picture

- Only 2 mechanisms can cause transverse motion in nuclear reactions:

  1) Baryon-baryon interactions induce random themal motion

  2) Collective degrees of freedom and compression of nuclear matter result in collective flow of energy along the direction of the pressure field gradient.

- Two types of collective motion:

  - directed "transverse" flow: compression of participant volume causes an anisotropy in pressure for nonzero impact parameter

  - elliptic flow (squeeze-out): azimuthal distributions show an enhancement in particle emission orthogonal to reaction plane at midrapidity at SIS, Bevalac energies

  - Elliptic flow (In-plane emission): rotational collective motion

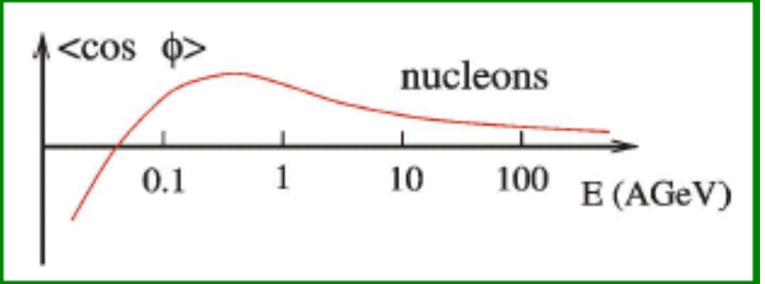

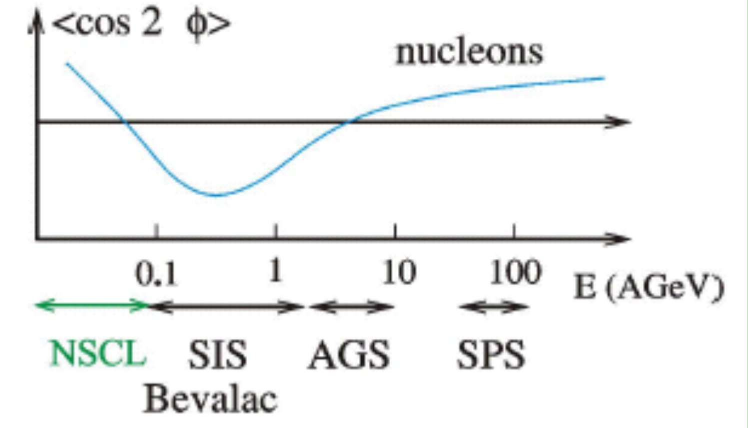

J. Ollitrault, Nuc. Phys. **A638** 195c (1997)

Transverse directed flow - Nuclear EOS

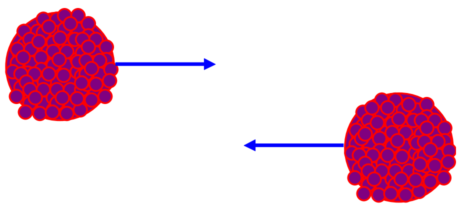

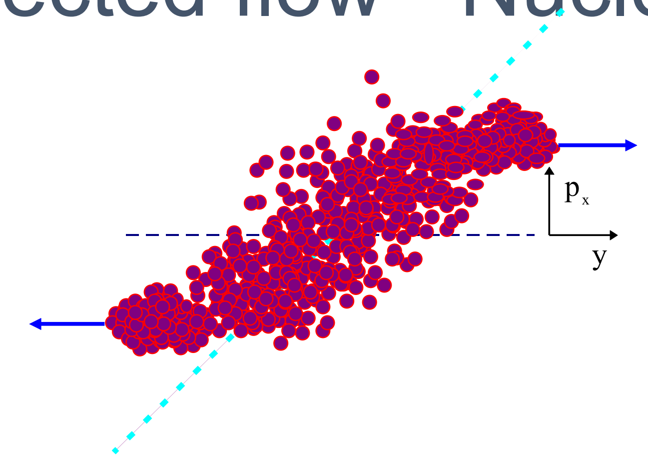

- **Flow Effects:**
  - **Transverse Directed Flow,**
  - **Radial Flow,**
  - **"Squeeze-Out" or elliptical flow.**

⇒reflect internal pressure.

- **Microscopic origins of pressure:**
  - **Nuclear Incompressibility,**
  - **Momentum dependence of nuclear mean field,**
  - **nucleon-nucleon scattering by the residual interaction.**

Directed flow at intermediate energies

Directed (sidewards) flow

- At low incident energies, the projectile and target nuclei will experience a force of attraction due to the nuclear mean field, causing a negative deflection

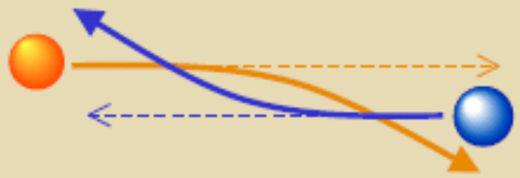

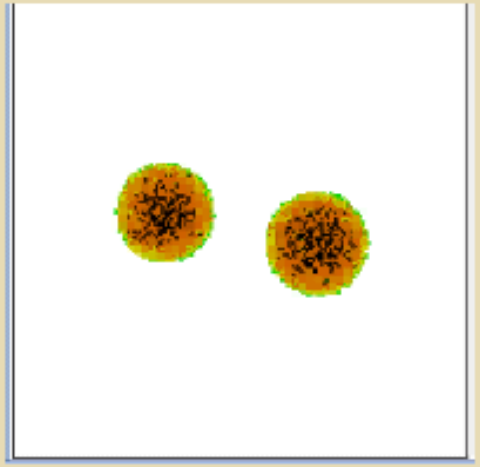

BUU, Ar+Sc, 40 MeV/nucleon

- In experiment, negative ("attractive") flow cannot be directly assigned.
- Reaction plane determination method causes negative flow to appear positive

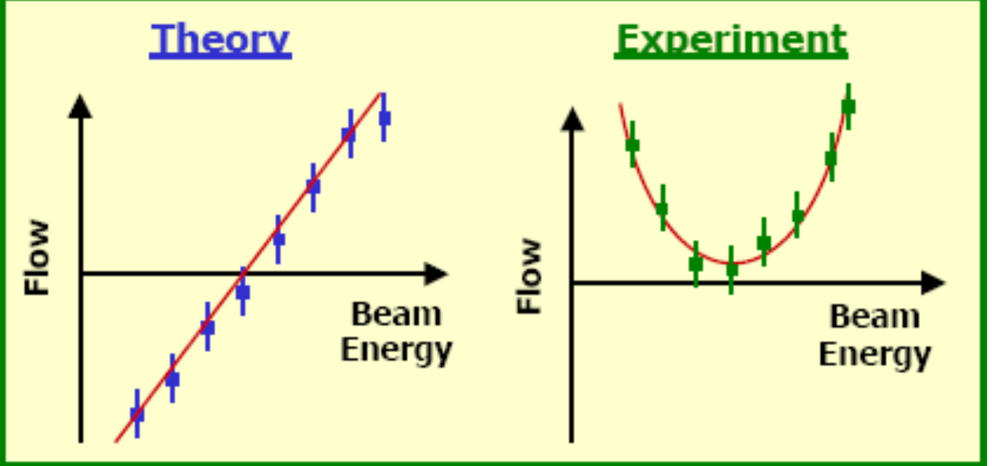

Directed flow at intermediate energies

Directed (sidewards) flow

- At high incident energies, the nuclei are repulsed due to nucleon-nucleon scattering.

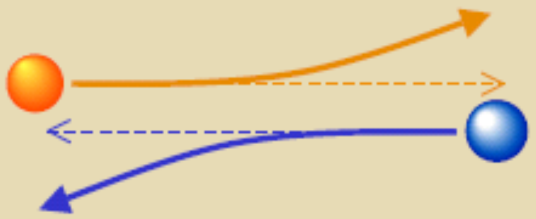

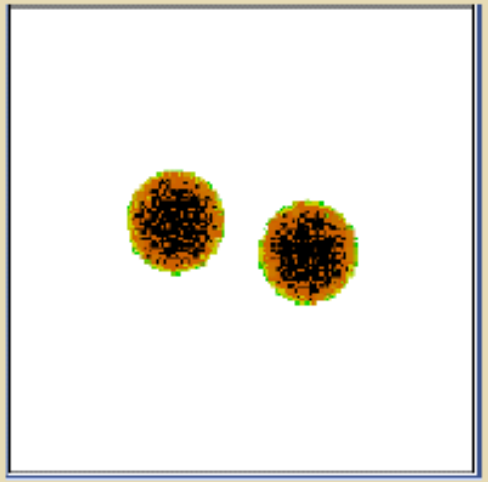

BUU, Au+Au, 150 MeV/nucleon

Theoretical problem: mass dependence of flow observables

- The measured transverse flows are mass dependent.

- Presents problem for models that do not explicitly predict cluster observables.
  - Molecular dynamics does explicitly predict clusters
  - BUU does not
    - **Coalescence invariant analyses.**

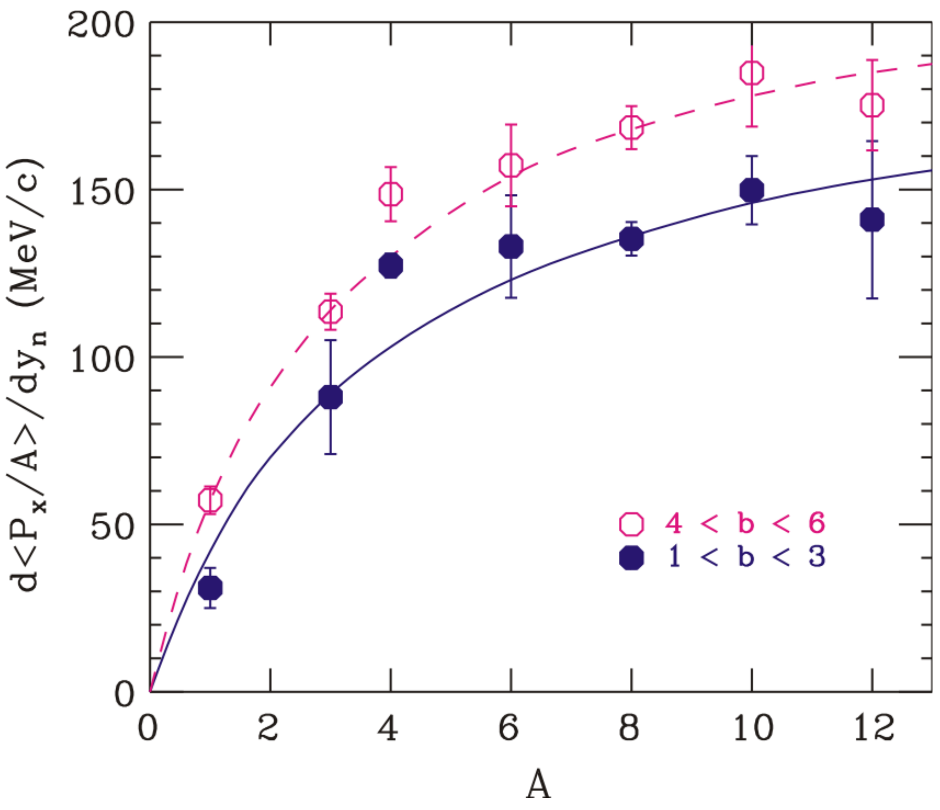

Huang, Phys. Rev. Lett. 77, 3739 (1996)

22 NOVEMBER 2002 VOL 298 SCIENCE

Determination of the Equation of State of Dense Matter

Paweł Danielewicz,[1,2] Roy Lacey,[3] William G. Lynch[1]*

Nuclear collisions can compress nuclear matter to densities achieved within neutron stars and within core-collapse supernovae. These dense states of matter exist momentarily before expanding. We analyzed the flow of matter to extract pressures in excess of 10^{34} pascals, the highest recorded under laboratory-controlled conditions. Using these analyses, we rule out strongly repulsive nuclear equations of state from relativistic mean field theory and weakly repulsive equations of state with phase transitions at densities less than three times that of stable nuclei, but not equations of state softened at higher densities because of a transformation to quark matter.

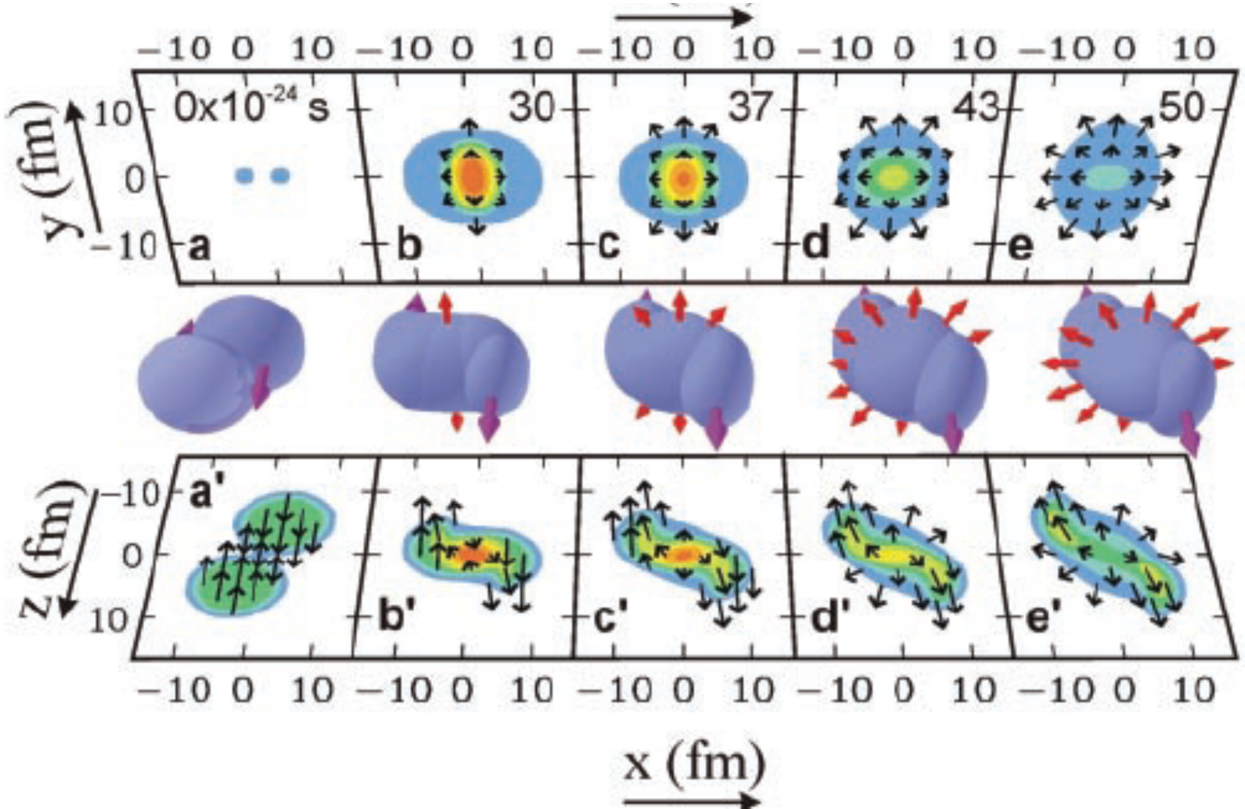

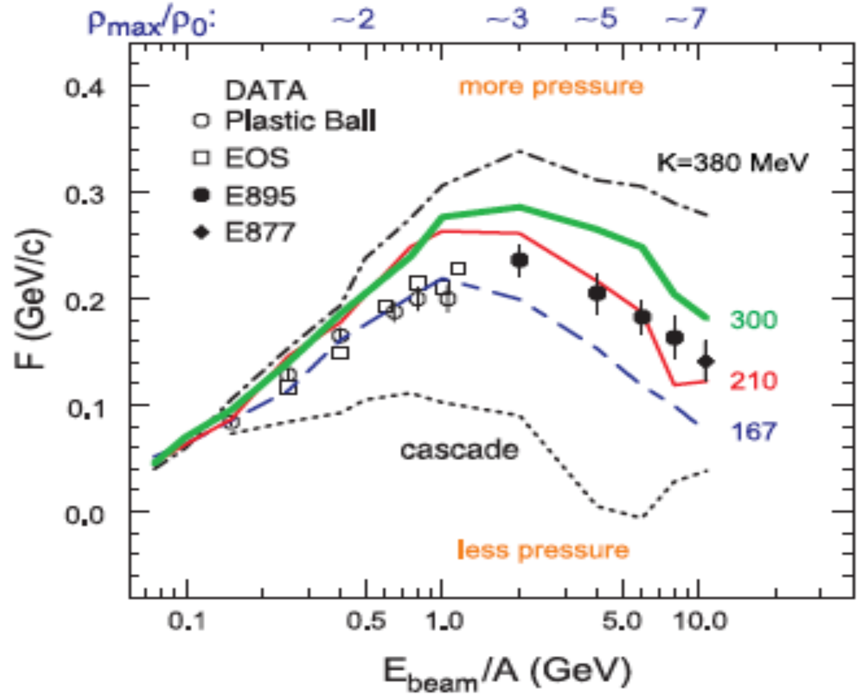

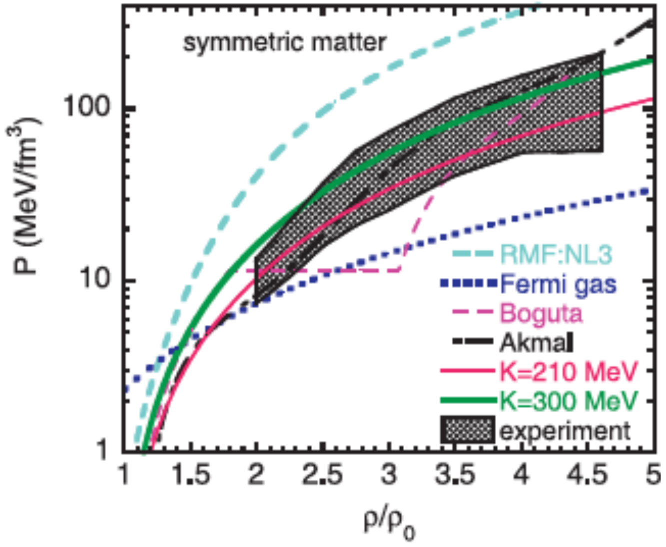

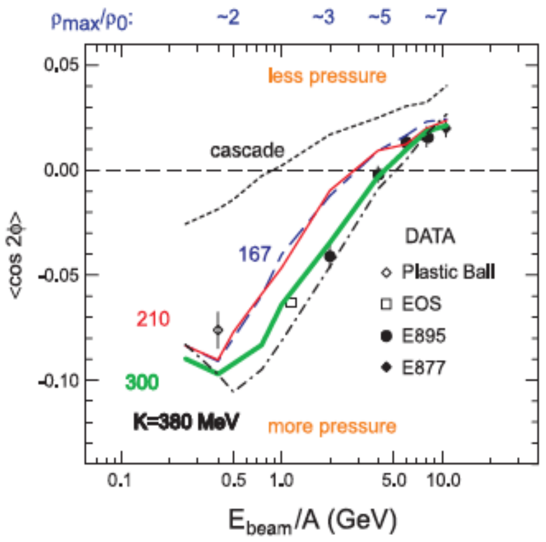

Ollitrault ('92)

Elliptic Flow @ RHIC

How does the system respond to initial spatial anisotropy?

Free streaming

$\lambda \to \infty$

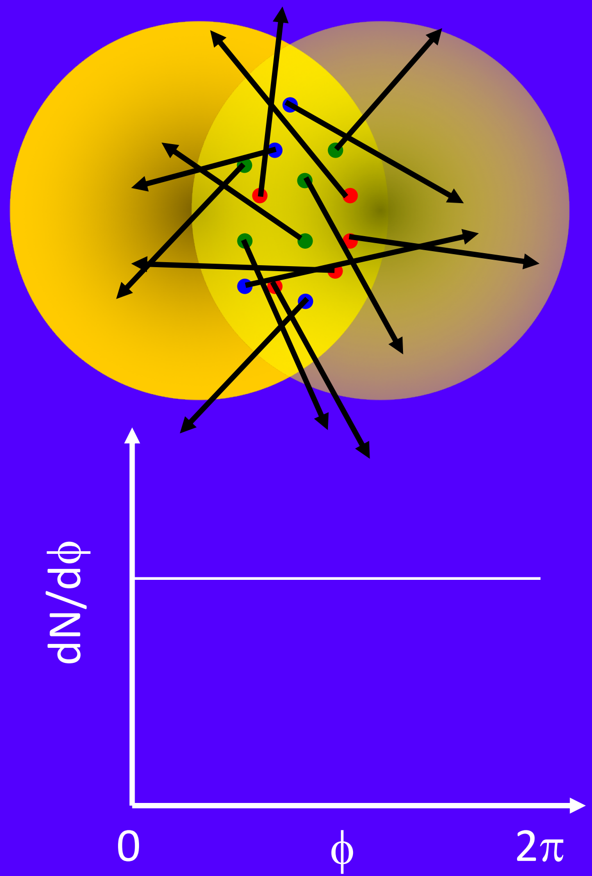

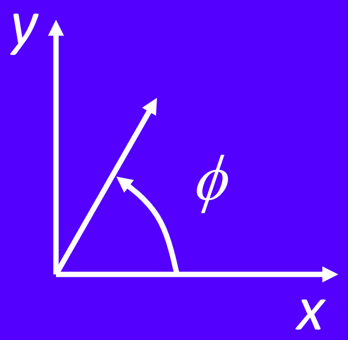

INPUT

Initial spatial anisotropy

Rescattering

OUTPUT

Final momentum anisotropy

Hydrodynamic expansion

$\lambda = 0$

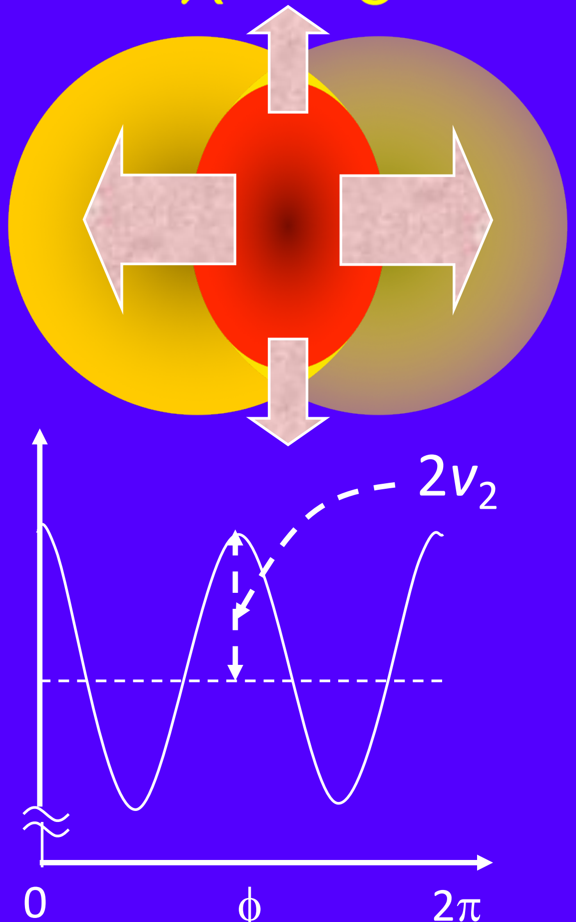

Elliptic flow v_2

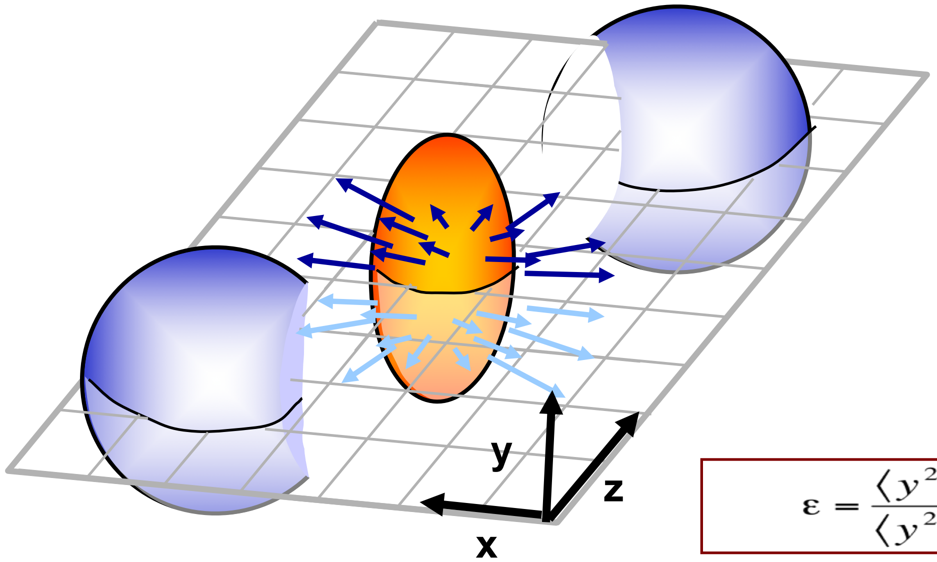

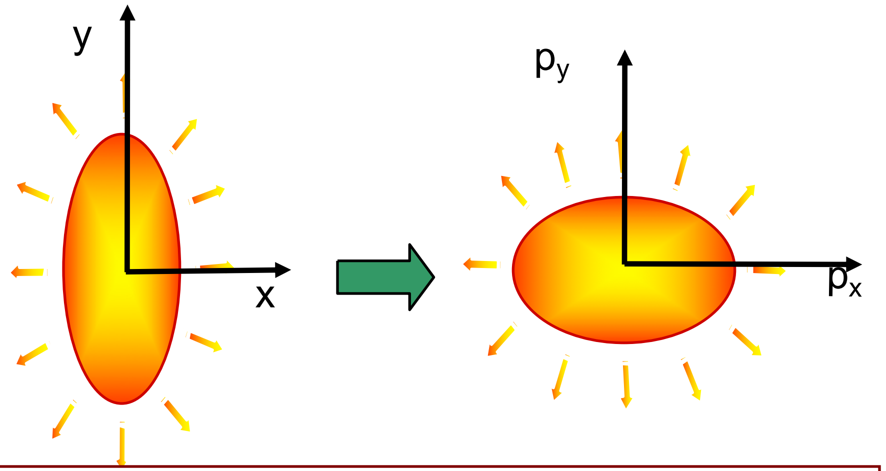

$$\varepsilon = \frac{\langle y^2 - x^2 \rangle}{\langle y^2 + x^2 \rangle} \qquad v_2 = \langle \cos 2\varphi \rangle, \quad \varphi = \tan^{-1}\left(\frac{p_y}{p_x}\right)$$

- *Non-central A+A collisions: azimuthally anisotropic distribution of particles in coordinate-space*
- *Density gradients and interactions between the particles: an asymmetry in momentum-space*
- *Signal is self-quenching with time – early time observable!*
- *Measurement: Fourier expansion of the azimuthal angle (φ-Ψ) distributions*

$$E\frac{d^3N}{d^3p} = \frac{1}{2\pi}\frac{d^2N}{p_T dp_T dy}\left[1 + 2v_1\cos(\varphi - \Psi_R) + 2v_2\cos(2[\varphi - \Psi_R]) + \ldots\right]$$

$$\frac{dN}{d(\varphi - \Psi_R)} = Norm * (1 + 2v_2\cos 2(\varphi - \Psi_R)) \quad \text{(mid-rapidity)}$$

Y.G.Ma

Resulting azimuthal distributions

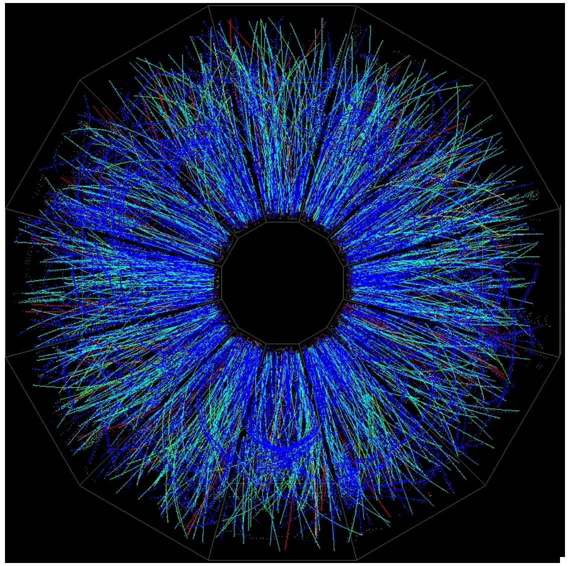

STAR, PRL**90** 032301 (2003)

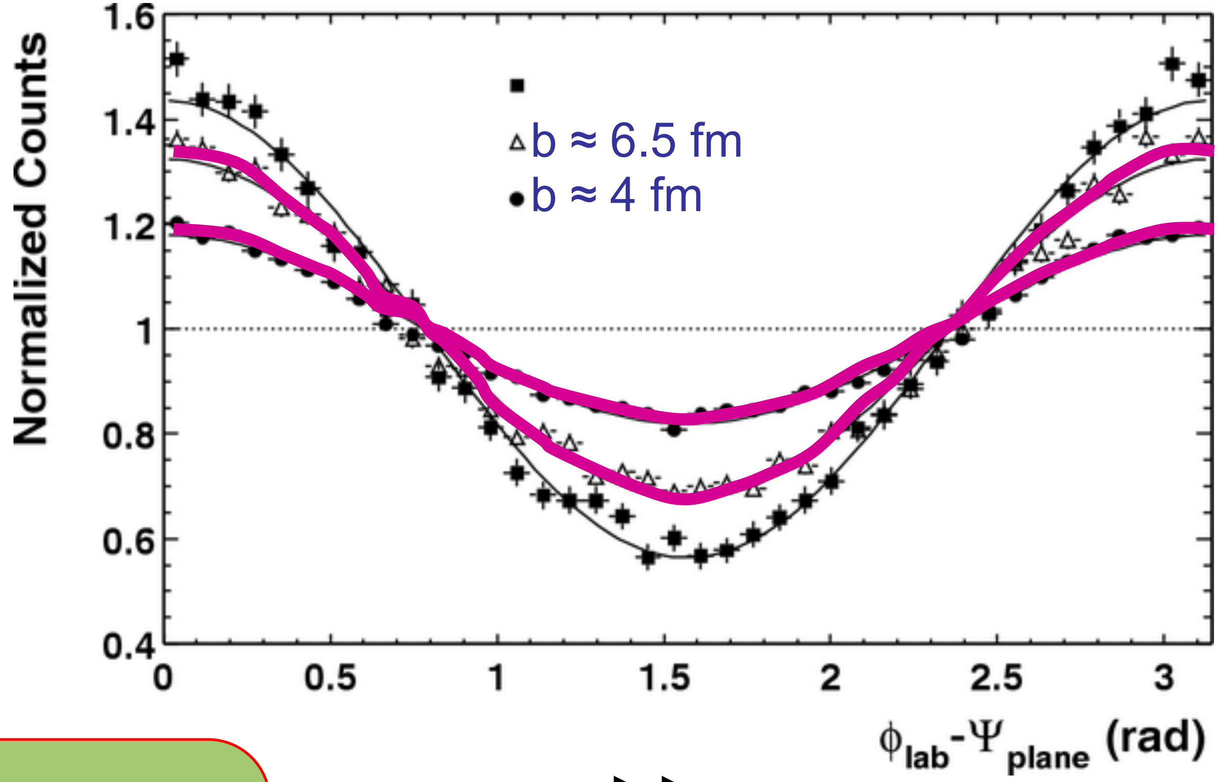

mid-central collisions

“central” collisions

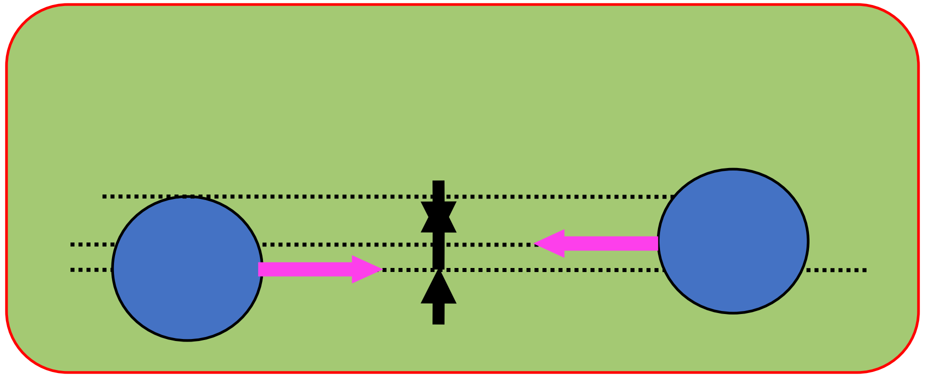

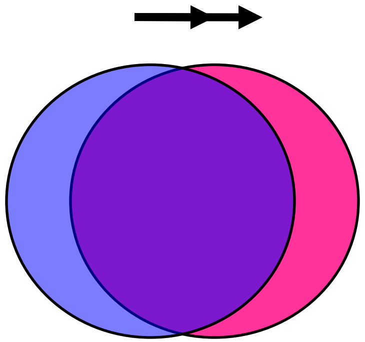

Resulting azimuthal distributions

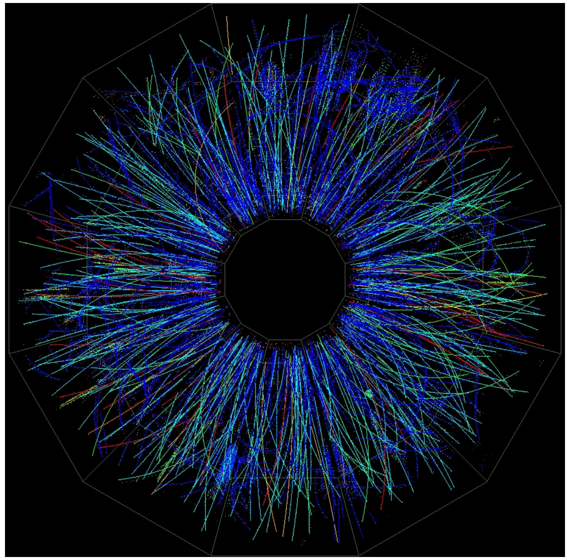

peripheral collisions

STAR, PRL**90** 032301 (2003)

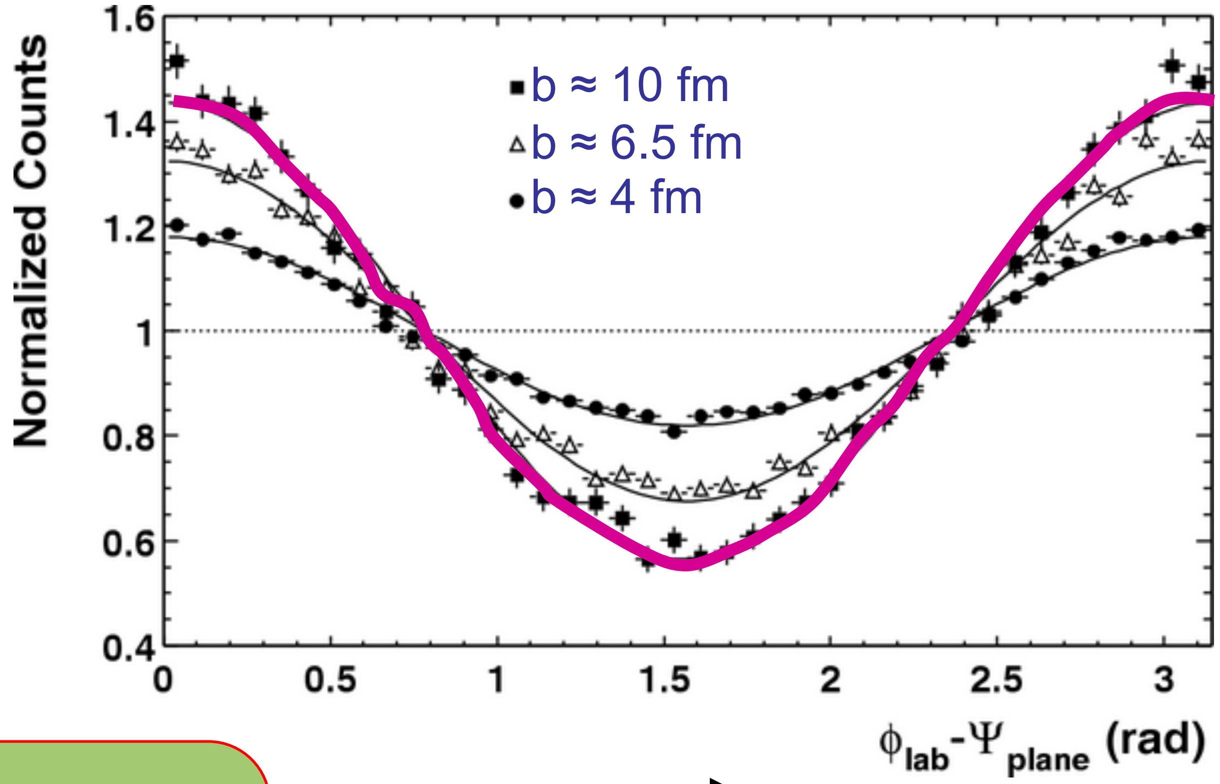

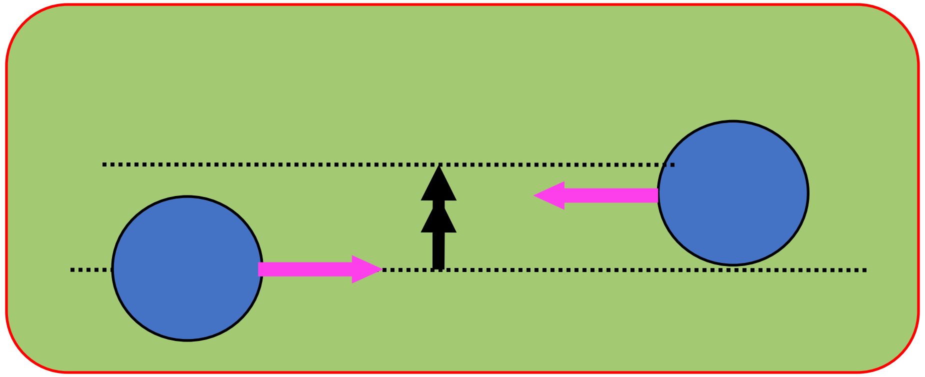

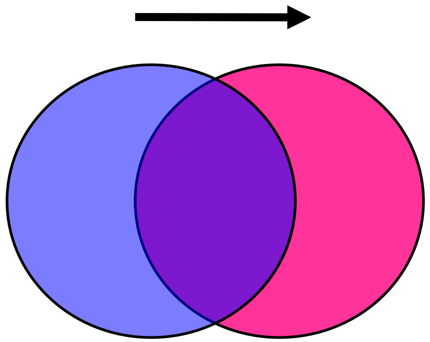

Elliptic flow

observed momentum anisotropy is largely elliptic deformation; its amplitude is denoted v2

RHIC v_2 reaches large values yielded by hydro (unlike lower energies)

STAR, PRL**90** 032301 (2003)

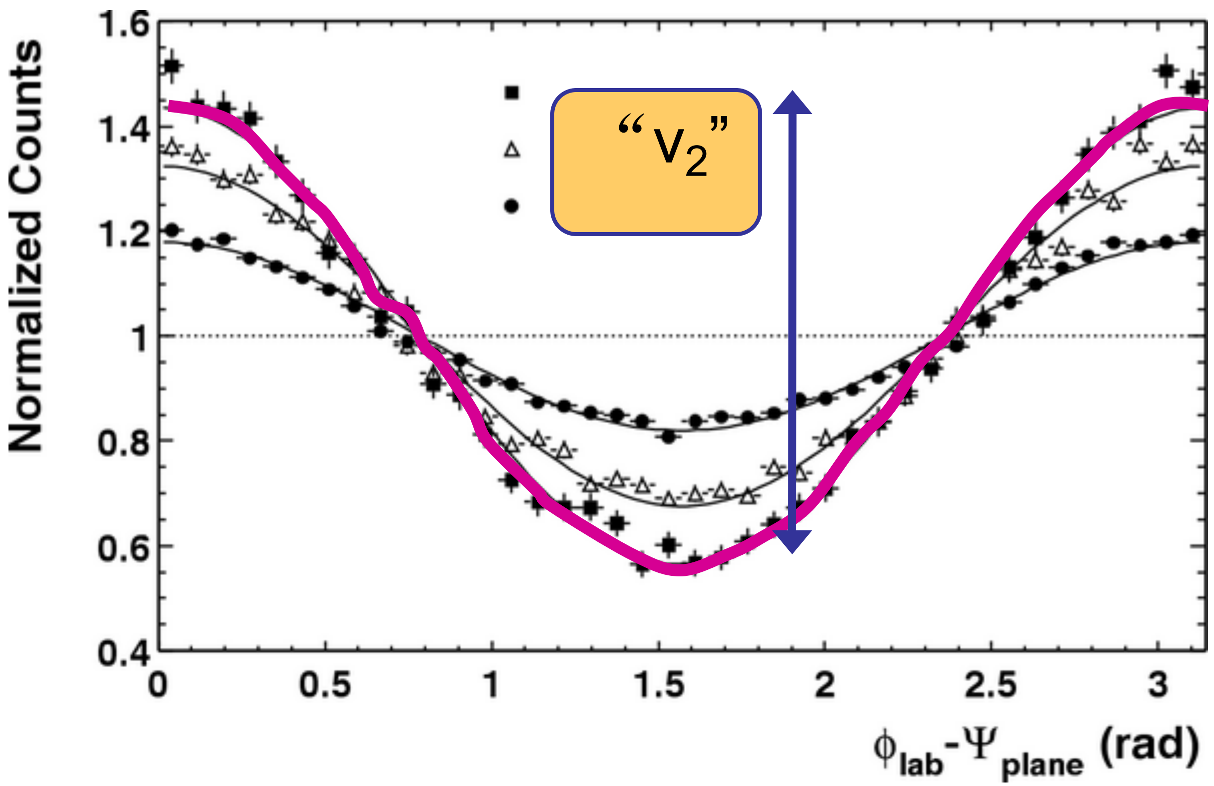

Hydrodynamic calculation of system evolution

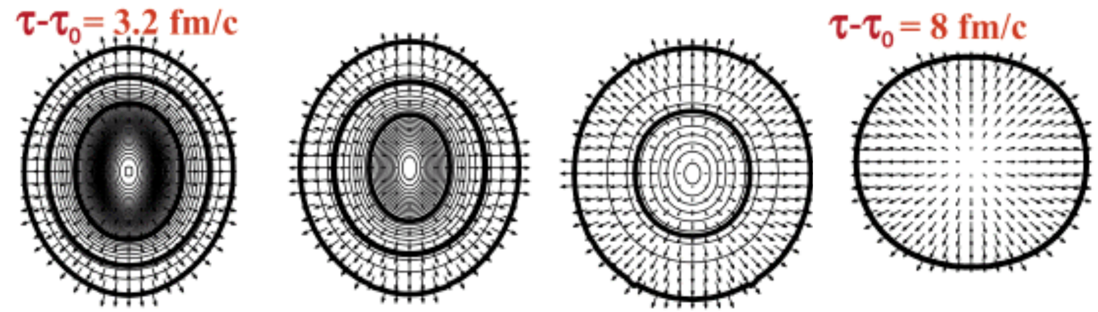

Elliptic flow - agreement with hydro

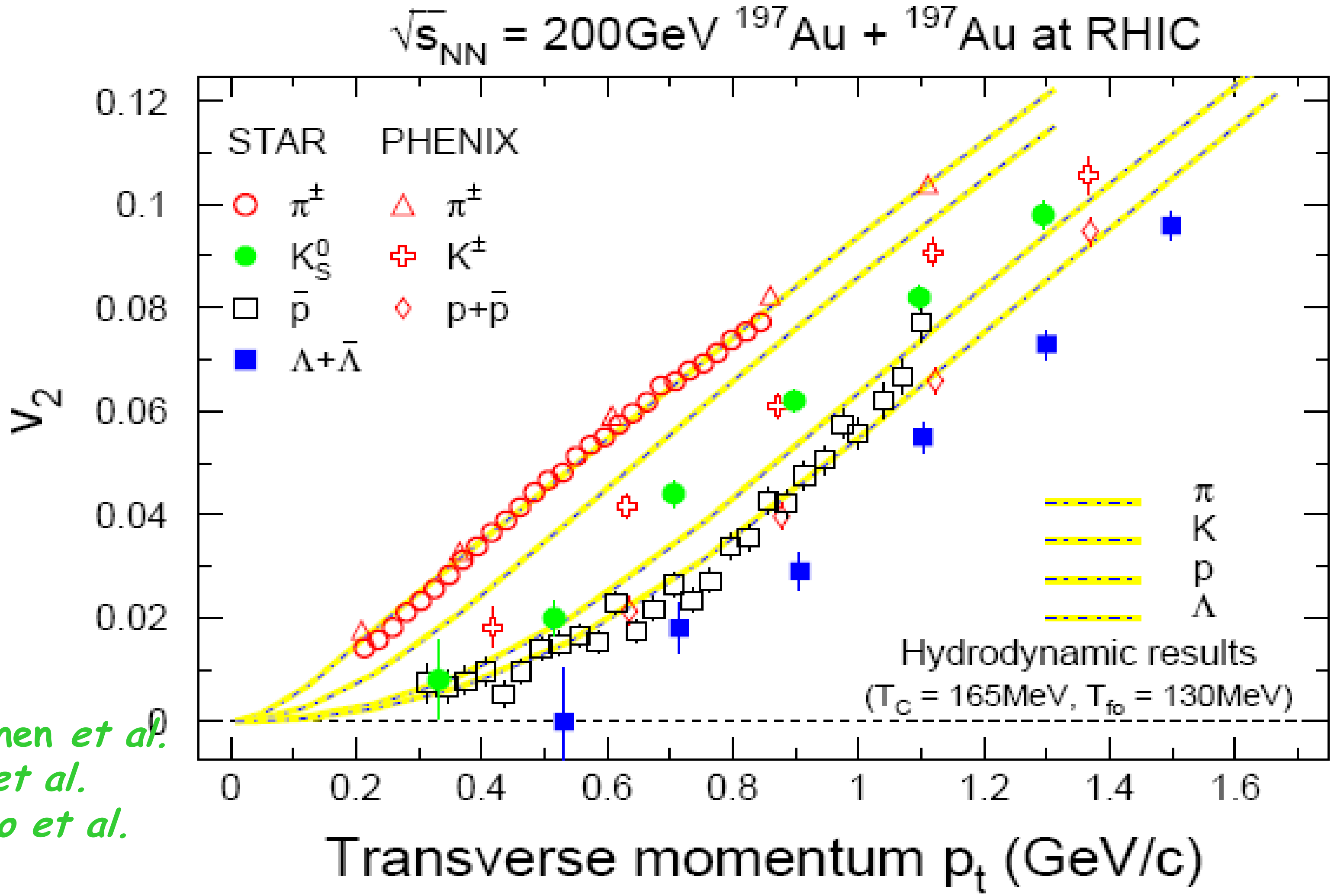

Huovinen *et al.*
Kolb *et al.*
Hirano *et al.*

dependence on particle mass follows hydro up to ~2 GeV/c

NCQ scaling in middle Pt

PRL. 98, 162301 (2007)

QuarkMatter2009

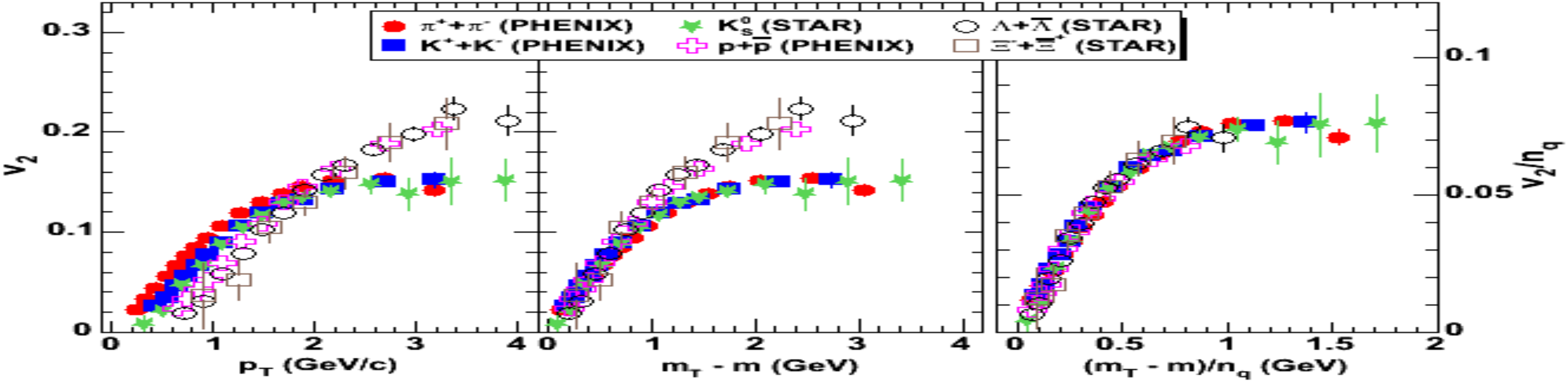

$KE_T = (m_T\text{-}m_0)/n_q$

$$\frac{d^3 n_M}{d^3 p_M} \propto [\frac{d^3 n_q}{d^3 p_q}(p_q \approx p_M/2)]^2 \quad \text{and} \quad \frac{d^3 n_B}{d^3 p_B} \propto [\frac{d^3 n_q}{d^3 p_q}(p_q \approx p_B/3)]^3,$$

1. Number-of-constituent-quark scaling (meson vs baryon)

2. $v_2(p_T)$ /n_{quark} vs. KE_T/n_{quark} becomes one curve independent of particle species.

Y.G.Ma

Multi-strange particle v2: Partonic Collectivity

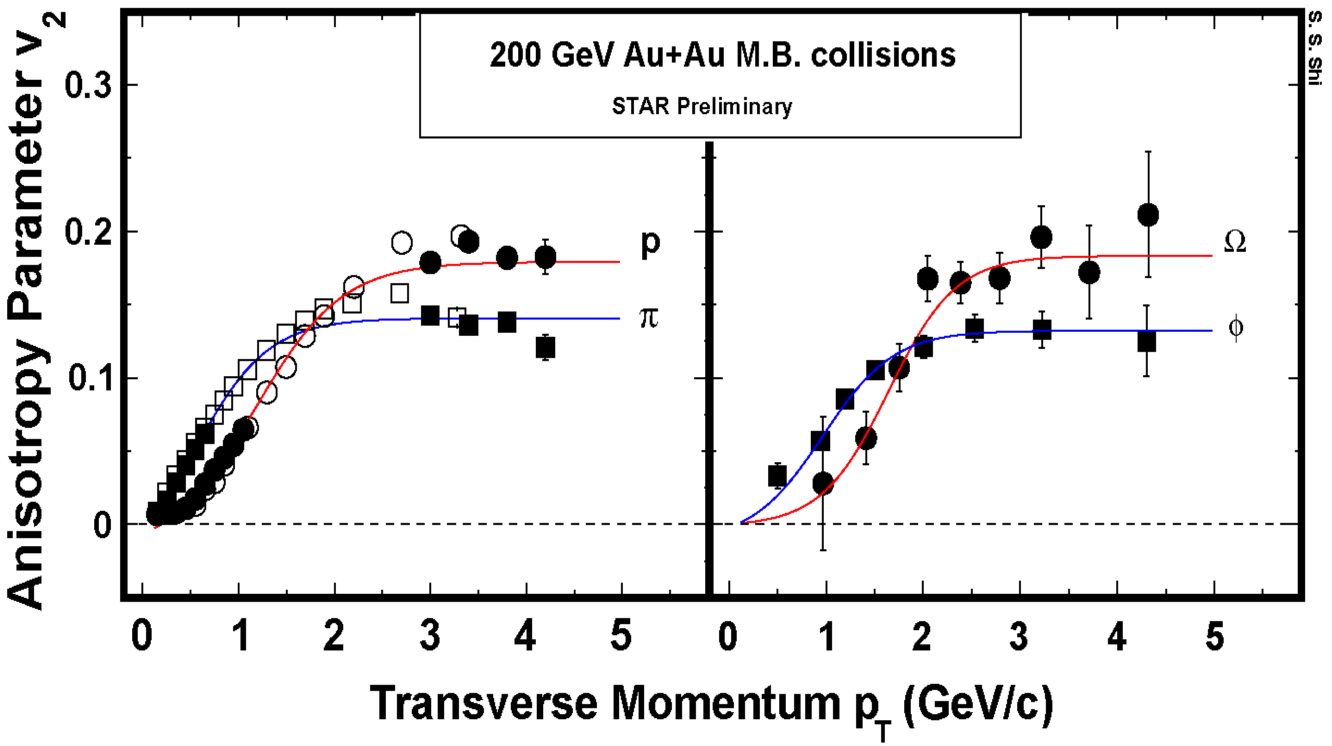

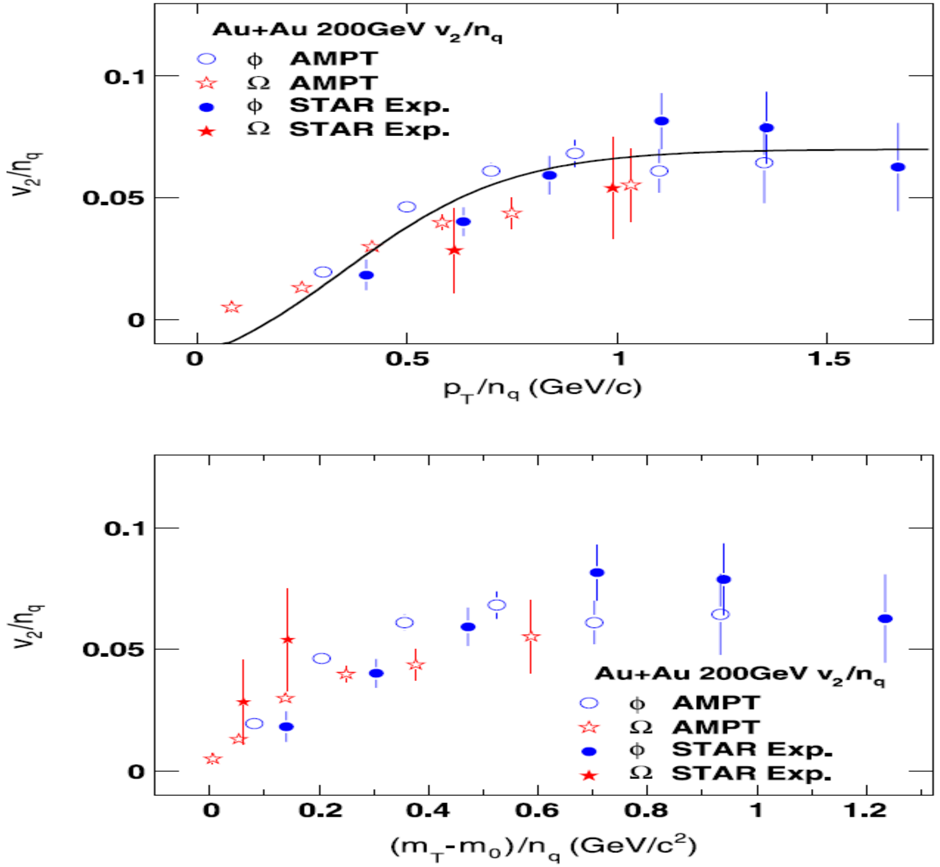

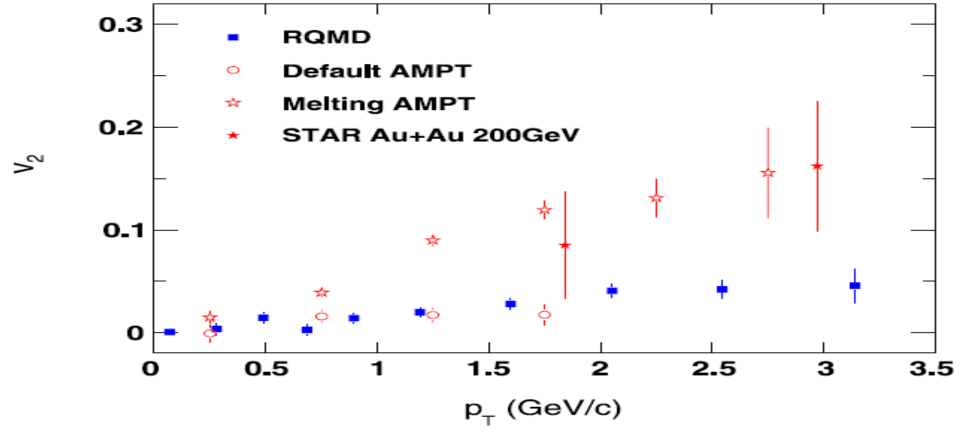

STAR data (S. Shi et al)

PHENIX π and p: nucl-ex/0604011v1
NQ inspired fit: X. Dong et al. Phy. Let. B 597 (2004) 328-332

J. Zuo, J.Y.Chen,X. Cai, YGM, F. Liu et al., EPJC 55,463(2008)

partonic collectivity at RHIC!

Y.G.Ma

组分夸克标度率：部分子集体性

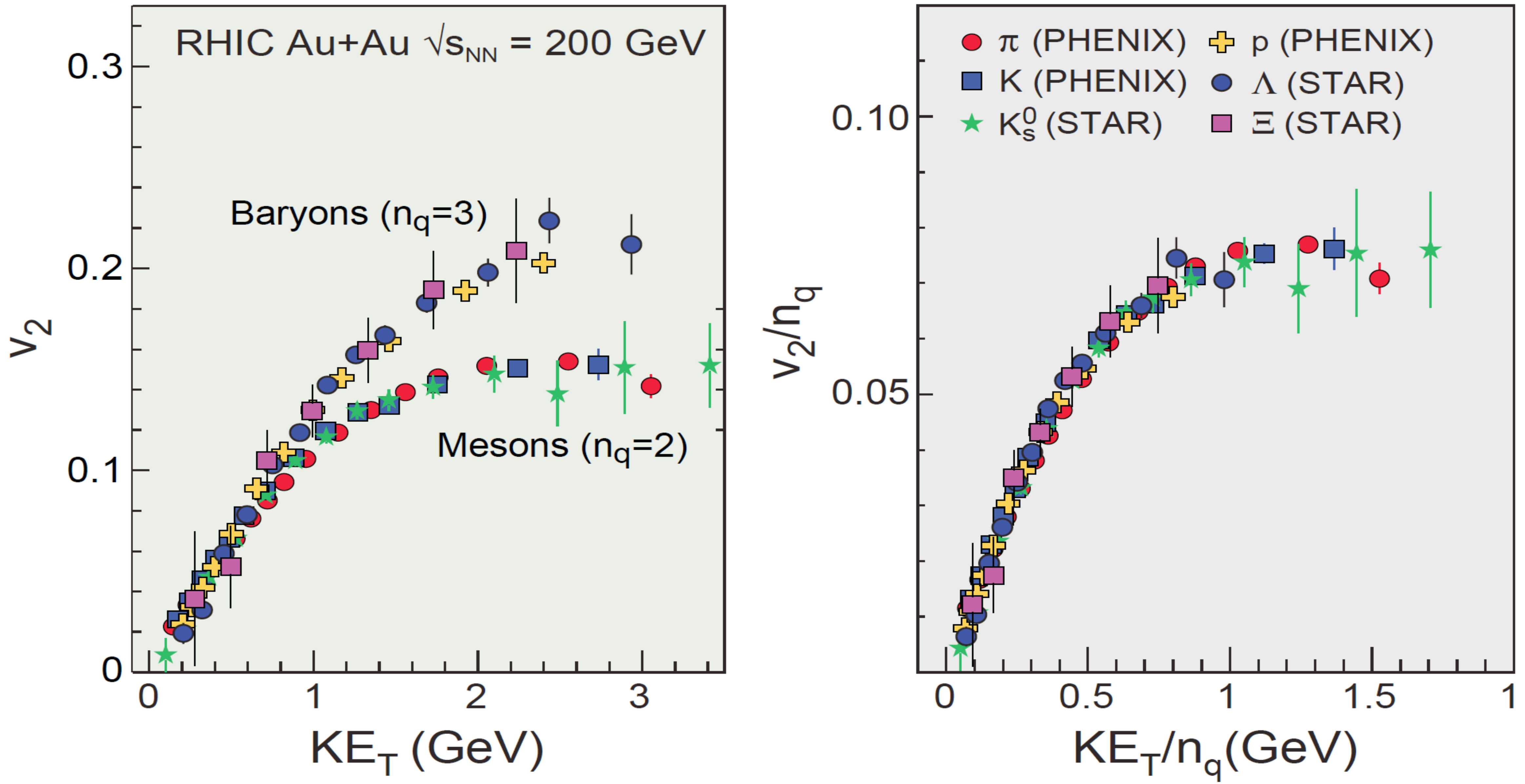

Coalescenece / Recombination

- If phase space is filled with partons, partons can be recombined/coalesced into hadrons.

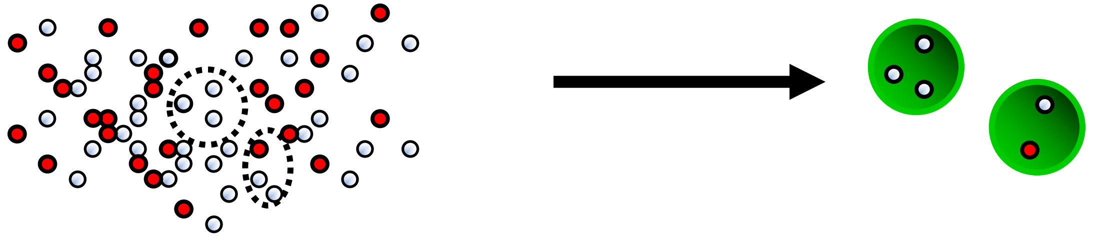

- Baryon: qqq$\rightarrow$B ; Meson: qq$\rightarrow$M

- <u>Three models:</u>

Ko, Greco, Lin, Chen et al.: TAMU Coalescence

Hwa & Yang, Oregon U

Fries, Muller et al: Duke U

K^0 and Λ elliptic flow

Quark coalescence?

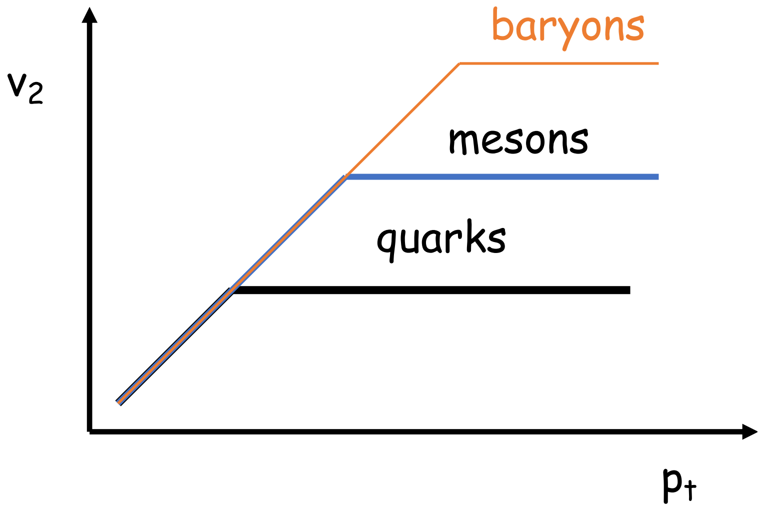

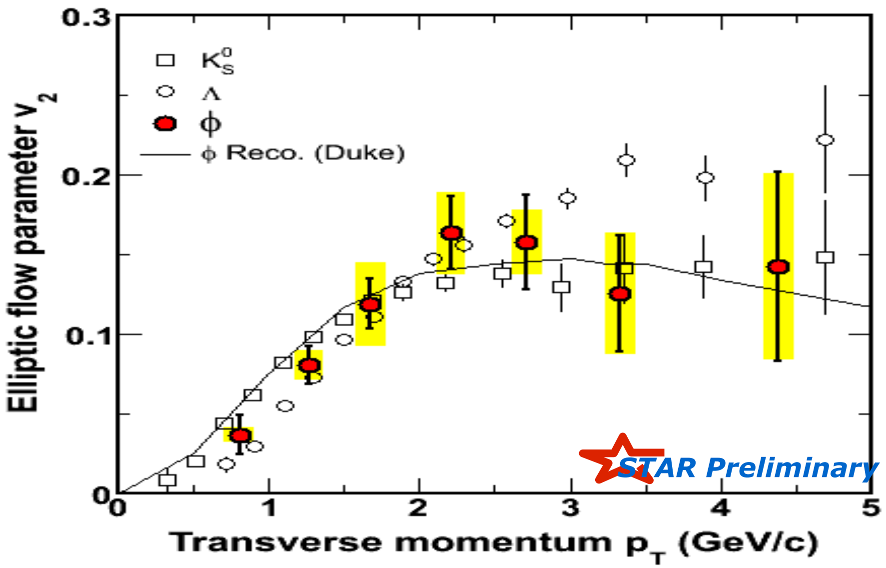

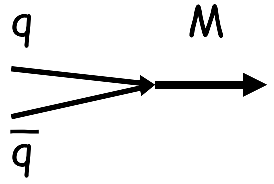

$$\frac{d^3 n_M}{d^3 p_M} \propto \left(\frac{d^3 n_q}{d^3 p_q} (p_q = p_M / 2) \right)^2$$

$$v_{2,M}(p_t) \approx 2 v_{2,q}(p_t / 2)$$

A good tool looking for phase transition at low energy scan: the breaking of NCQ scaling of elliptic flow

J. Tian, J. H. Chen, Y. G. Ma et. al., Phys. Rev. C 79, 067901 (2009)

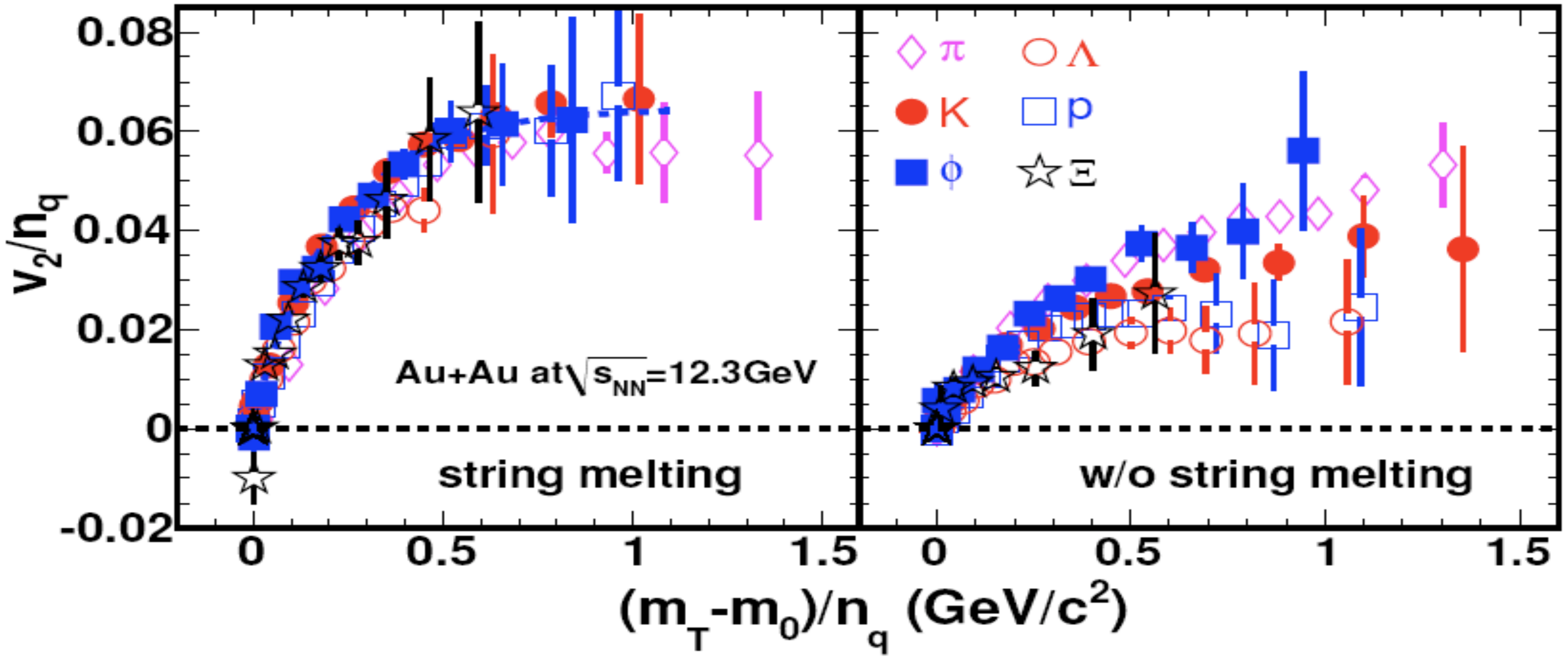

- NCQ scaling for the identified-particle elliptic flow may serve as a probe for searching for critical point.

v_2 Excitation Function

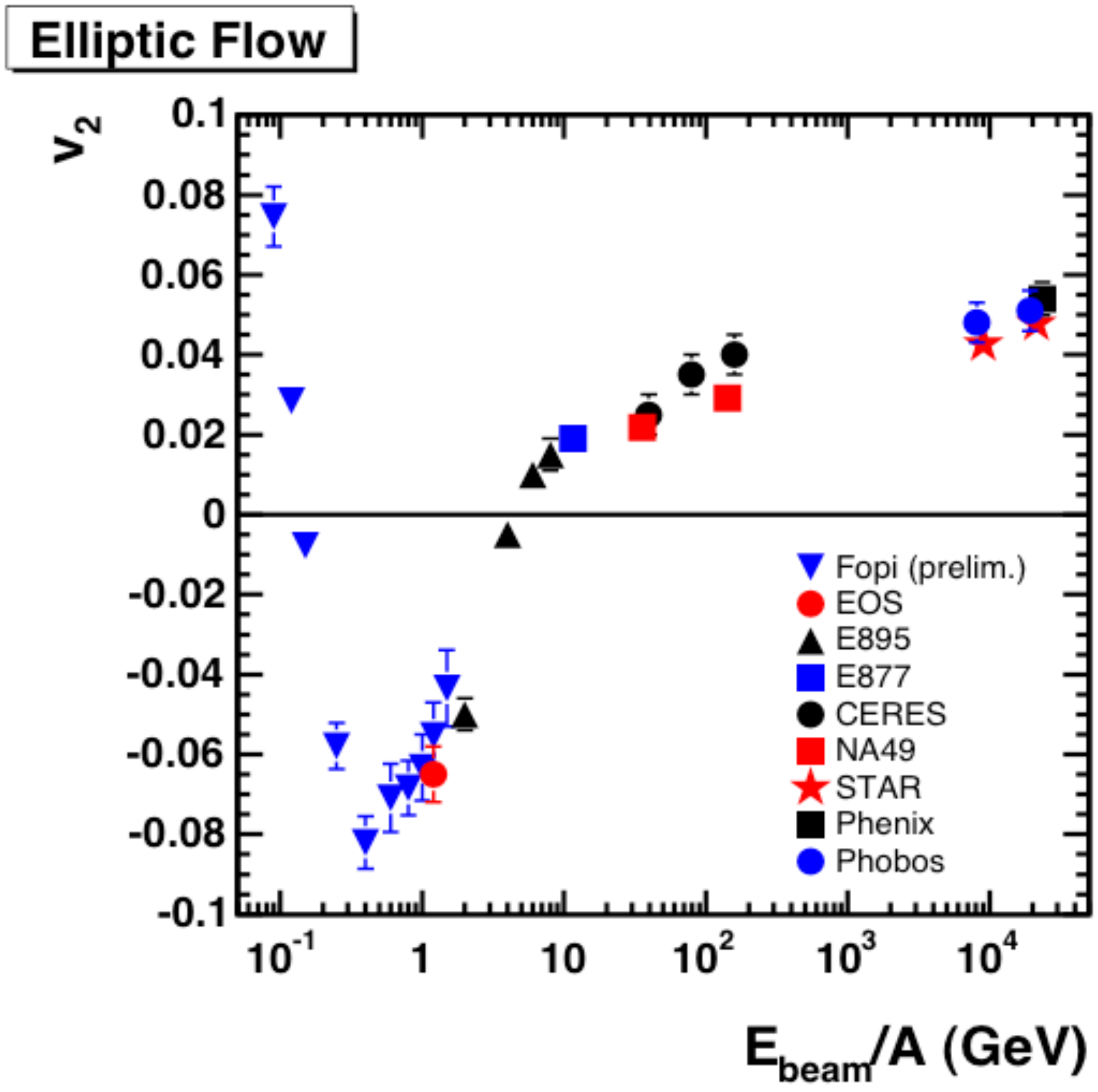

Rich structure:

Transition from in-plane to out-of-plane and back to in-plane emission:

Low Ebeam: rotational behavior;
Mid Ebeam: squeeze-out
High Ebeam: pressure-induced in-plane emission

RAPID COMMUNICATIONS

PHYSICAL REVIEW C VOLUME 48, NUMBER 4 OCTOBER 1993

Rotational behavior in intermediate energy heavy ion collisions

Y. G. Ma and W. Q. Shen
Chinese Center of Advanced Science and Technology (World Laboratory), P.O. Box 8730, Beijing 100080, People's Republic of China
and Institute of Nuclear Research, Academia Sinica, P.O. Box 800-204, Shanghai 201800, People's Republic of China

J. Feng
Institute of Nuclear Research, Academia Sinica, P.O. Box 800-204, Shanghai 201800, People's Republic of China

Y. Q. Ma
Chinese Center of Advanced Science and Technology (World Laboratory), P.O. Box 8730, Beijing 100080, People's Republic of China
and Physics Department, Nanjing University, Nanjing 210008, People's Republic of China

(Received 18 May 1992)

$$\frac{\partial f}{\partial t} + \mathbf{v}\cdot\nabla_r f - \nabla_r U \cdot \nabla_p f = \frac{4}{(2\pi)^3}\int d^3p_2 d^3p_3 d\Omega \frac{d\sigma_{NN}}{d\Omega} V_{12} \times [f_3 f_4 (1-f)(1-f_2) - f f_2 (1-f_3)(1-f_4)]\delta^3(\mathbf{p}+\mathbf{p}_2-\mathbf{p}_3-\mathbf{p}_4)$$

$$U = A\rho/\rho_0 + B(\rho/\rho_0)^\gamma + C\varepsilon_i(\rho_n - \rho_p)/\rho_0$$

$$\phi = \arctan(P_y/P_x)$$

$$dN/d\phi = a_0 + a_1 \cos\phi + a_2 \cos(2\phi)$$

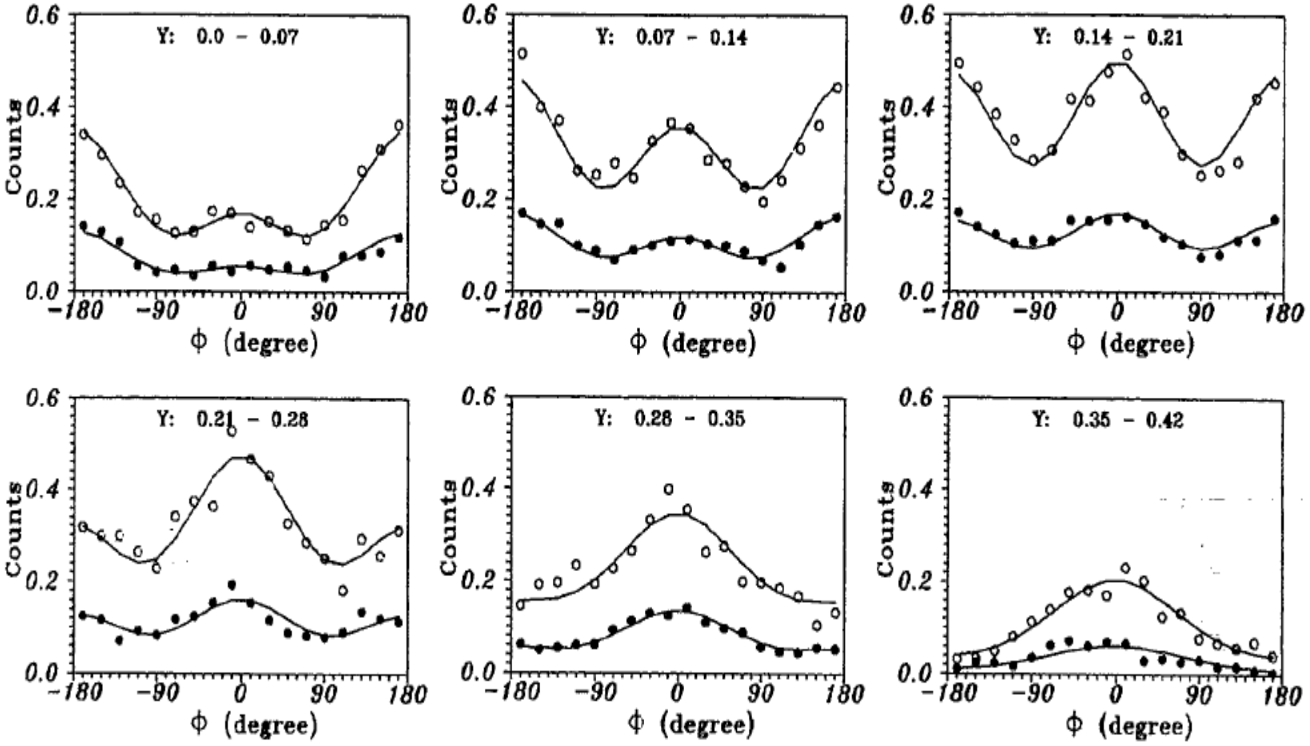

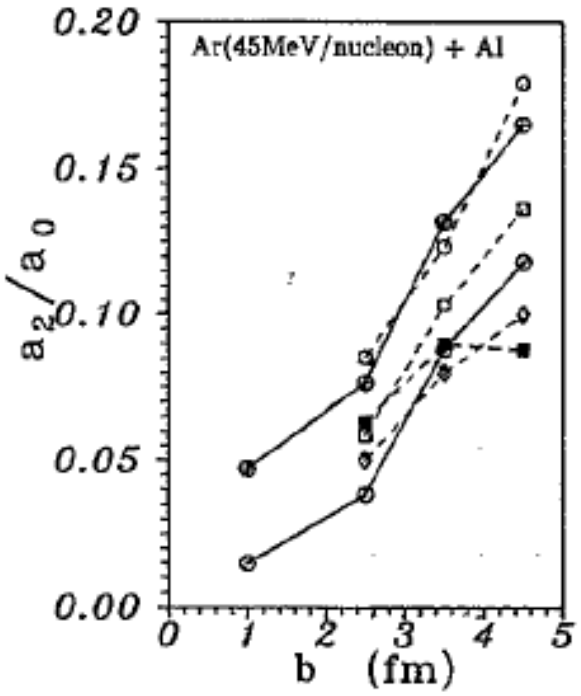

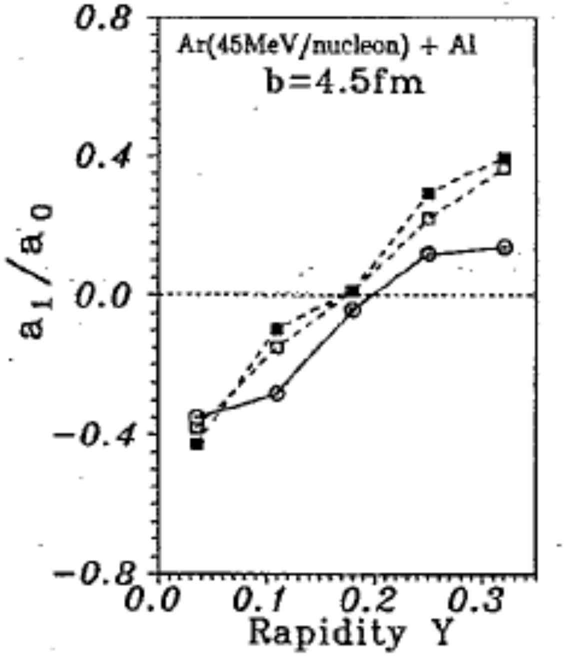

Nucleonic transport: Quantum Molecular Dynamics

Isospin-dependent Quantum Molecular Dynamics Model:

N-body transportation theory model

Including the most important parts for nuclear reaction at intermediate energy

$$\Psi_i(\mathbf{r},_t)=\frac{1}{(2\pi_L)^{3/4}}e^{-[\mathbf{r}-\mathbf{r}_i(_t)]^2/(4_L)}e^{i\mathbf{p}_i\cdot\mathbf{r}/\hbar}.$$

Performing a Wigner transformation for Eq. (1), we get the nucleon's Wigner density distribution in phase space:

$$f_i(\mathbf{r},\mathbf{p},_t)=\frac{1}{(\pi\hbar)^3}\exp\left[-\frac{[\mathbf{r}-\mathbf{r}_i(_t)]^2}{2_L}-\frac{[\mathbf{p}-\mathbf{p}_i(_t)]^2 2_L}{\hbar^2}\right],$$

Nuclear mean field:

$$U(\rho,\tau_z)=\alpha(\frac{\rho}{\rho_0})+\beta(\frac{\rho}{\rho_0})^{\gamma}+\frac{1}{2}(1-\tau_z)V_c\ +C_{sym}\frac{(\rho_n-\rho_p)}{\rho_0}\tau_z+U^{Yuk}$$

Nucleon-nucleon collision and Pauli blocking etc are considered

.Fragment Recognition, a naive coalescence model

□ R≤3.5fm; □ P≤300MeV/c

PHYSICAL REVIEW C VOLUME 51, NUMBER 2 FEBRU

Collective motion of reverse-reaction system in the intermediate-energy domain via the quantum-molecular-dynamics approach

Y. G. Ma* and W. Q. Shen
Chinese Center of Advanced Science and Technology (World Laboratory), P.O. Box 8730, Beijing 100080, China
and Institute of Nuclear Research, Academia Sinica, P.O. Box 800-204, Shanghai 201 800, China

Z. Y. Zhu
Institute of Nuclear Research, Academia Sinica, P.O. Box 800-204, Shanghai 201800, China
(Received 1 April 1994; revised manuscript received 11 October 1994)

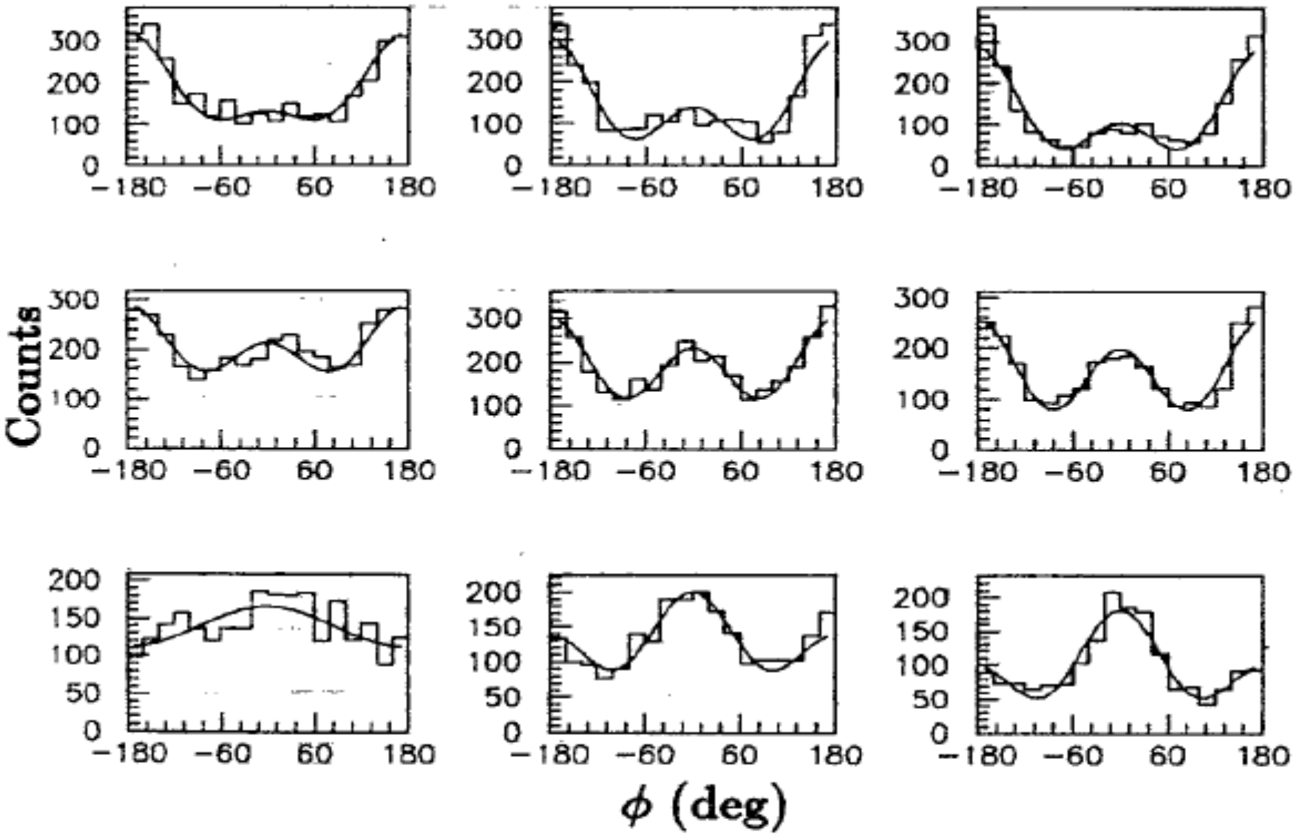

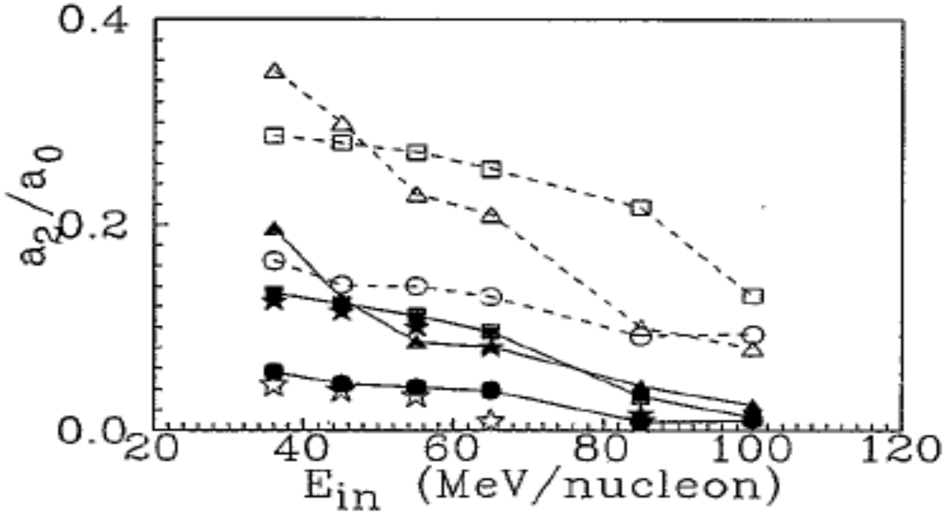

FIG. 2. The comparison of QMD calculations with the experimental data for the midrapidity rotational coefficient a_2/a_0. Dashed lines represent the original calculation and solid lines show their correction with the finite dispersion of the reaction plane determination. ○, □, and △ correspond to $b = 2.5$, 4.5, and 6.5 fm, respectively. Empty stars and full stars represent the experimental data for $b \sim 2.5$ and 4.5 fm.

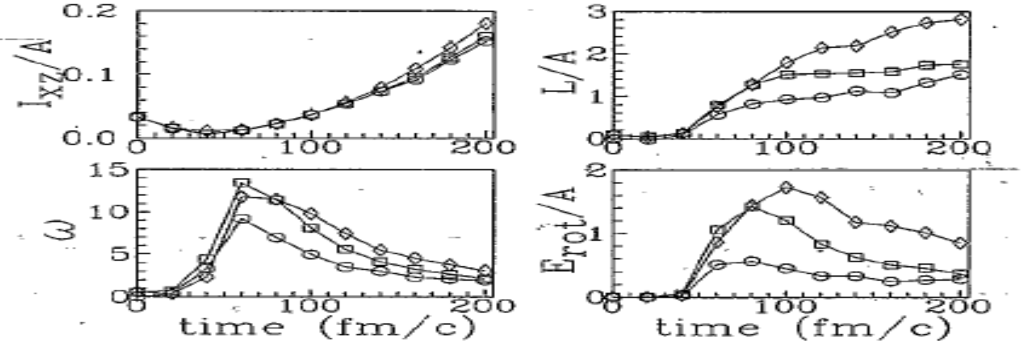

FIG. 3. The time evolution of the moment of inertia per nucleon I_{xz}/A, angular momentum per nucleon L/A, angular velocity ω, and rotational energy per nucleon E_{rot}/A for 36 MeV/nucleon ^{40}Ar+^{27}Al. Their units are 10^3 GeV fm$^2/c^2$ nucleon, $\hbar$/nucleon, $10^{-3}c$/fm, and MeV/nucleon, respectively. ○, □, and △ represent 2.5, 4.5, and 6.5 fm, respectively.

Results (1): NNS of flow

System: 86Kr + 124Sn, 25 MeV/u, 7-10fm; 50,000 events accumulated; freeze-out time: ~120fm/c; results: extracted @ 200fm/c; Hard EOS is used in the present work;

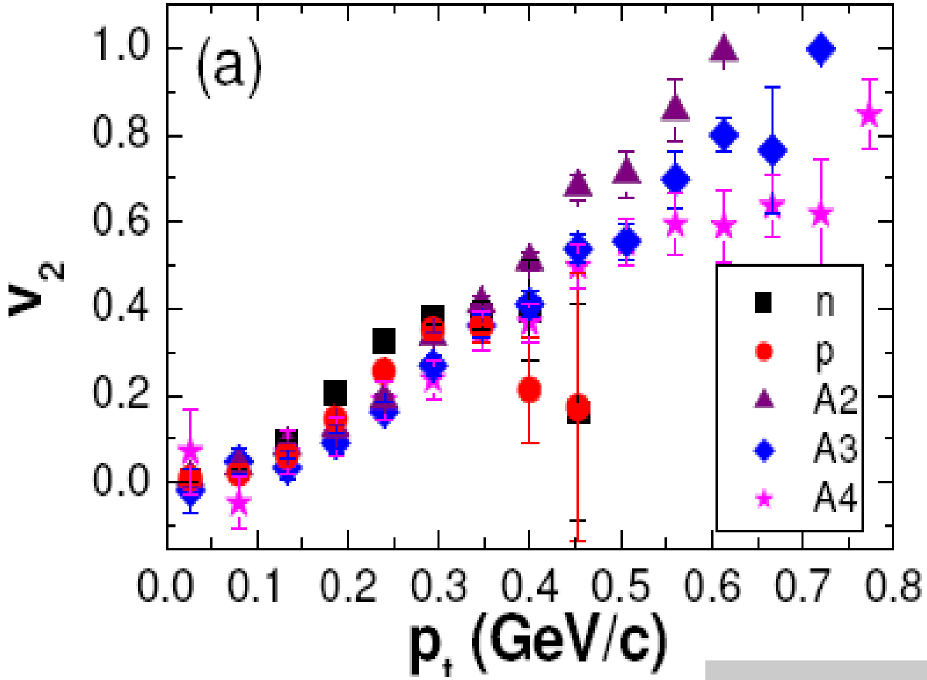

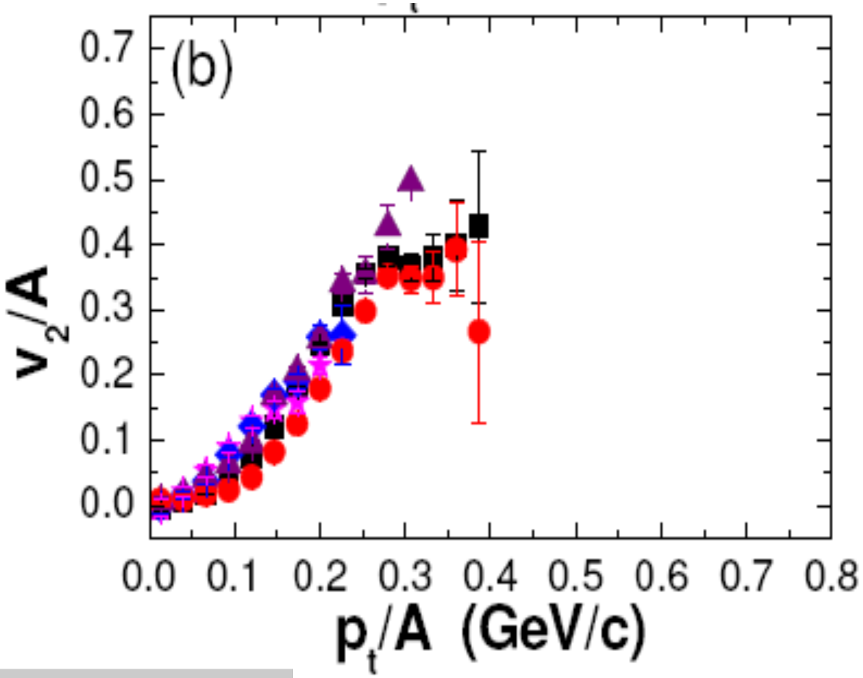

$$v_2 = \langle cos(2\phi) \rangle = \langle \frac{p_x^2 - p_y^2}{p_t^2} \rangle$$

Number-of-nucleon scaling of the elliptic flow !

Low energy: FLOW scaling V2 & v4/v2^2 scaling: nucleonic coalescence below 100A MeV

Physics Letters B 638 (2006) 50–54

Scaling of anisotropic flow and momentum-space densities for light particles in intermediate energy heavy ion collisions

T.Z. Yan [a,b], Y.G. Ma [a,*], X.Z. Cai [a], J.G. Chen [a], D.Q. Fang [a], W. Guo [a,b], C.W. Ma [a,b], E.J. Ma [a,b], W.Q. Shen [a], W.D. Tian [a], K. Wang [a,b]

In hydro by Kolb et al, assuming that quarks have no higher-order anisotropic flows

$$v_4 = \left\langle \frac{p_x^4 - 6p_x^2p_y^2 + p_y^4}{p_t^4} \right\rangle$$

$$v_{4,M}(p_t) = (1/4)v_{2,M}^2(p_t)$$
$$v_{4,B}(p_t) = (1/3)v_{2,B}^2(p_t)$$

If quarks also flow, one get

$$\frac{v_{4,M}}{v_{2,M}^2} \approx \frac{1}{4} + \frac{1}{2}\frac{v_{4,q}}{v_{2,q}^2},$$

$$\frac{v_{4,B}}{v_{2,B}^2} \approx \frac{1}{3} + \frac{1}{3}\frac{v_{4,q}}{v_{2,q}^2},$$

Similarly, if v4/v^2 = ½ for nucleons, then
V4/v2^2(A=2) = ¼+1/2*1/2=1/2
V4/v2^2(A=3) = 1/3+1/3*1/2=1/2
<u>This is the case for the right bottom plot!</u>

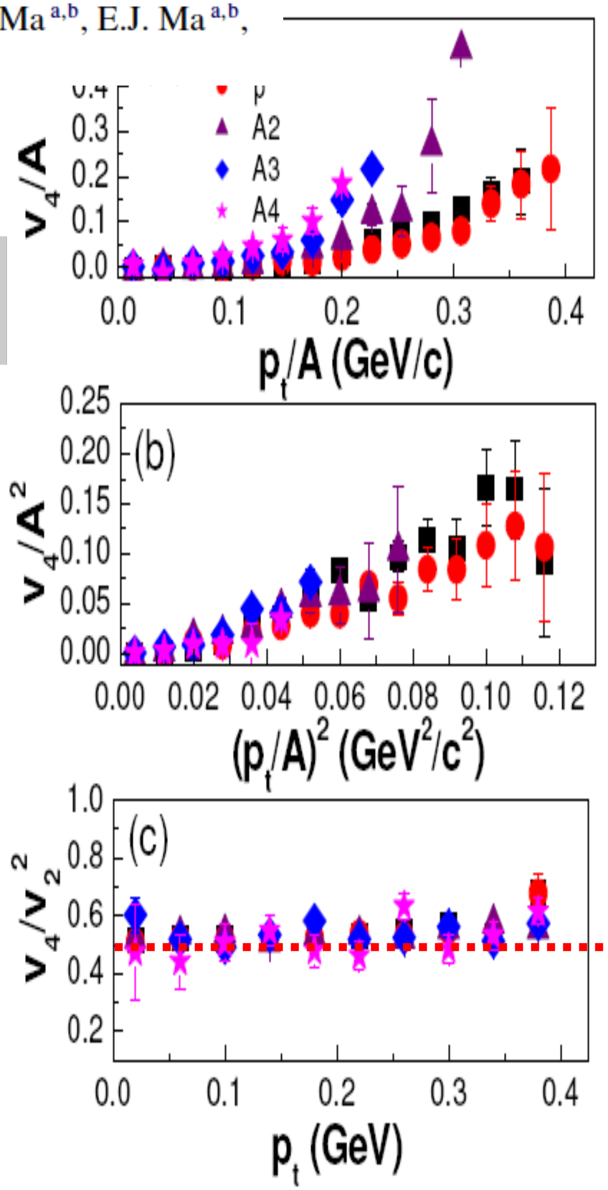

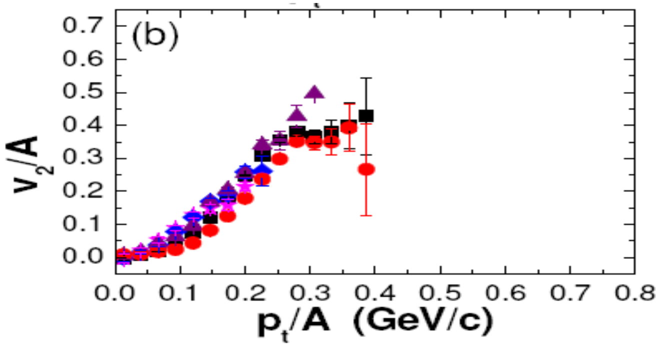

V2/A vs Pt/A
&
V4/V2^2 ~ cst

V4/A^2 vs (Pt/A)^2

T.Z. Yan, YGM et al., Physics Letters B 638 (2006) 50

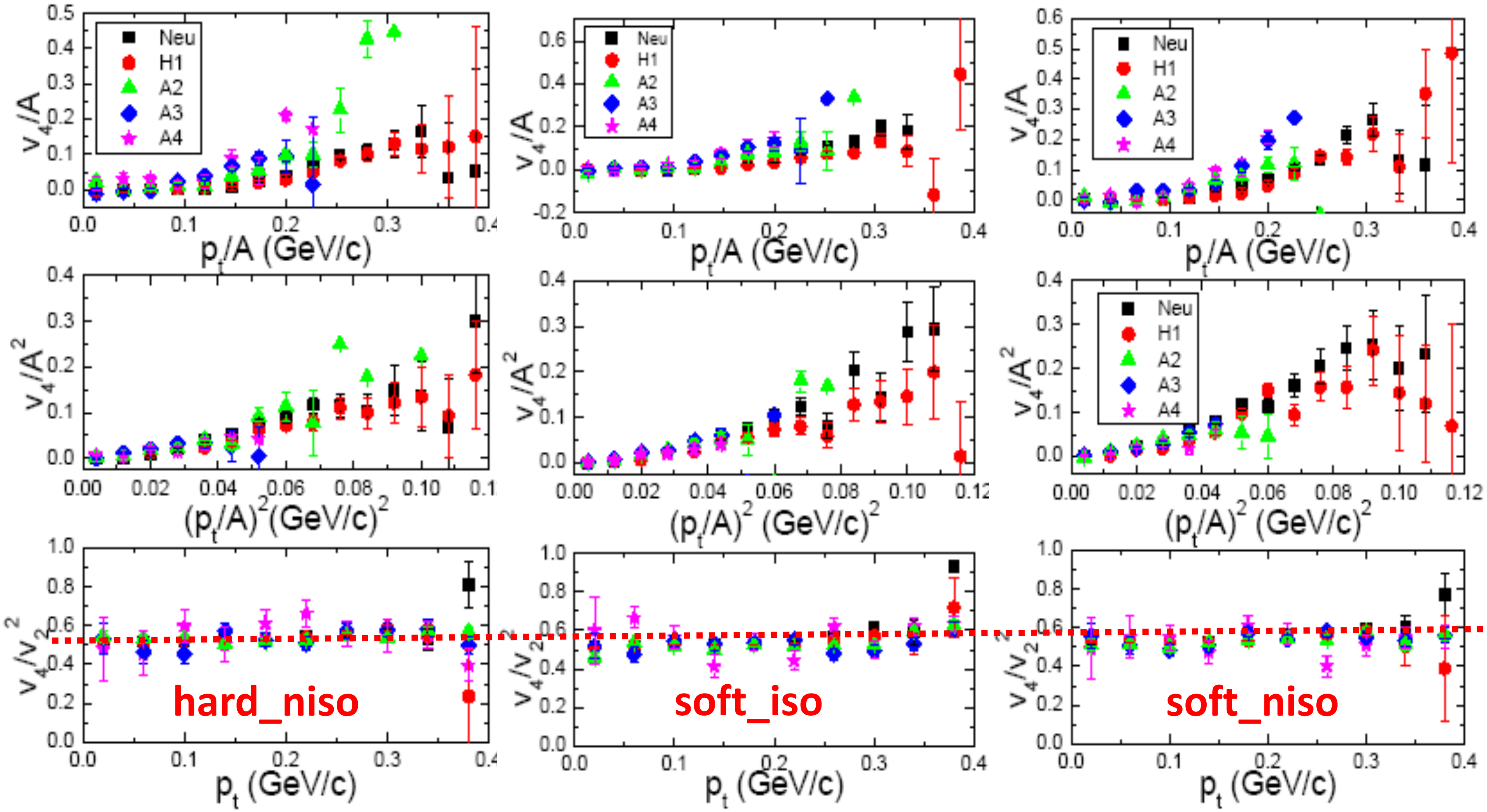

The behavior of scaling is independent of hard or soft EOS and isospin effect !

→ It is a parameter independent observable!

Y.G.Ma

Power-law in momentum space: 0.25-1.15GeV/A

Coalescence:

Assuming the production probability of p is p1, and n is p2, if deutron is formed by coalescence, its production probability should be: p1*p2.

Similarly, probability of fragments with A mass (Coulomb is ignored) should be prob = p1^n

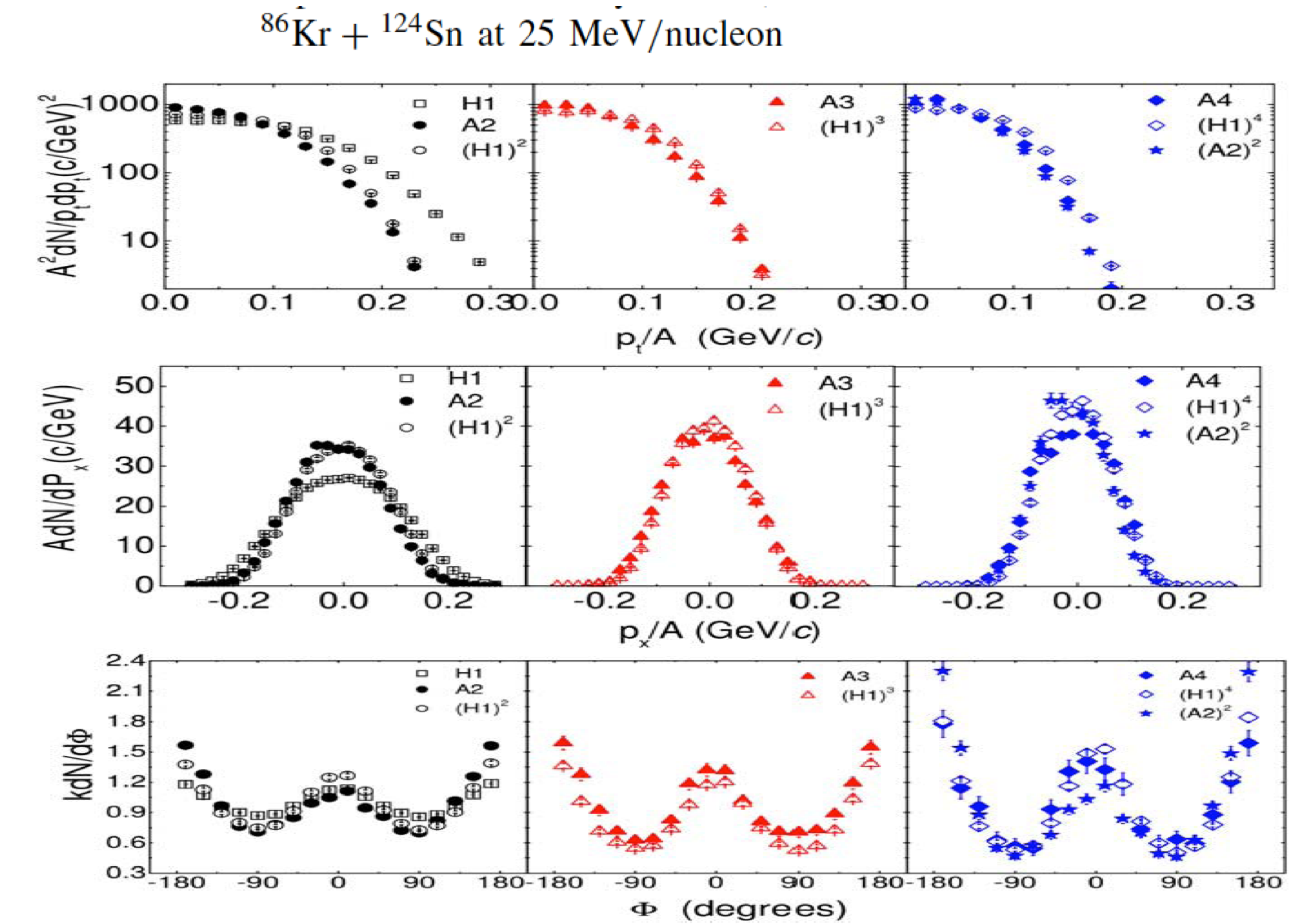

Eur. Phys. J. A (2019) 55: 102
DOI 10.1140/epja/i2019-12788-0

THE EUROPEAN PHYSICAL JOURNAL A

Regular Article – Theoretical Physics

0.4A GeV Au+Au

Nucleon-number scalings of anisotropic flows and nuclear modification factor for light nuclei in the squeeze-out region

负的椭圆流

T.T. Wang[1,2] and Y.G. Ma[1,3,a]

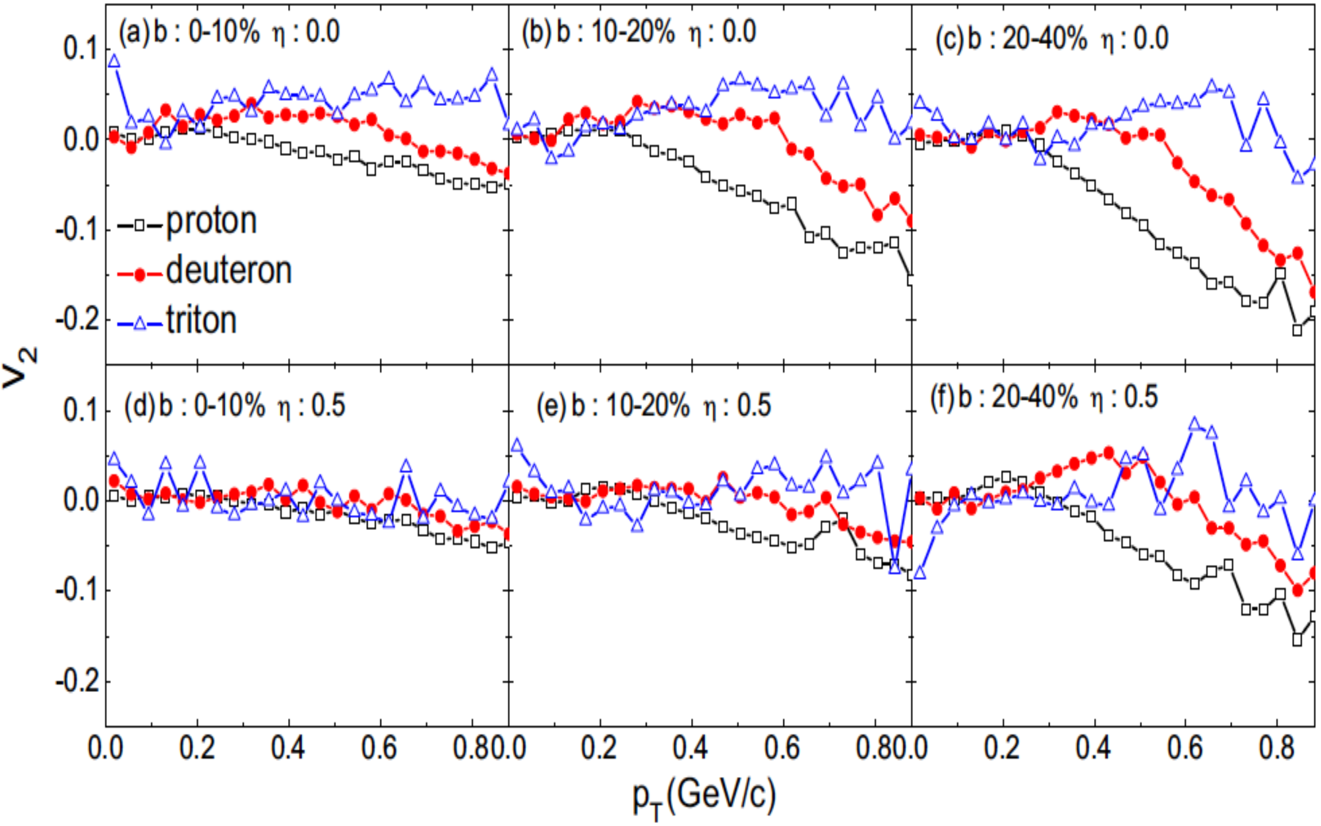

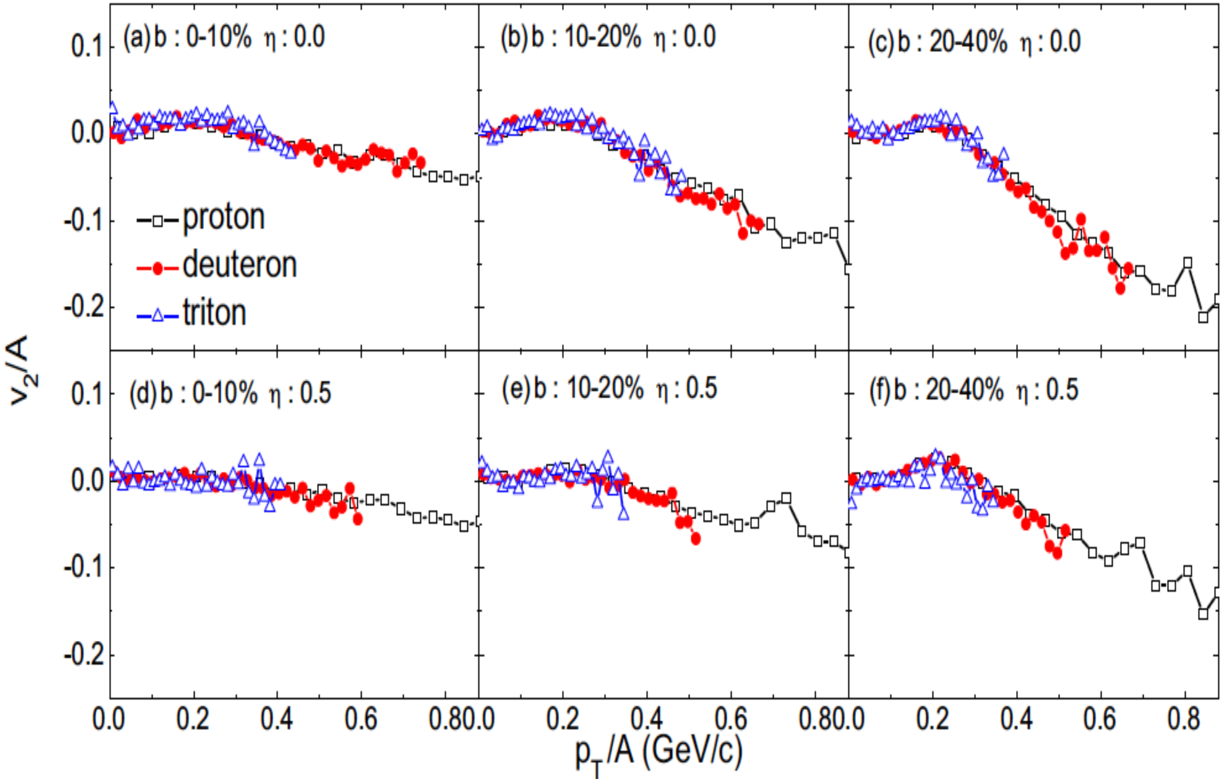

2006年我们提出的轻碎片的椭圆流存在核子数标度率得到STAR合作组的验证

（唯一参考文献[46]）

PHYSICAL REVIEW C **94**, 034908 (2016)

Measurement of elliptic flow of light nuclei at $\sqrt{s_{NN}} = 200, 62.4, 39, 27, 19.6, 11.5$, and 7.7 GeV at the BNL Relativistic Heavy Ion Collider

L. Adamczyk,[1] J. K. Adkins,[20] G. Agakishiev,[18] M. M. Aggarwal,[31] Z. Ahammed,[49] I. Alekseev,[16] A. Aparin,[18] D. Arkhipkin,[3] E. C. Aschenauer,[3] A. Attri,[31] G. S. Averichev,[18] X. Bai,[7] V. Bairathi,[27] R. Bellwied,[45] A. Bhasin,[17] A. K. Bhati,[31] P. Bhattarai,[44] J. Bielcik,[10] J. Bielcikova,[11] L. C. Bland,[3] I. G. Bordyuzhin,[16] J. Bouchet,[19] J. D. Brandenburg,[37] H. Caines,[53] M. Calderón de la Barca Sánchez,[5] J. M. Campbell,[29] D. Cebra,[5]

Figure 9 presents the light-nuclei v_2/A as a function of p_T/A, where A is the atomic mass number of the corresponding light nuclei. The main goal of this study is to understand whether light (anti) nuclei production is consistent with coalescence of (anti) nucleons. The model predicts that, if a composite particle were produced by coalescence of n number of particles that are very close to each other in phase space, then $v_2(p_T)$ of the composite will be n times that of the constituents [46]. In Fig. 9 it is observed that the (anti) nuclei v_2/A closely follows v_2 of p ($\overline{p}$) for p_T/A up to 1.5 GeV/c. The scaling behavior holds ($p_T/A < 1.5$ GeV/c) within 5%–20% for all beam energy range presented. The scaling behavior of these nuclei suggest that d ($\overline{d}$) within $p_T <$ 3.0 GeV/c and t, ^{3}He ($^3\overline{\text{He}}$) within $p_T < 4.5$ GeV/c might have formed via the coalescence of nucleons (antinucleons).

almost similar magnitude of v_2 for all collision energies. The fact that all the light-nuclei v_2 generally follow an atomic mass number scaling indicates that the coalescence of nucleons might be the underlying mechanism of light-nuclei formation in high-energy heavy-ion collisions. This observation is further

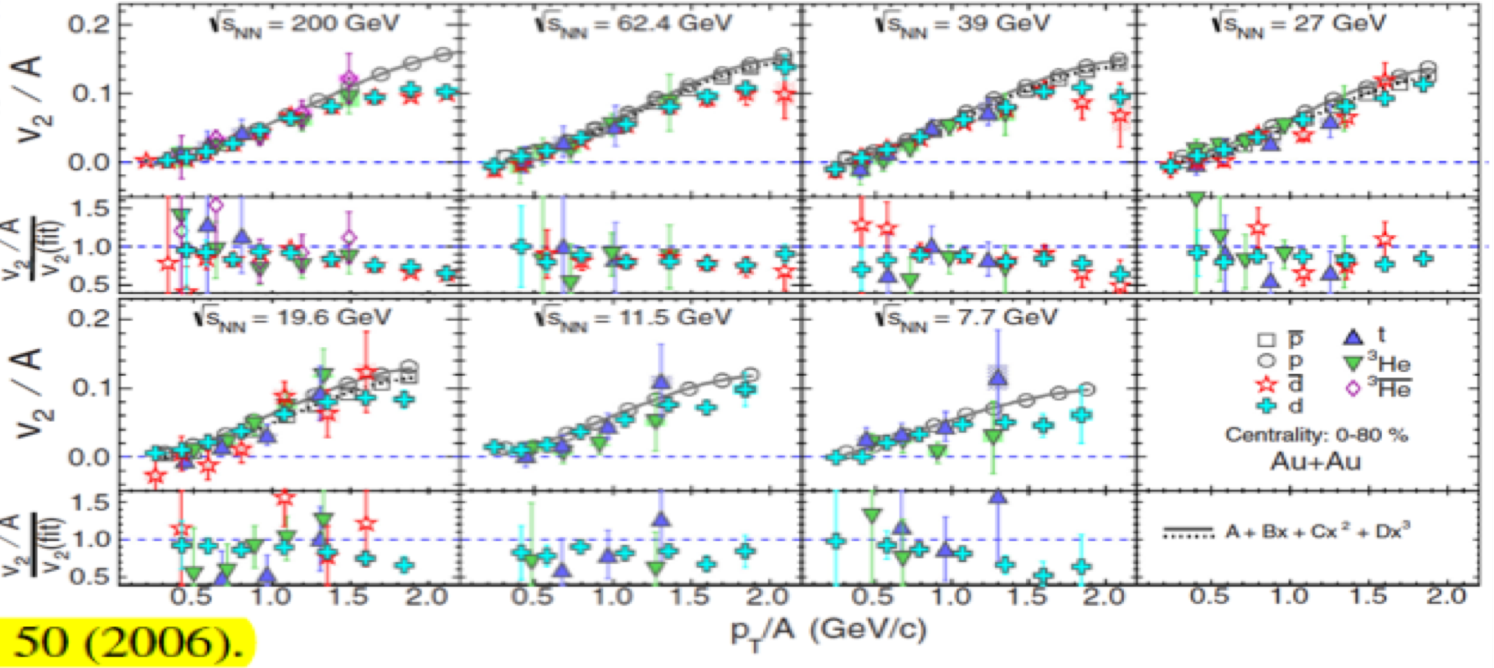

[46] T. Z. Yan *et al.*, Phys. Lett. B **638**, 50 (2006).

PHYSICS LETTERS B

Scaling of anisotropic flow and momentum-space densities for light particles in intermediate energy heavy ion collisions

T.Z. Yan [a,b], Y.G. Ma [a,*], X.Z. Cai [a], J.G. Chen [a], D.Q. Fang [a], W. Guo [a,b], C.W. Ma [a,b], E.J. Ma [a,b], W.Q. Shen [a], W.D. Tian [a], K. Wang [a,b]

Alpha Clustering effects

an example of nuclear structure effect in HIC

轻核区基态、激发态及远离β稳定线区团簇的不同存在形式

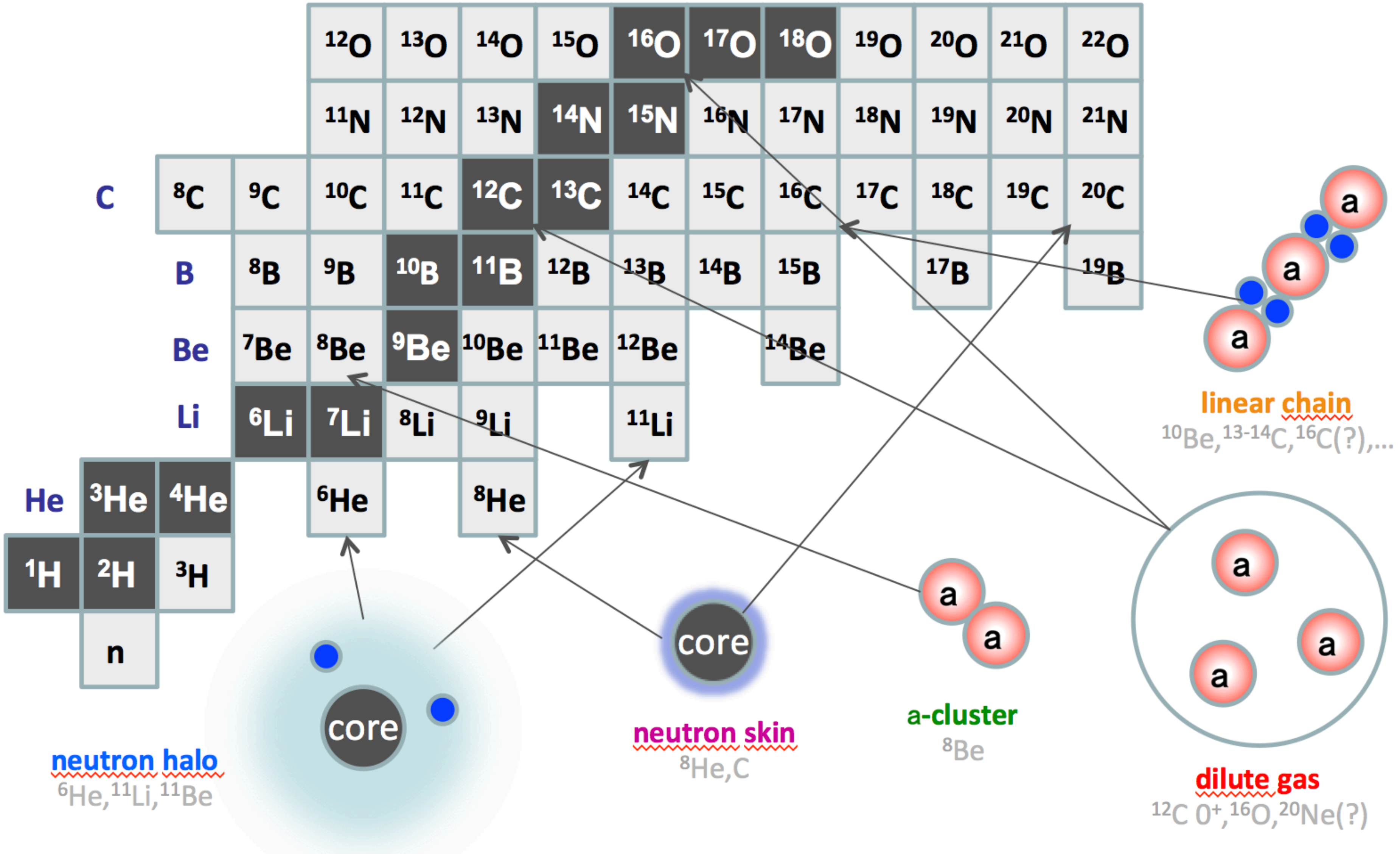

See D Dell'Aquila talk on SOTANCP4

✓ Alpha-cluster is predicted to appear near cluster decay threshold in α conjugate nuclei about 50 years ago

The α cluster is the most prominent case since (1) the high binding energy of α-conjugate nuclei and (2) high energy of it's first excitation state.

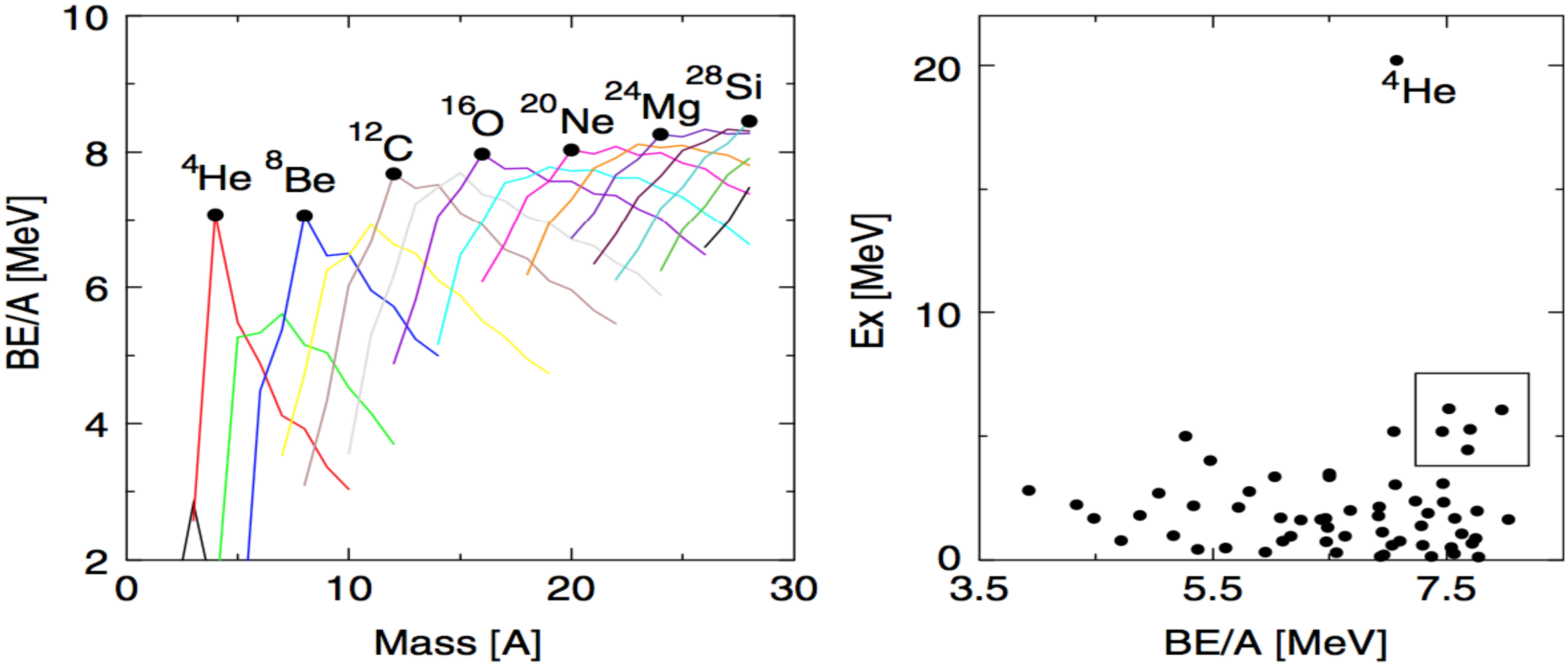

He burning Chain

The Triple-Alpha Process

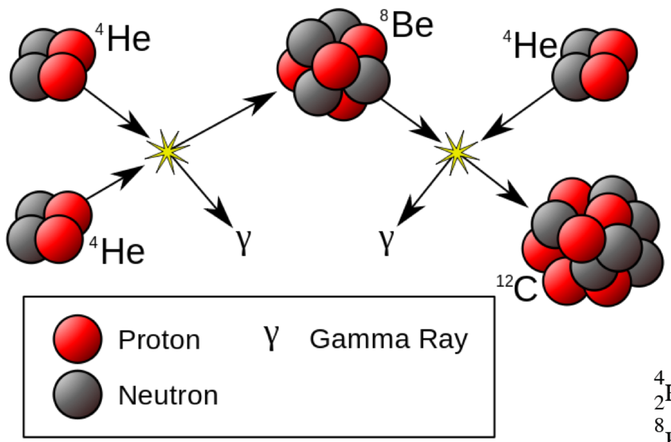

$$^{4}_{2}\mathrm{He} + ^{4}_{2}\mathrm{He} \rightarrow ^{8}_{4}\mathrm{Be} \quad (-93.7\ \mathrm{keV})$$
$$^{8}_{4}\mathrm{Be} + ^{4}_{2}\mathrm{He} \rightarrow ^{12}_{6}\mathrm{C} \quad (+7.367\ \mathrm{MeV})$$

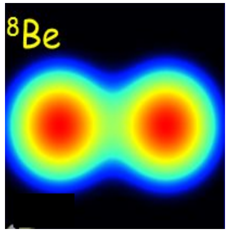

Facilitated by the cluster structure of the ^{8}Be and the ^{12}C Hoyle State

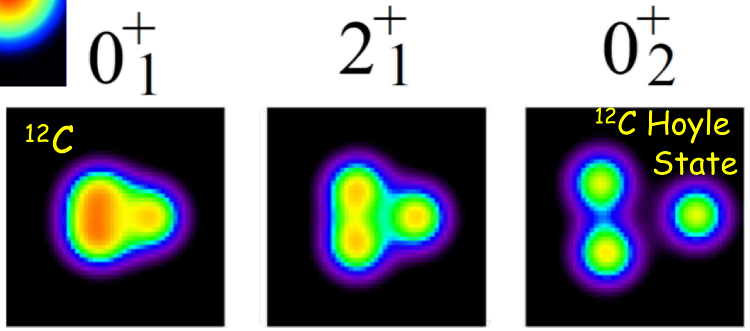

Y. Kanada En'yo, M. Kimura, A. Ono, **Prog. of Theo. Exp.Phys..2012 (2012) 01A202**

The ^{12}C(alpha,gamma)^{16}O

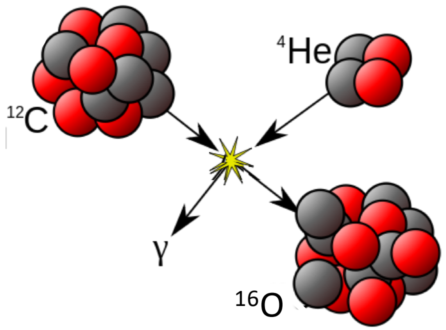

Facilitated by the cluster structure of bound and unbound ^{16}O states

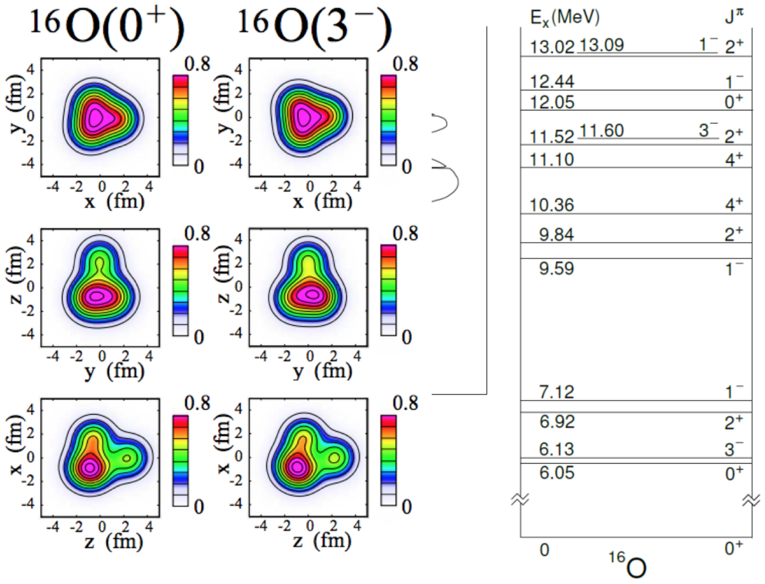

From M. Wiescher talk on SOTANCP4

稳定核中以α和类α团簇为主

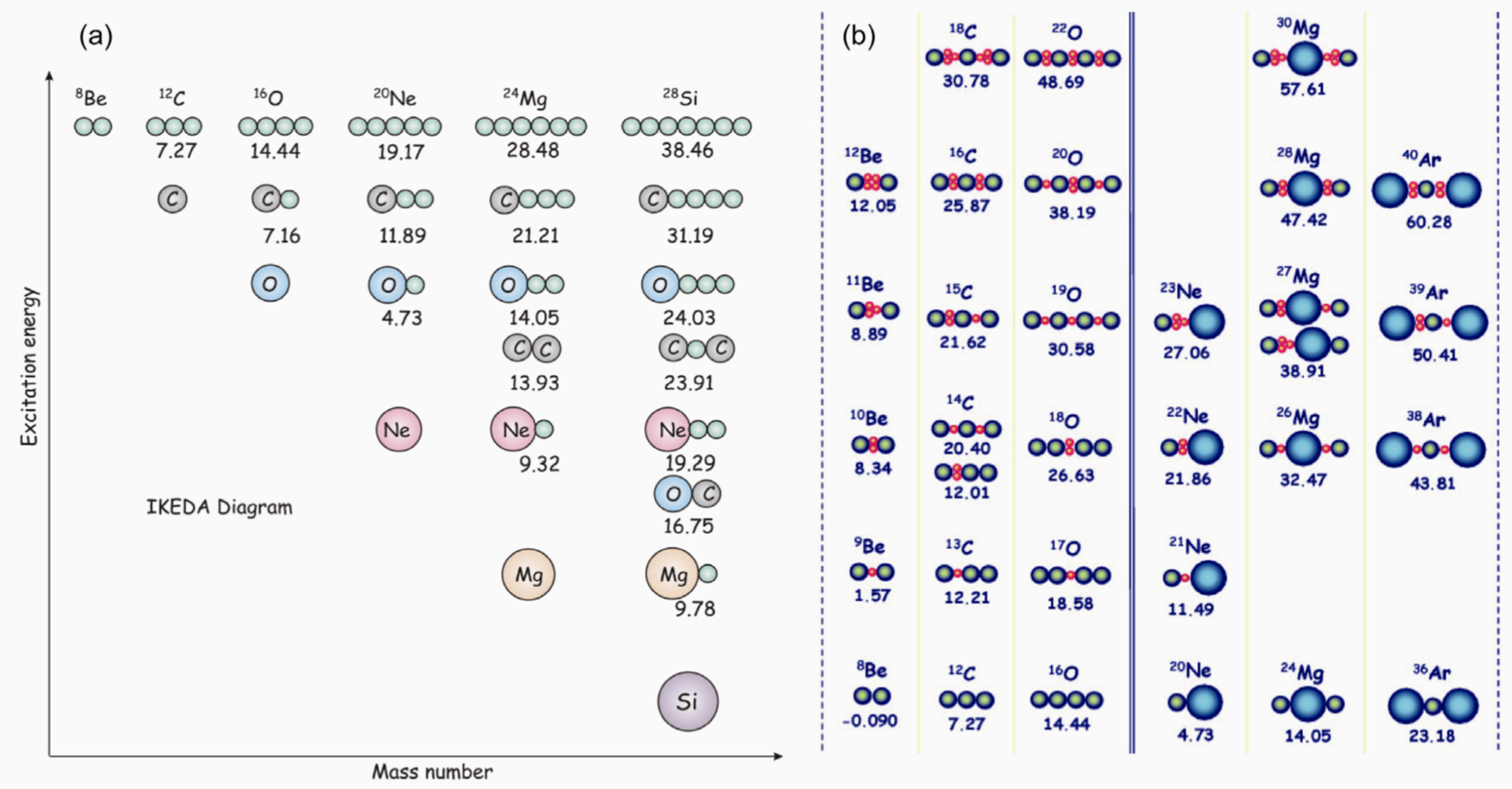

The first condition is the stability of the constituent clusters which is necessary for keeping the identity of the clusters. The second condition is the weakness of inter-cluster interaction.

The weakness of the inter-cluster interaction results in the energy location of the cluster state near the breakup threshold into constituent clusters.

LETTER

doi:10.1038/nature11246

How atomic nuclei cluster

J.-P. Ebran[1], E. Khan[2], T. Nikšić[3] & D. Vretenar[3]

Fully microscopic descrip- tion based on the framework of energy-density functionals (EDFs).

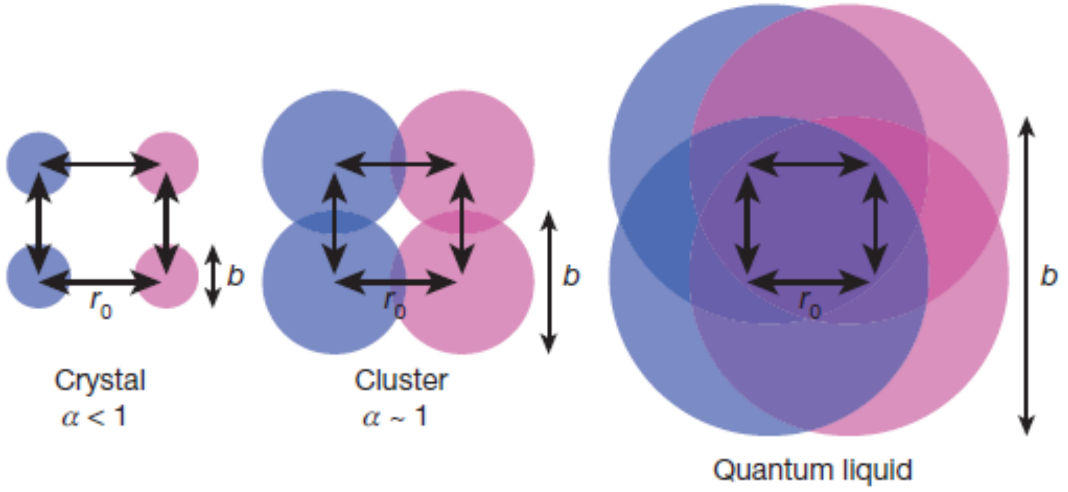

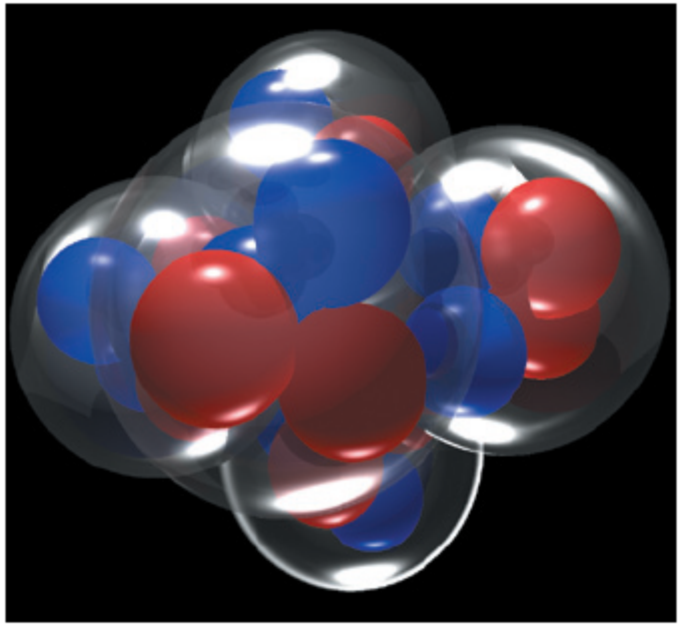

NUCLEAR PHYSICS

Nucleons come together

MARTIN FREER

The transformation from the fermionic liquid to the bosonic crystal-like cluster structures reveals key features of the strong nucleon–nucleon interaction within nuclei, and the current work is a step forward in our understanding of this interaction. ■

So, is this the complete picture of nuclear clustering? Although the depth of the potential may emphasize the cluster symmetries, it does not describe the emergence of clustering close to the energy threshold for α-particle decay — the Ikeda picture[3]. There is, therefore, a missing component in this explanation of clustering. Weakly bound nuclei close to

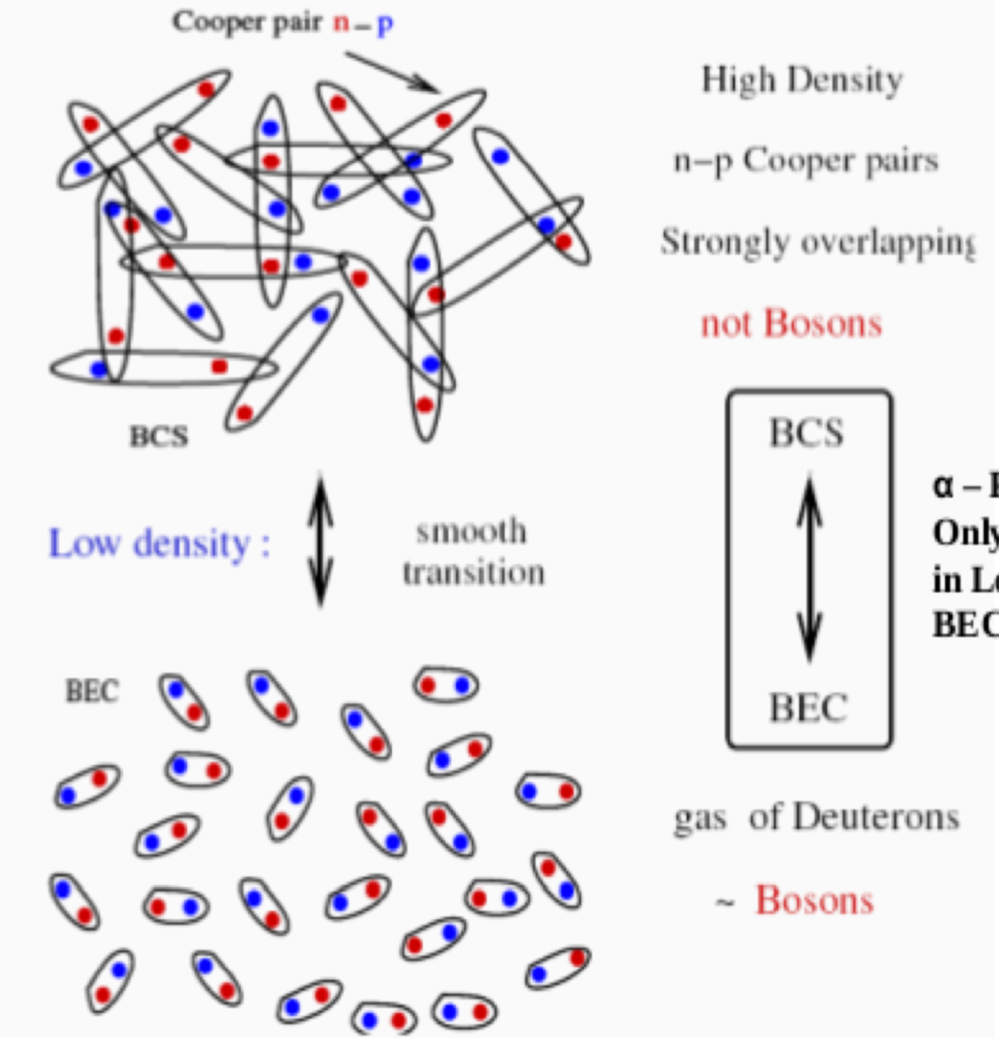

α – Particles Only Exist in Low Density BEC Phase

Quartetting

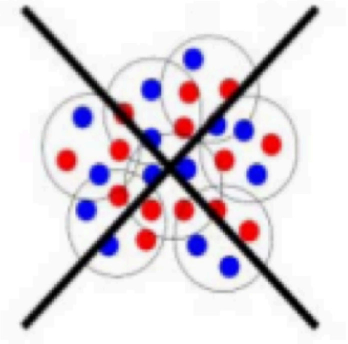

No BCS phase (dense phase) of α-particles possible!

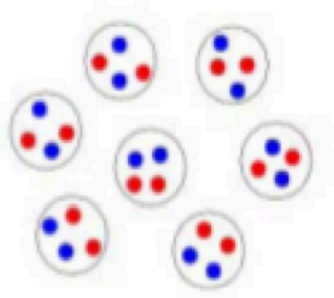

Bose-Einstein-Condensation of α-particles (dilute)

See P. Schuck talk on SOTANCP4

Triple-alpha process occuring in Red Giants => Origin of carbon !

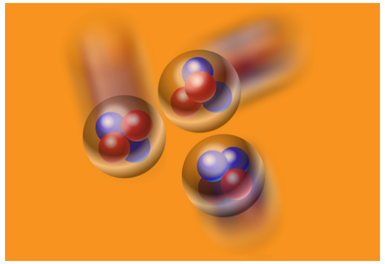

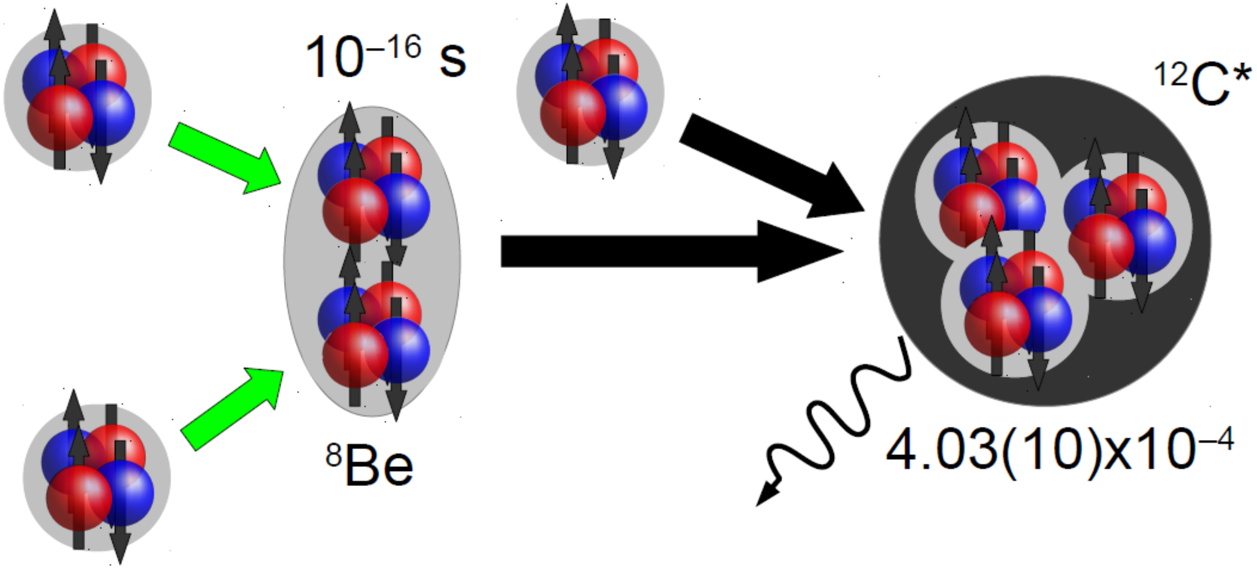

Most important nuclear reaction during Helium burning !

Schematic of the triple alpha process at T~10^8 K.

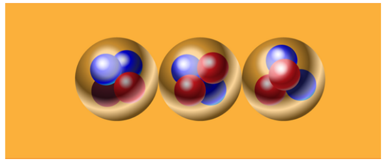

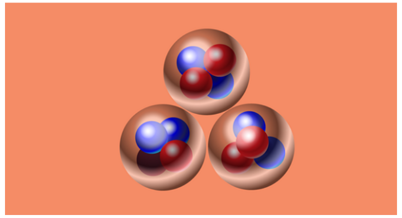

$\alpha+\alpha$ → ^{8}Be – 0.092 MeV; ^{8}Be is unstable with $\tau_{1/2}$ ~ 10^{-16} s and decays quickly into two α-particles !
Carbon production is possible only via a resonance reaction
$\alpha+\alpha+\alpha$ → ^{12}C* → ^{12}C + 2γ + 7.37 MeV

$\boxed{J^{\pi}=0^{+},\ E_x=7.654\ \text{MeV}}$

predicted by Fred Hoyle in 1953

^{40}Ca case:

109, 232503 (2012) PHYSICAL REVIEW LETTERS week ending 7 DECEMBER 2012

Existence of an Exotic Torus Configuration in High-Spin Excited States of ^{40}Ca

T. Ichikawa,[1] J. A. Maruhn,[2] N. Itagaki,[1] K. Matsuyanagi,[1,3] P.-G. Reinhard,[4] and S. Ohkubo[5,6]
[1]Yukawa Institute for Theoretical Physics, Kyoto University, Kyoto 606-8502, Japan
[2]Institut für Theoretische Physik, Universität Frankfurt, D-60438 Frankfurt, Germany
[3]RIKEN Nishina Center, Wako 351-0198, Japan
[4]Institut für Theoretische Physik, Universität Erlangen, D-91058 Erlangen, Germany
[5]Department of Applied Science and Environment, University of Kochi, Kochi 780-8515, Japan
[6]Research Center for Nuclear Physics, Osaka University, Ibaraki, Osaka 567-0047, Japan
(Received 26 July 2012; published 5 December 2012)

We investigate the possibility of the existence of the exotic torus configuration in the high-spin excited states of ^{40}Ca. We here consider the spin alignments about the symmetry axis. To this end, we use a three-dimensional cranked Skyrme Hartree-Fock method and search for stable single-particle configurations. We find one stable state with the torus configuration at the total angular momentum $J = 60\hbar$ and an excitation energy of about 170 MeV in all calculations using various Skyrme interactions. The total angular momentum $J = 60\hbar$ consists of aligned 12 nucleons with the orbital angular momenta $\Lambda = +4$, $+5$, and $+6$ for spin-up or -down neutrons and protons. The obtained results strongly suggest that a macroscopic amount of circulating current breaking the time-reversal symmetry emerges in the high-spin excited state of ^{40}Ca.

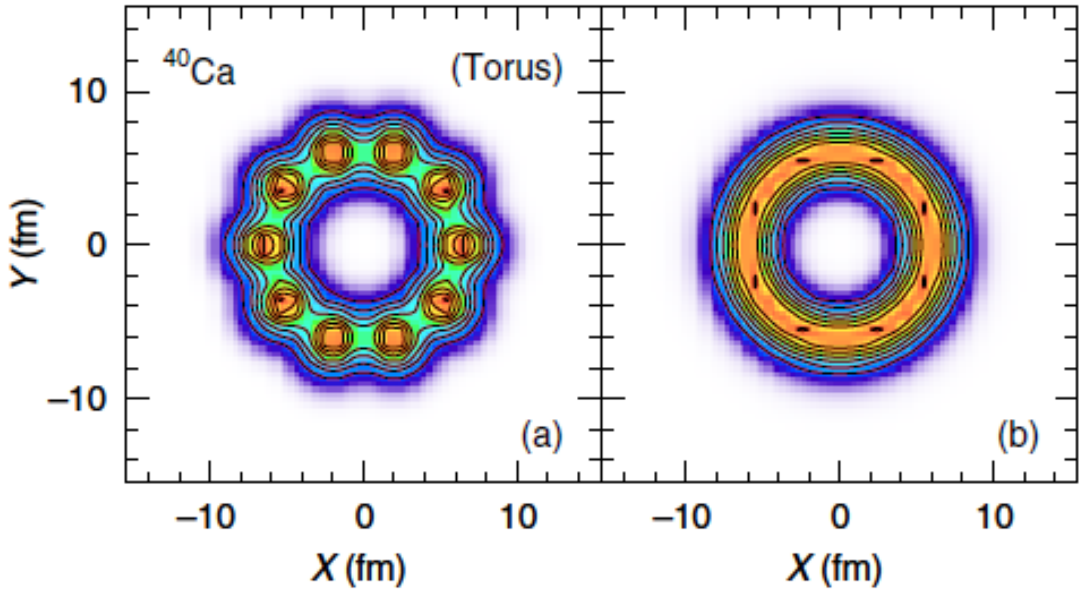

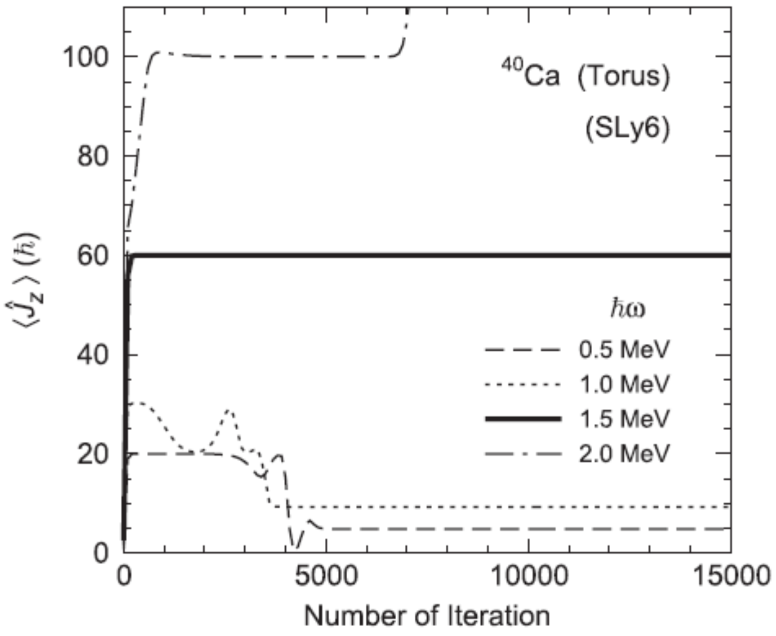

首次发现原子核极高激发能共振实验证据

约翰·惠勒在20世纪五六十年代预言在一定的条件下原子核可能呈现准一维的环形结构

J. A. Wheeler, Nucleonics Notebook, 1950 (unpublished), see also p. 297 in G. Gamow, Biography of Physics, Harper & Brothers Publishers, N.Y. 1961

C. Y. Wong's predictions, Phys Lett B 41, 446 (1972)， Phys Lett B 738, 401 (2014)

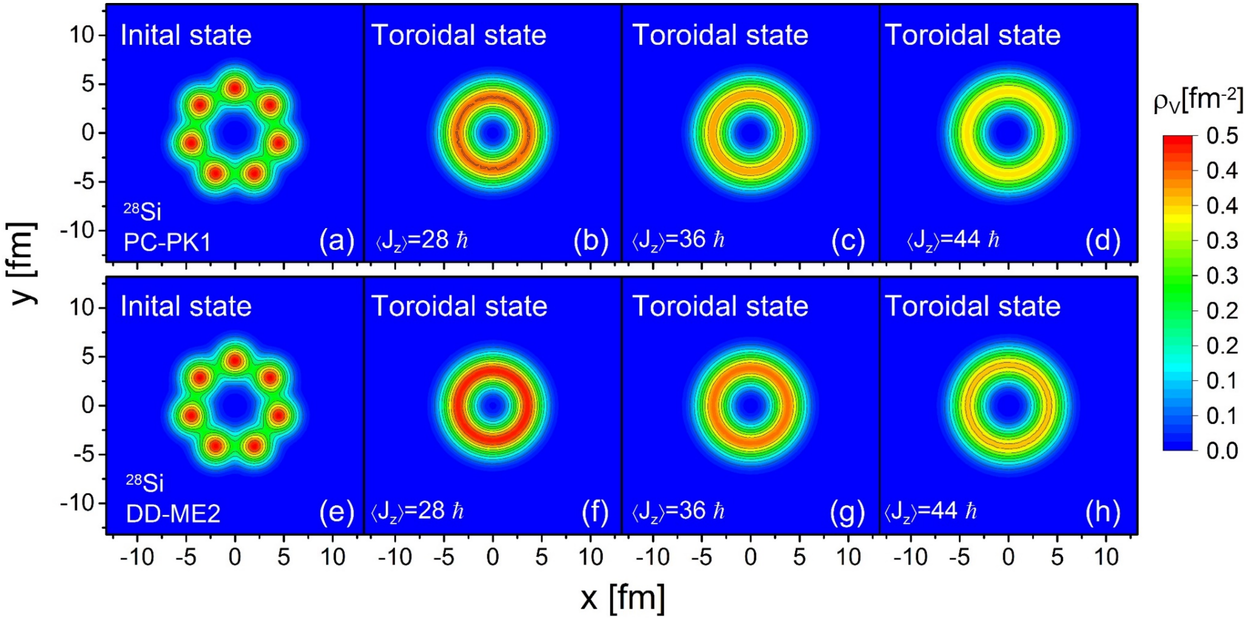

实验探测器布局

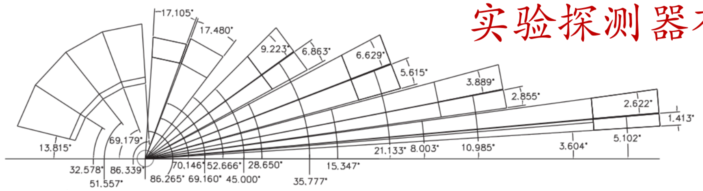

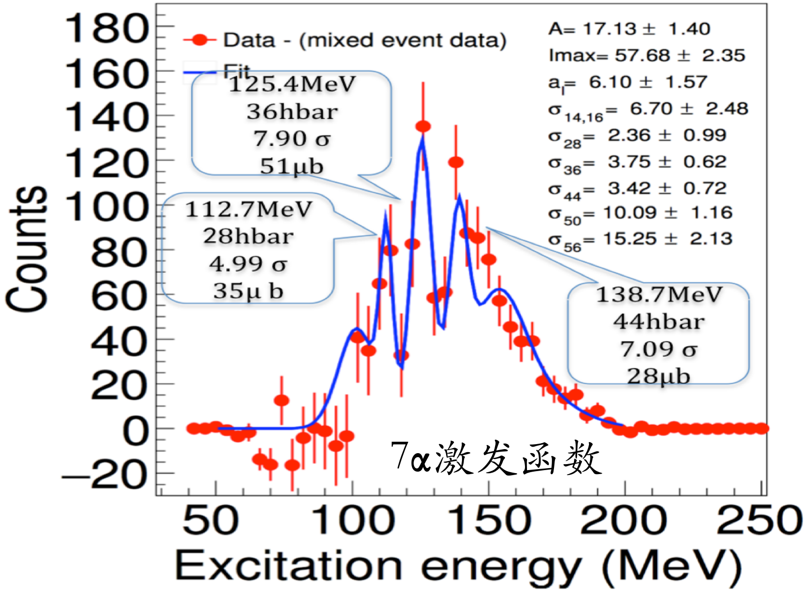

X. G. Cao et al., Phys Rev C 99, 014606 (2019)

- ✓ 实验首次测量到^{28}Si高激发态的7α发射道
- ✓ 首次发现远高于已知共振能区存在3个明显共振峰(置信度大于5个σ)，与理论预言定量符合
- ✓ 探测原子核的极限状态: 极高激发能(139MeV)、极高角动量(44hbar)、形状极限(准2维空心圆环和1维长链等)
- ✓ 7α发射来自低密度状态，核相图低密度区的α波色-爱因斯坦凝聚?

Model: EQMD- An extension of QMD

-- microscopic dynamical model

Maruyama, T., Niita, K., & Iwamoto, A. (1996). Phys. Rev. C, 53(1), 297 – 304.

- Gaussian wave packets of nucleons:

$$\phi_i(\mathbf{r}_i) = \left(\frac{\nu_i + \nu_i^*}{2\pi}\right)^{3/4} \exp\left[-\frac{\nu_i}{2}(\mathbf{r}_i - \mathbf{R}_i)^2 + \frac{i}{\hbar}\mathbf{P}_i \cdot \mathbf{r}_i\right] \qquad \nu_i = \frac{1}{\lambda_i} + i\delta_i$$

$$\varphi_i(\mathbf{p}_i) = \left(\frac{\nu_i + \nu_i^*}{2\pi\hbar^2\nu_i^2}\right)^{3/4} \exp\left[-\frac{1}{2\nu_i\hbar^2}(\mathbf{p}_i - \mathbf{P}_i)^2 - \frac{i}{\hbar}\mathbf{p}_i \cdot \mathbf{R}_i\right]$$

- Density distribution:

$$\rho(\mathbf{r}_i) = \varphi_i(\mathbf{r}_i)^*\varphi_i(\mathbf{r}_i) = \left(\frac{1}{\pi\lambda_i}\right)^{\frac{3}{2}} \exp\left[-\frac{1}{\lambda_i}(\mathbf{r}_i - \mathbf{R}_i)^2\right]$$

$$\rho(\mathbf{p}_i) = \varphi_i(\mathbf{p}_i)^*\varphi_i(\mathbf{p}_i) = \left(\frac{1}{\pi} \cdot \frac{\lambda_i}{1 + \lambda_i^2\delta_i^2}\right)^{\frac{3}{2}} \exp\left[-\frac{\lambda_i}{1 + \lambda_i^2\delta_i^2}(\mathbf{p}_i - \mathbf{P}_i)^2\right]$$

- Wigner function:

$$W(\mathbf{r}, \mathbf{p}) = \left(\tfrac{1}{\pi\hbar}\right)^3 \sum_i^A exp$$
$$\left[-\tfrac{1+\lambda_i^2\delta_i^2}{\lambda_i}(\mathbf{r} - \mathbf{R}_i)^2 - \tfrac{2\lambda_i\delta_i}{\hbar}(\mathbf{r} - \mathbf{R}_i) \cdot (\mathbf{p} - \mathbf{P}_i) - \tfrac{\lambda_i}{\hbar^2}(\mathbf{p} - \mathbf{P}_i)^2\right]$$

- Effective interaction：

$$H_{int} = H_{Skyrme} + H_{Coulomb} + H_{Symmetry} + H_{Pauli}$$

- Pauli potential：

$$H_{\mathrm{Pauli}} = \frac{c_{\mathrm{P}}}{2} \sum_{i} (f_i - f_0)^{\mu} \theta(f_i - f_0),$$

$$f_i \equiv \sum_{j} \delta(S_i, S_j) \delta(T_i, T_j) |\langle \phi_i | \phi_j \rangle|^2,$$

The Pauli potential gives the nucleons repulsive potential for the same spin and isospin to avoid close to each other in the phase space.

Dynamic width wave packets of nucleons and the Pauli potential are the key extension of EQMD

For transport model, one has to prepare energy-minimum states as initial ground nuclei. They are obtained by starting from a random configuration and by solving the damped equations of motion.

- Friction cooling：

$$\dot{\mathbf{R}}_i=\frac{\partial H}{\partial \mathbf{P}_i},\quad \dot{\mathbf{P}}_i=-\frac{\partial H}{\partial \mathbf{R}_i},$$

$$\frac{3\hbar}{4}\dot{\lambda}_i=-\frac{\partial H}{\partial \delta_i},\quad \frac{3\hbar}{4}\dot{\delta}_i=\frac{\partial H}{\partial \lambda_i}.$$

Equations of motion

Add damping term

$$\dot{\mathbf{R}}_i=\frac{\partial H}{\partial \mathbf{P}_i}+\boxed{\mu_{\mathbf{R}}\frac{\partial H}{\partial \mathbf{R}_i}},\quad \dot{\mathbf{P}}_i=-\frac{\partial H}{\partial \mathbf{R}_i}+\boxed{\mu_{\mathbf{P}}\frac{\partial H}{\partial \mathbf{P}_i}},$$

$$\frac{3\hbar}{4}\dot{\lambda}_i=-\frac{\partial H}{\partial \delta_i}+\boxed{\mu_{\lambda}\frac{\partial H}{\partial \lambda_i}},\quad \frac{3\hbar}{4}\dot{\delta}_i=\frac{\partial H}{\partial \lambda_i}+\boxed{\mu_{\delta}\frac{\partial H}{\partial \delta_i}}.$$

Equations of cooling

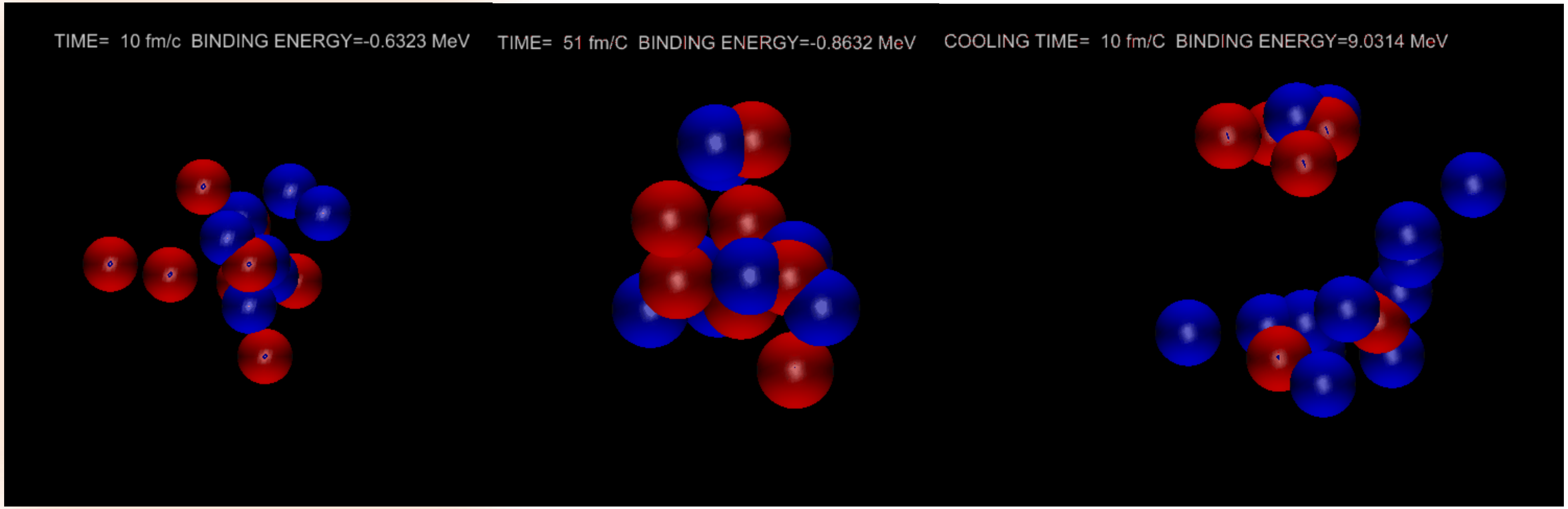

^{16}O initial state before cooling　^{16}O cooling to ground state　^{19}C cooling to halo structure

There are three main excitation modes studied widely: GDR, PDR, GMR

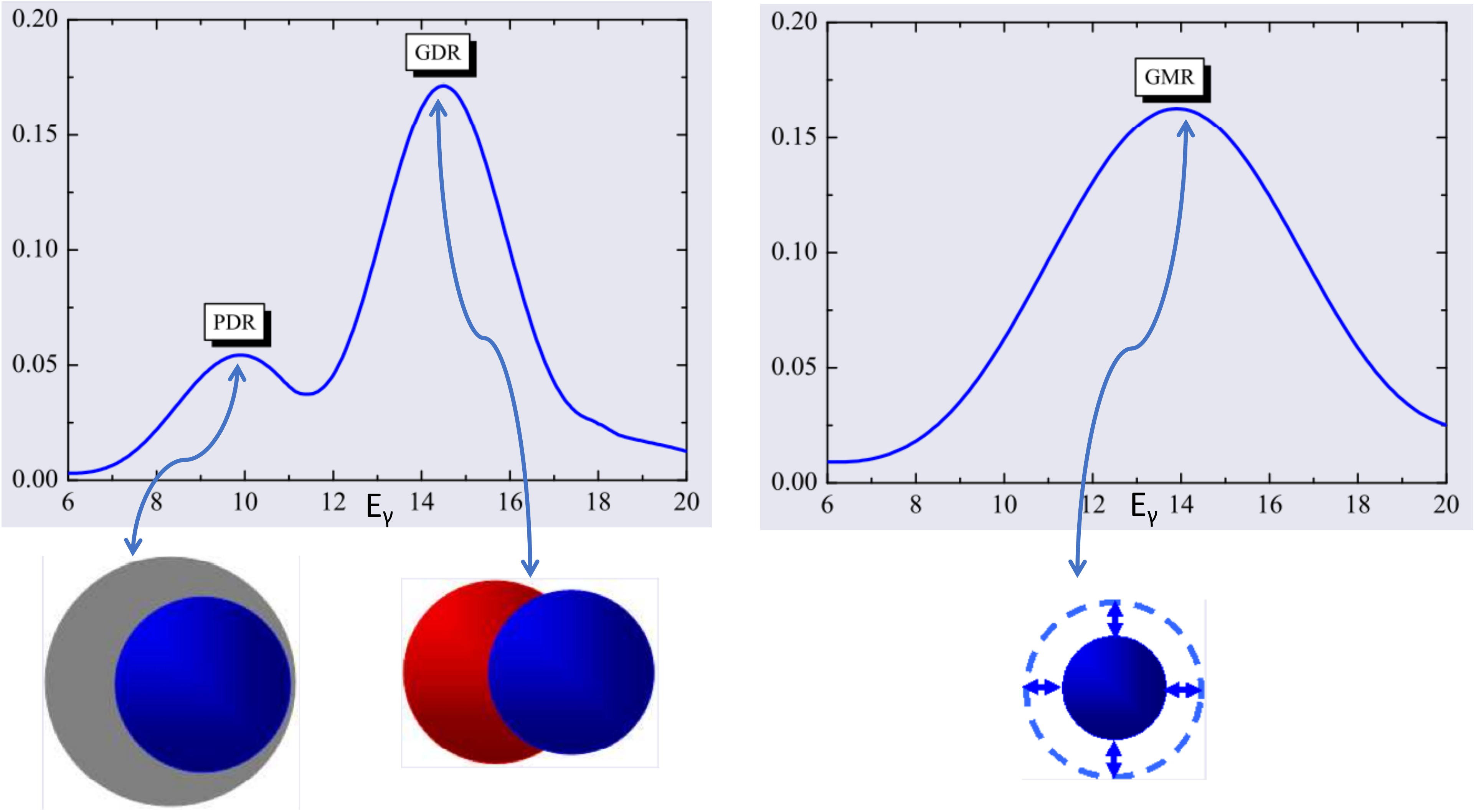

Valence neutron <=> Core   Proton <=> Neutron

☐ GDR algorithm & verification

-- How to extract giant resonance from QMD

Dipole excitation

V. Baran et al, Nucl. Phys.A 679,373 (2001)

$$H_{GDR}(t) = \frac{\Pi^2(t)}{2M} + \frac{M\omega^2(t)}{2} X^2(t)$$

$$\Pi = \frac{NZ}{A}\left(\frac{P_Z}{Z} - \frac{P_N}{N}\right) \qquad X = R_Z - R_N$$

Dipole moments are:

$$D_G(t) = \frac{NZ}{A}\left[R_Z(t) - R_N(t)\right],$$

$$K_G(t) = \frac{NZ}{A\hbar}\left[\frac{P_Z(t)}{Z} - \frac{P_N(t)}{N}\right],$$

Fourier transformation

- ✓ $\mathrm{DR}(t) = \frac{NZ}{A}(R_p - R_n)$ ← Dipole moment

  $R_p(R_n)$ is center of mass for protons (neutrons

- ✓ $\bar{V} \equiv \overline{\frac{dDR(t)}{dt}}$,
- ✓ $\frac{dV}{dt}(E) = \int_0^\infty \frac{d^2DR(t)}{dt^2} e^{i\left(\frac{Et}{\hbar c}\right)} dt$
- ✓ $\frac{dP}{dE} = \frac{2}{3\pi}\frac{e^2}{E\hbar c}\left|\overline{\frac{dV}{dt}}(E)\right|^2$

dP/dE is GDR strength

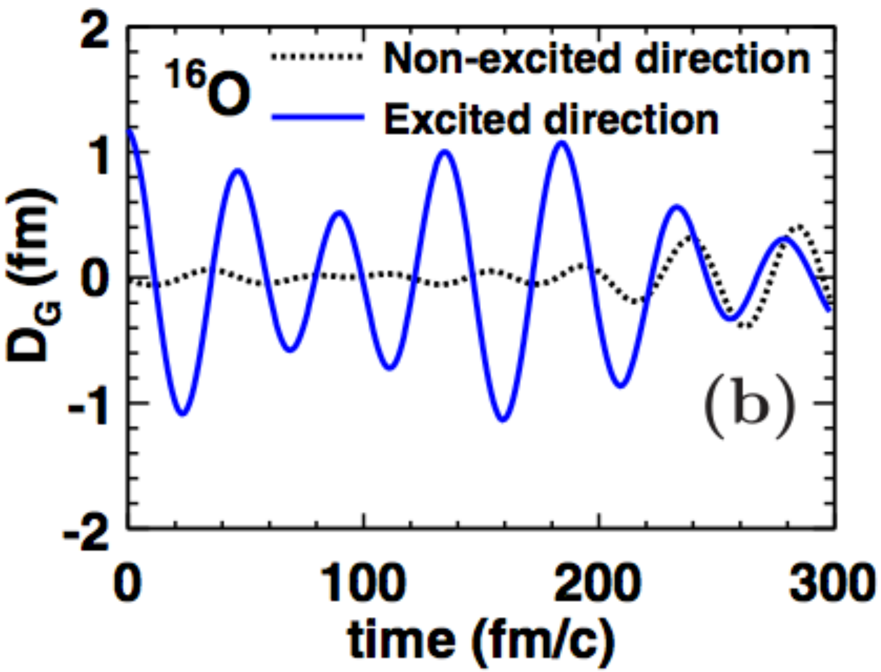

Density of each nucleon in nuclei with alpha-clustering configuration

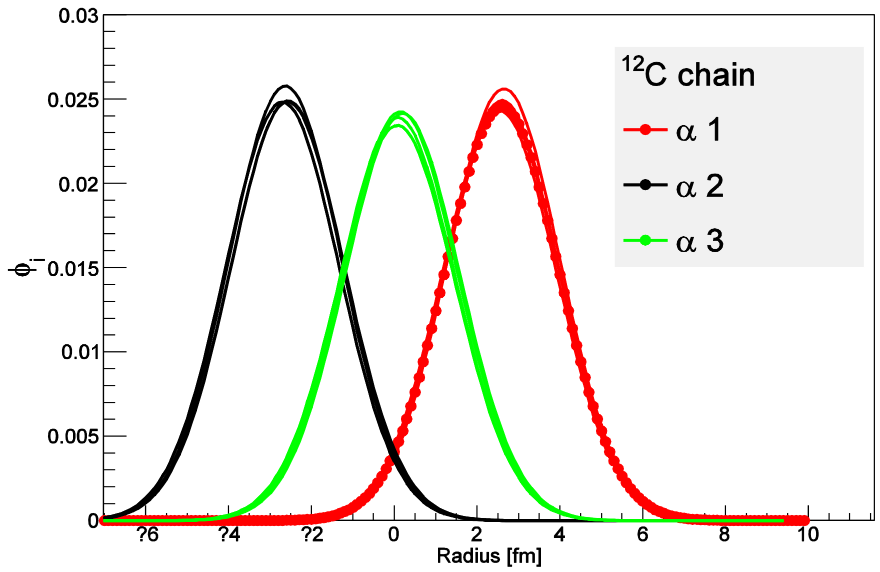

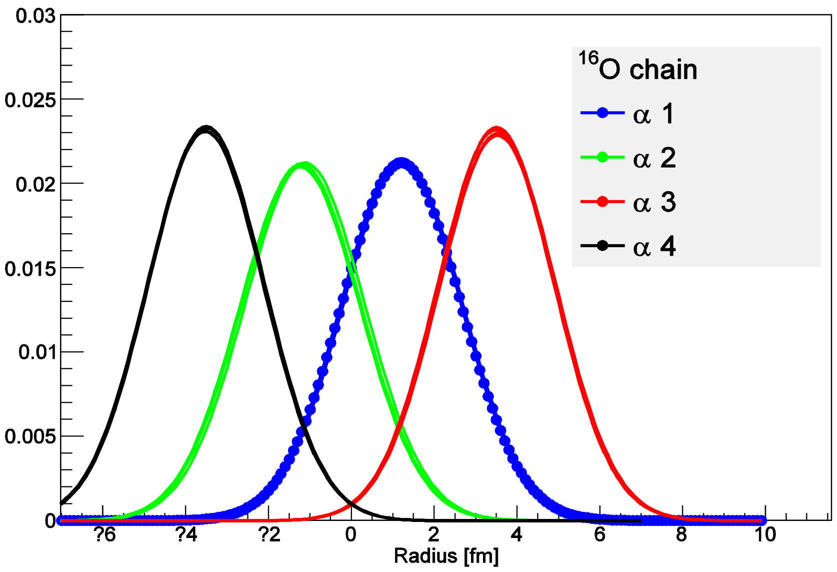

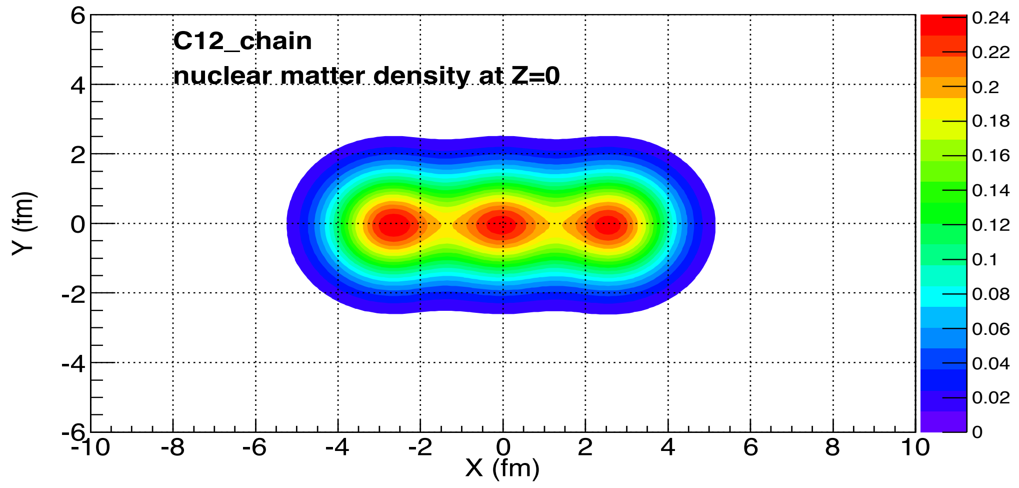

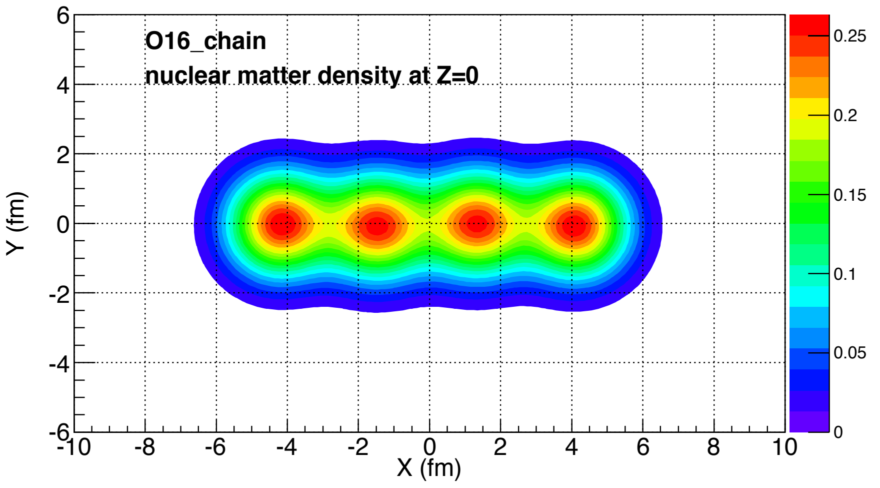

^{12}C

Long axis

Short axis

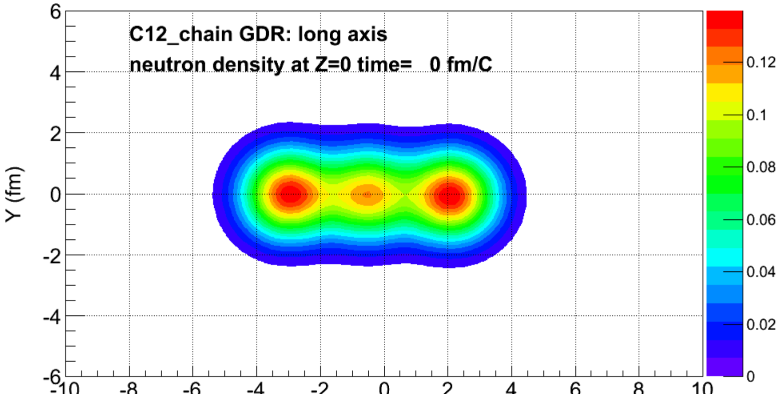

neutrons

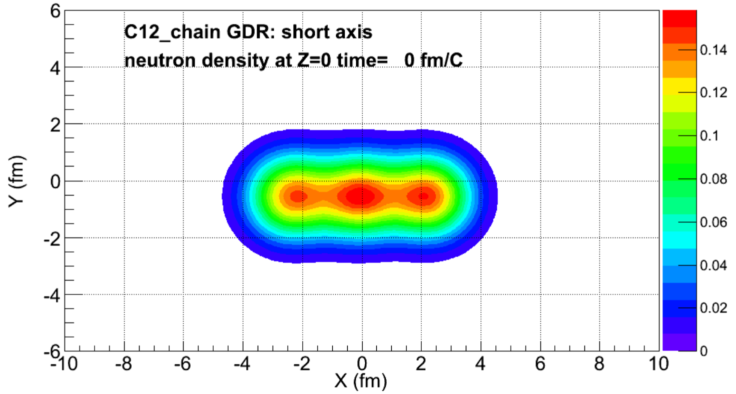

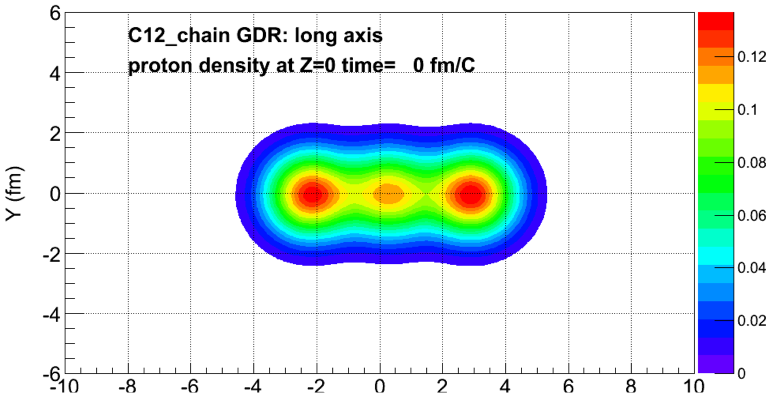

protons

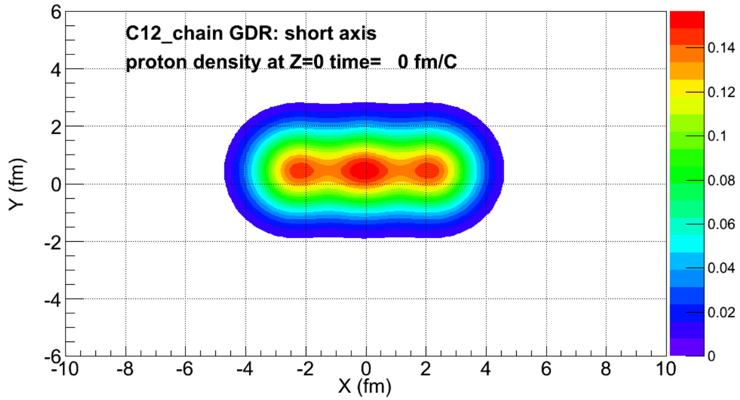

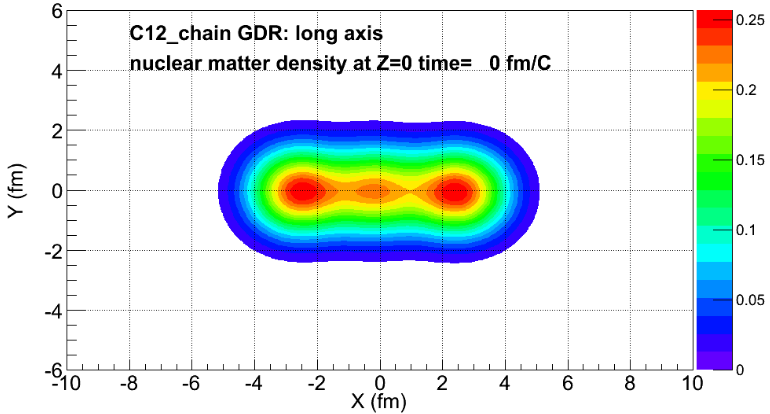

total

CM keeps zero

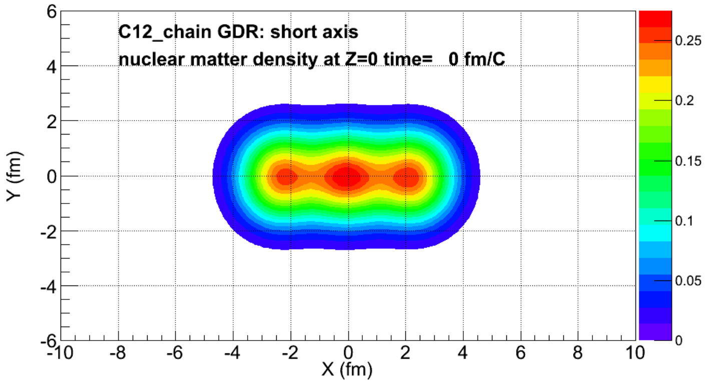

Long axis

^{16}O

Short axis

neutrons

protons

total

CM keeps zero

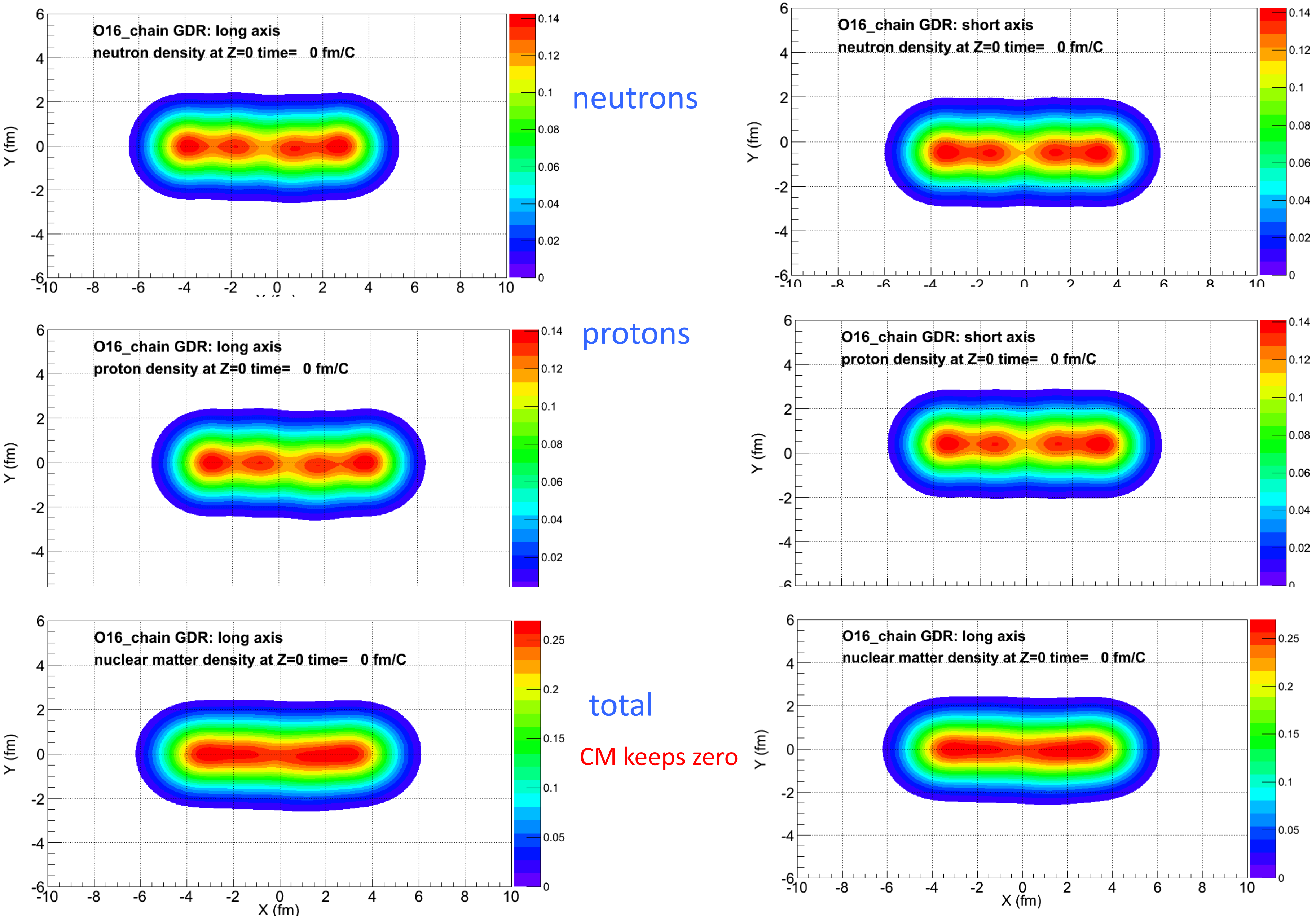

C12-triangle & 16O kite

neutrons

protons

total

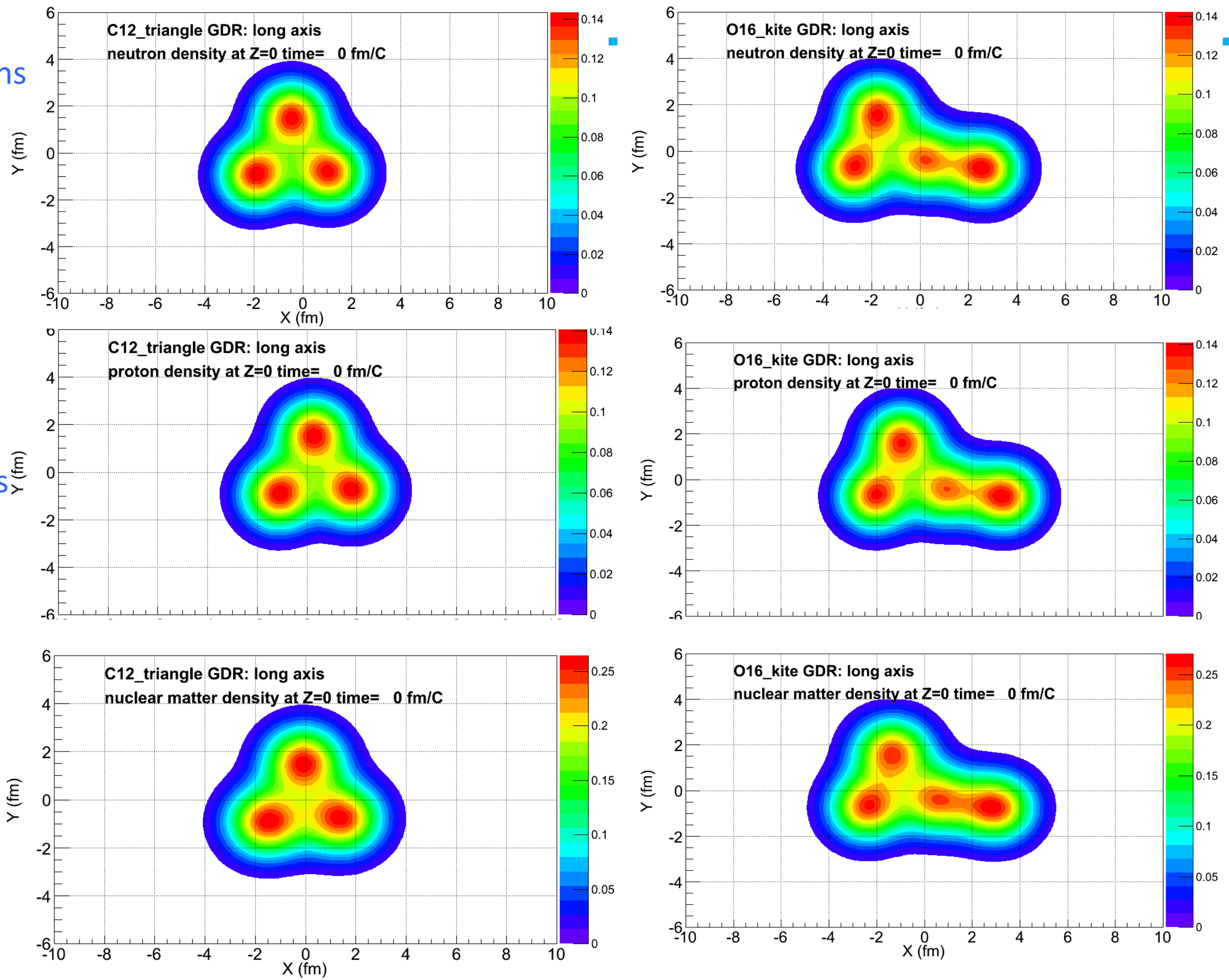

O16-tetrahadral & 16O square

neutrons

protons

total

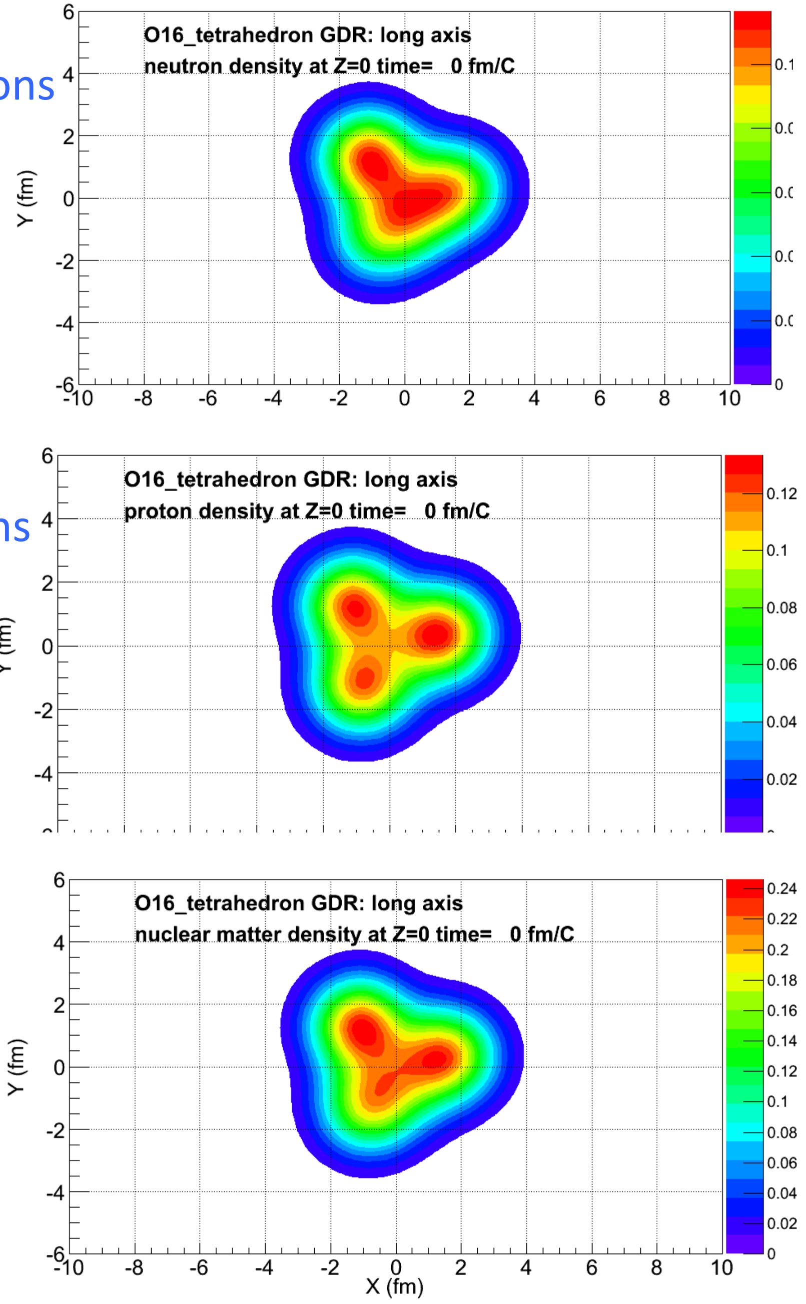

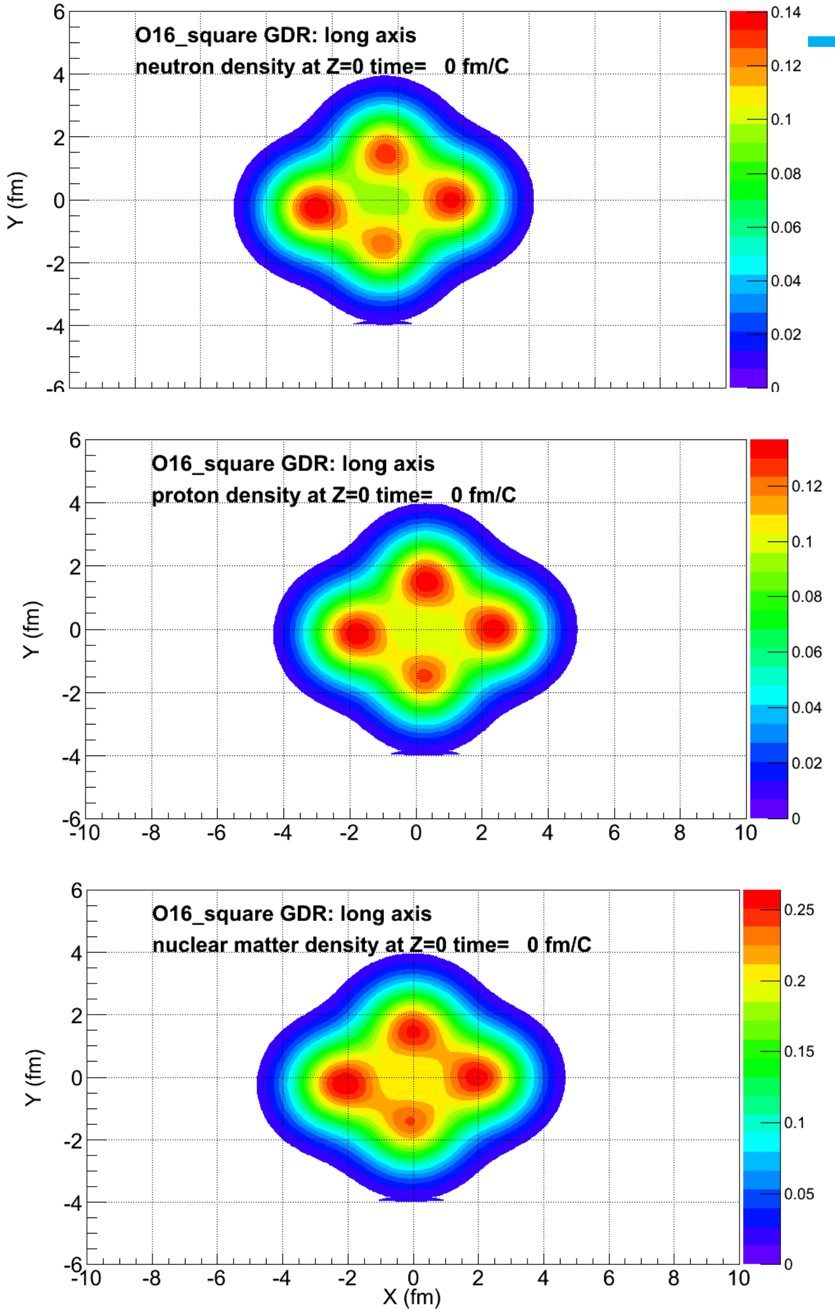

Results & discussion

-- GDR of ^{8}Be, ^{12}C & ^{16}O with different α configurations

EQMD calculation supports ^{16}O ground state with tetrahedron

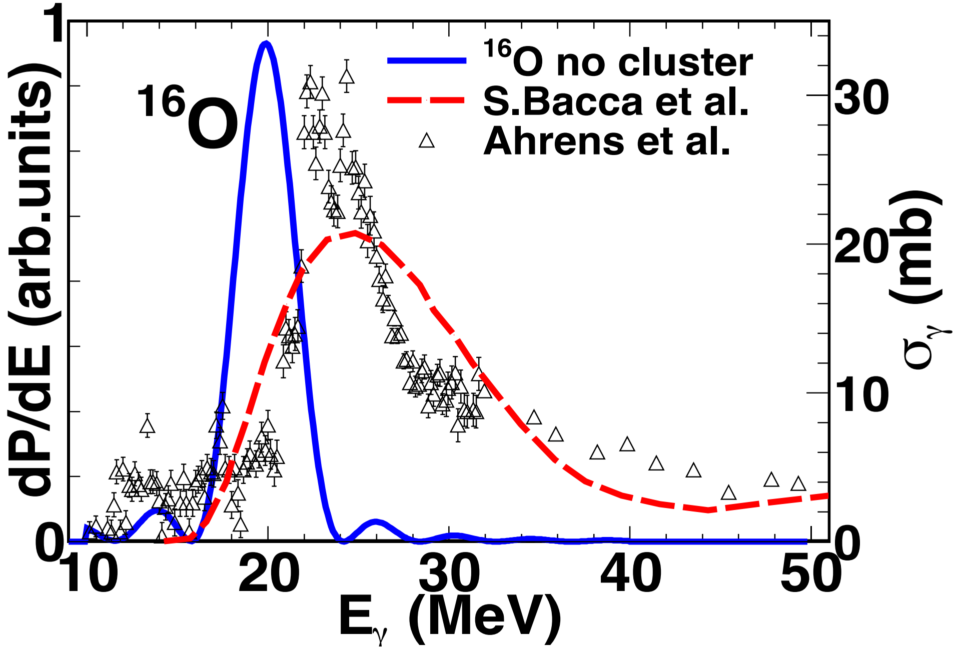

^{16}O ground state w/o alpha clusters

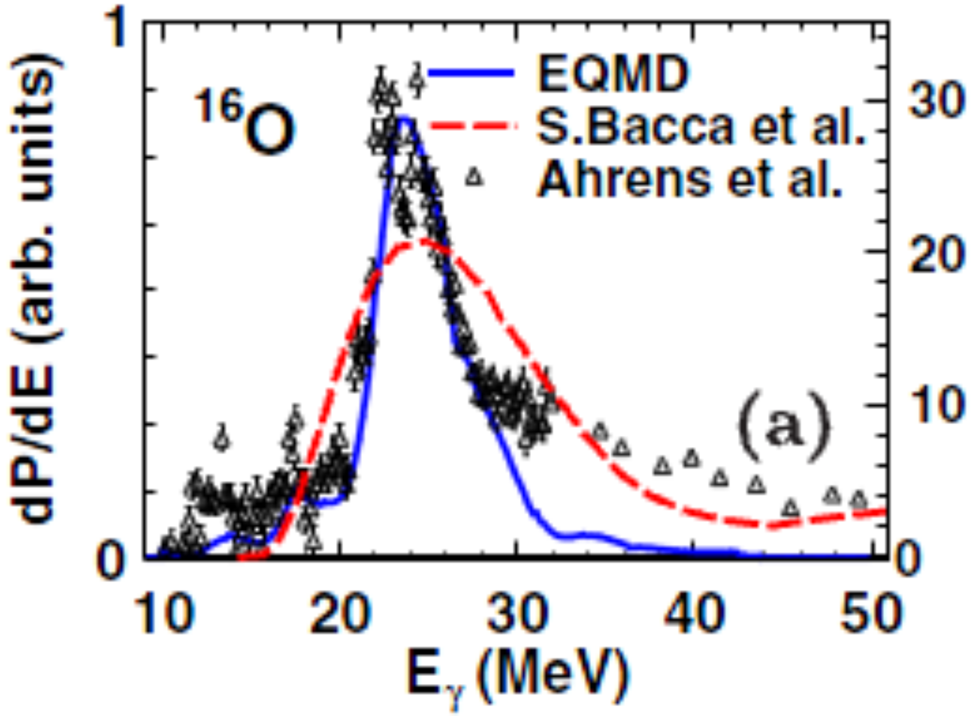

^{16}O ground state with tetrahedron structure

The data is from J. Ahrens, H. Borchert, K. H. Czock et al., Nucl. Phys. A251, 479 (1975).
The first principle calculation is from S. Bacca et al., Phys. Rev. Lett. 111, 122502 (2013).

◆ EQMD calculation indicates the ground of ^{12}C is a multiconfiguration mixing of shell-model-like and cluster-like configurations, which is consistent with the prediction of AMD [Y. Kanada-En'yo, Phys. Rev. Lett 81, 5291 (1998)] and FMD [M. Chernykh et al., Phys. Rev. Lett. 98, 032501 (2007)]

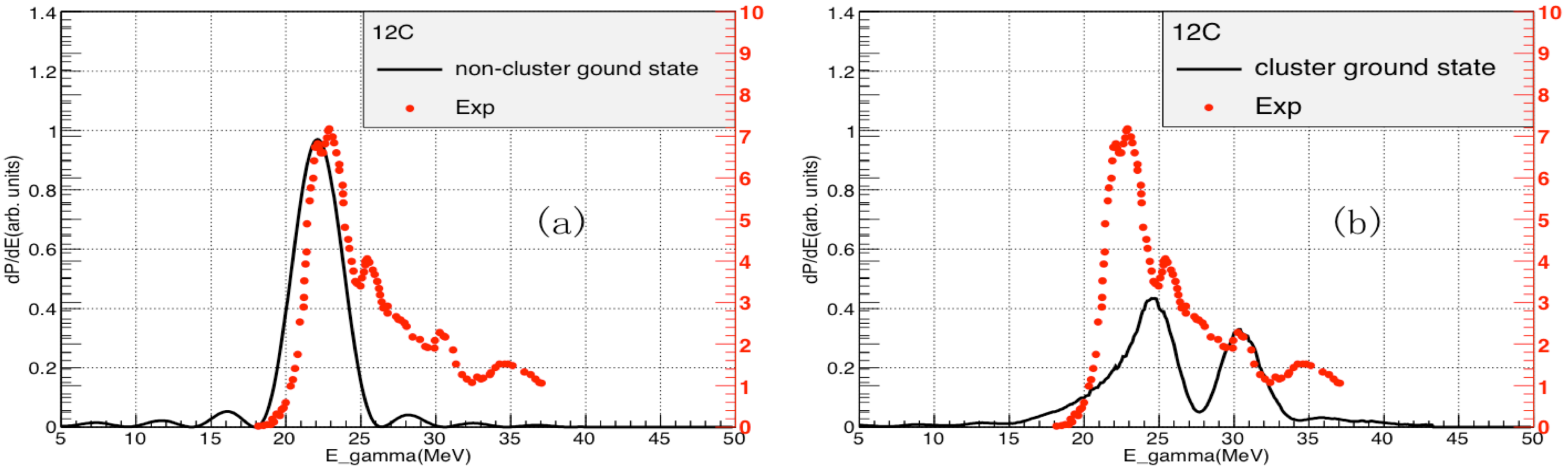

^{12}C GDR without (left panel) and with (right panel) cluster configuration with data.

The data is from J. Ahrens, H. Borchert, K. H. Czock et al., Nucl. Phys. A251, 479 (1975).

Giant Dipole Resonance as a Fingerprint of α Clustering Configurations in ^{12}C and ^{16}O

W. B. He (何万兵),[1,2] Y. G. Ma (马余刚),[1,3,*] X. G. Cao (曹喜光),[1,†] X. Z. Cai (蔡翔舟),[1] and G. Q. Zhang (张国强)[1]
[1]*Shanghai Institute of Applied Physics, Chinese Academy of Sciences, Shanghai 201800, China*
[2]*University of the Chinese Academy of Sciences, Beijing 100080, China*
[3]*Shanghai Tech University, Shanghai 200031, China*

(Received 6 May 2014; published 17 July 2014)

Correspondence between GDR and α cluster configurations

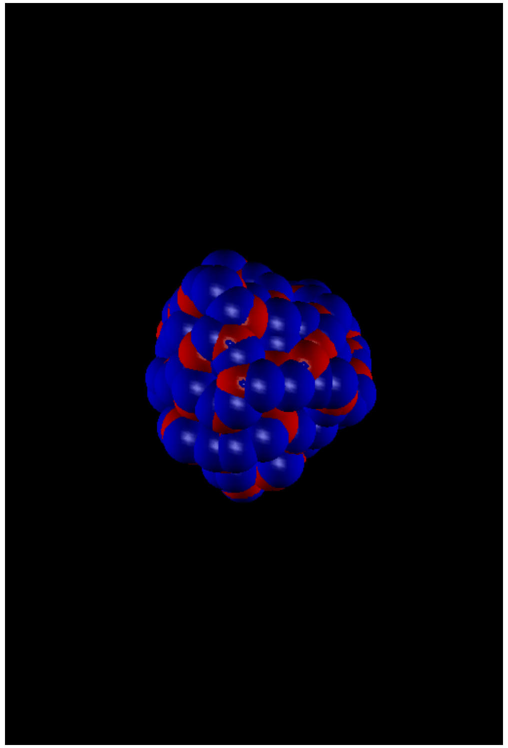

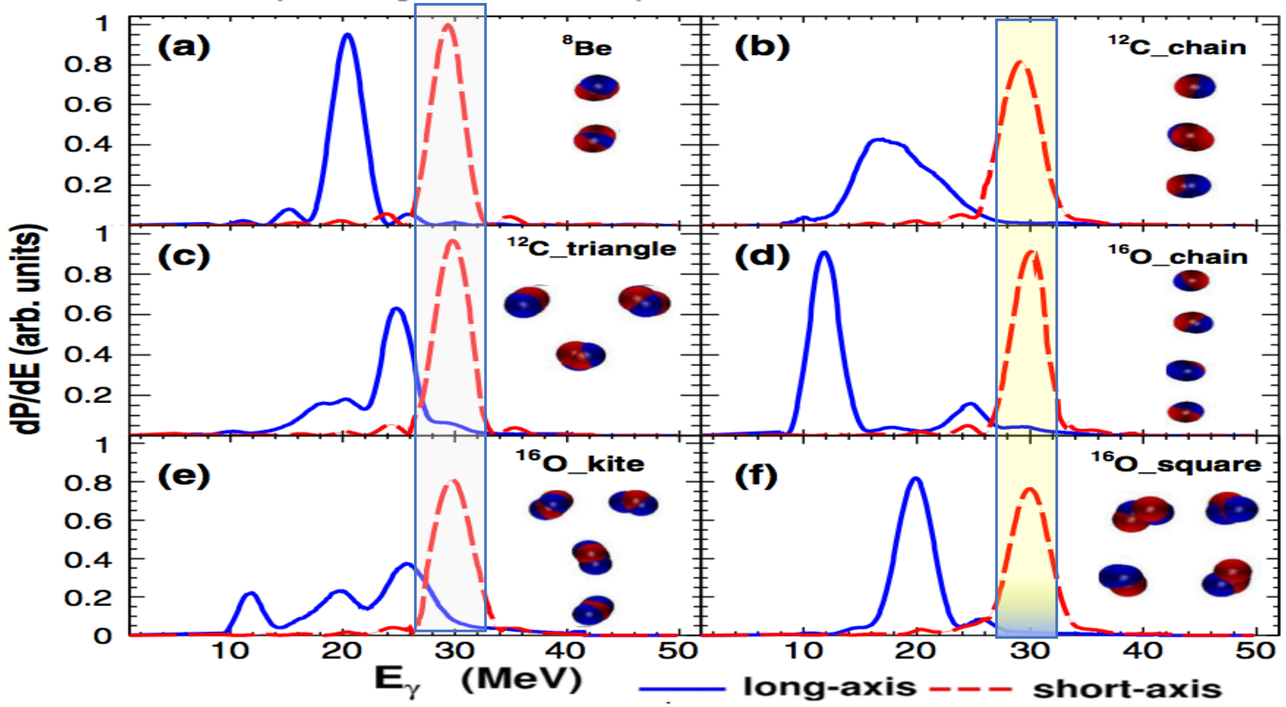

FIG. 2 (color online). ^{8}Be, ^{12}C, and ^{16}O GDR spectra with different cluster configurations. The corresponding α cluster configuration in the present EQMD model calculation is drawn in each panel, in which blue and red balls indicate protons and neutrons, respectively. The dynamical dipole evolution of ^{8}Be, ^{12}C, and ^{16}O with linear-chain configurations are shown in [51].

Photo-excitation of 6Li. Second bump at ∼ 33 MeV is GDR of alpha particle.
About 7 MeV higher than in free space but very similar shape.

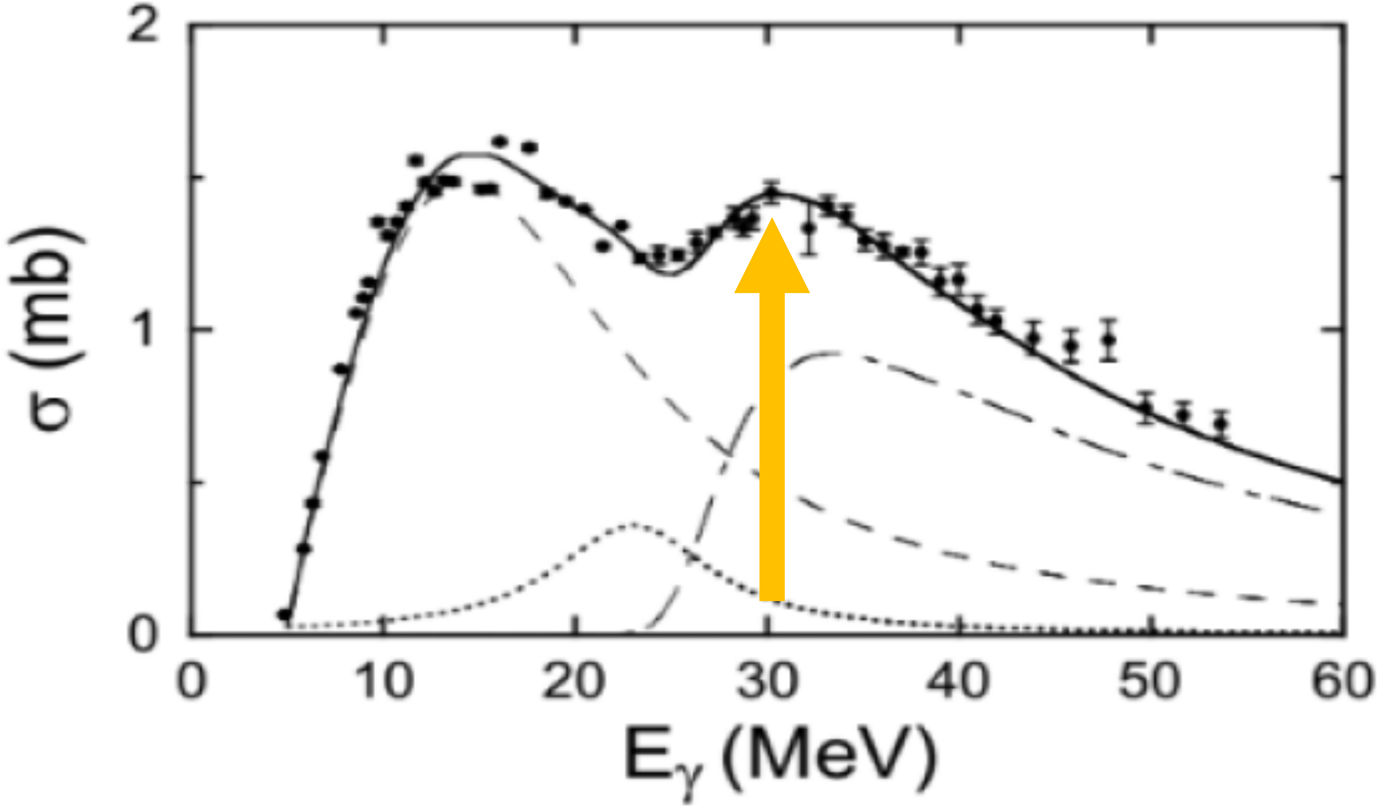

FIG. 11. Fitting of the present data assuming the LEDR at $E_r =$ 12 MeV and $\Gamma = 21$ MeV (dashed curve) and the HEDR at $E_r =$ 33 MeV and $\Gamma = 30$ MeV (dash-dotted curve). A small resonance was introduced at $E_r = 23$ MeV and $\Gamma = 10$ MeV (dotted curve). The solid curve is the fitting result. See text.

- **Alpha-clustering effect on nucleon correlation by Photonuclear reaction**

PHYSICAL REVIEW C **95**, 034606 (2017)

Photonuclear reaction as a probe for α-clustering nuclei in the quasi-deuteron region

B. S. Huang (黄勃松),[1,2] Y. G. Ma (马余刚),[1,3,*] and W. B. He (何万兵)[1,4]

If photons hit alpha cluster, what happens?

We consider: $^{12}C(\gamma,np)^{10}B$

(a) chain **(b) triangle** **(c) spherical**

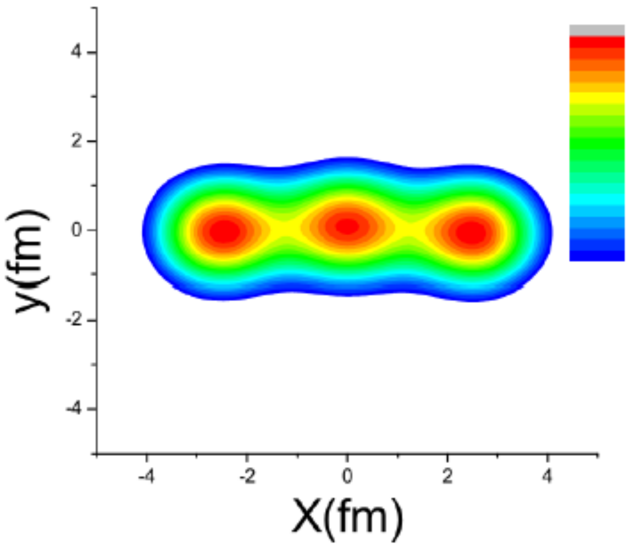

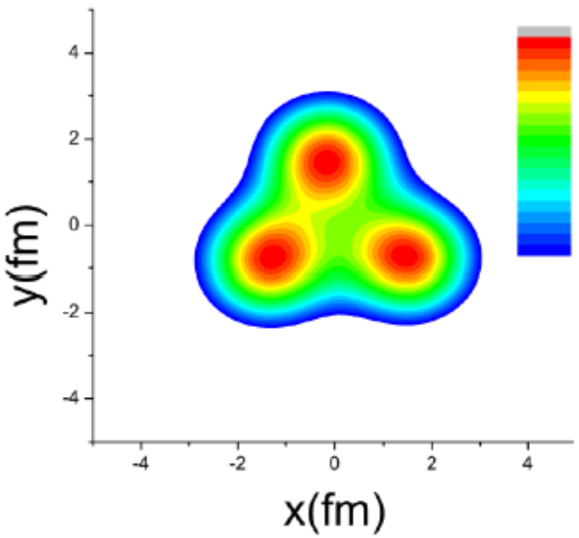

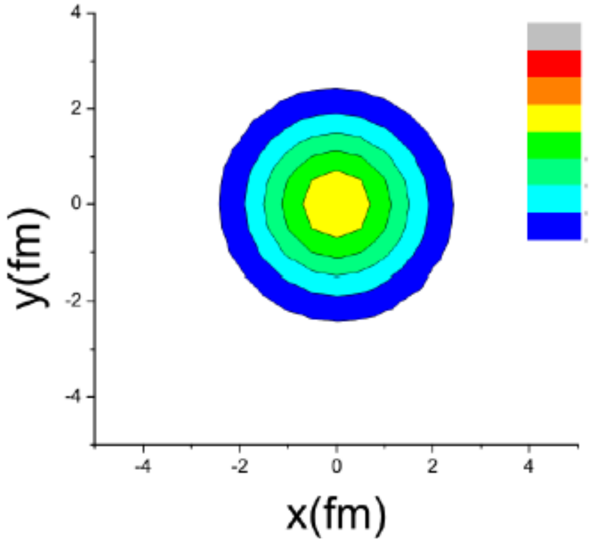

Quasi-deuteron: ~70-140MeV

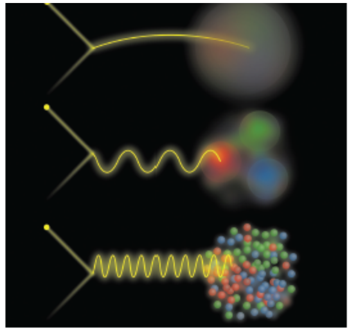

TABLE I: RMS radius and binding energy of different configurations of 12C and the ground state data.

Configuration	r_{RMS} (fm)	E_{bind} (MeV/nucleon)
Chain	2.71	7.17
Triangle	2.35	7.12
Sphere	2.23	7.60
Exp. Data	2.47	7.68

np emission from Tetrahedron 16O

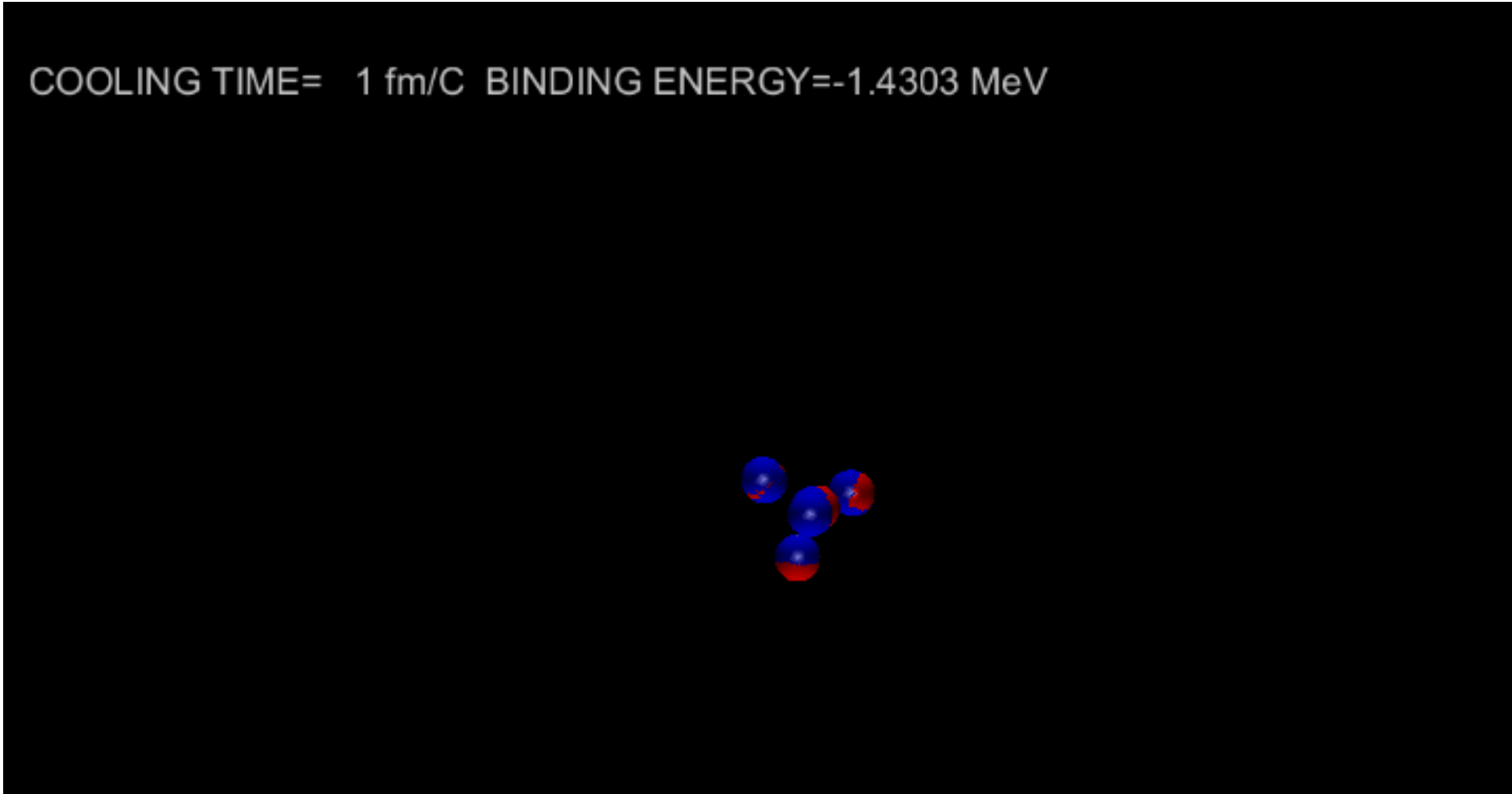

Chain 16O

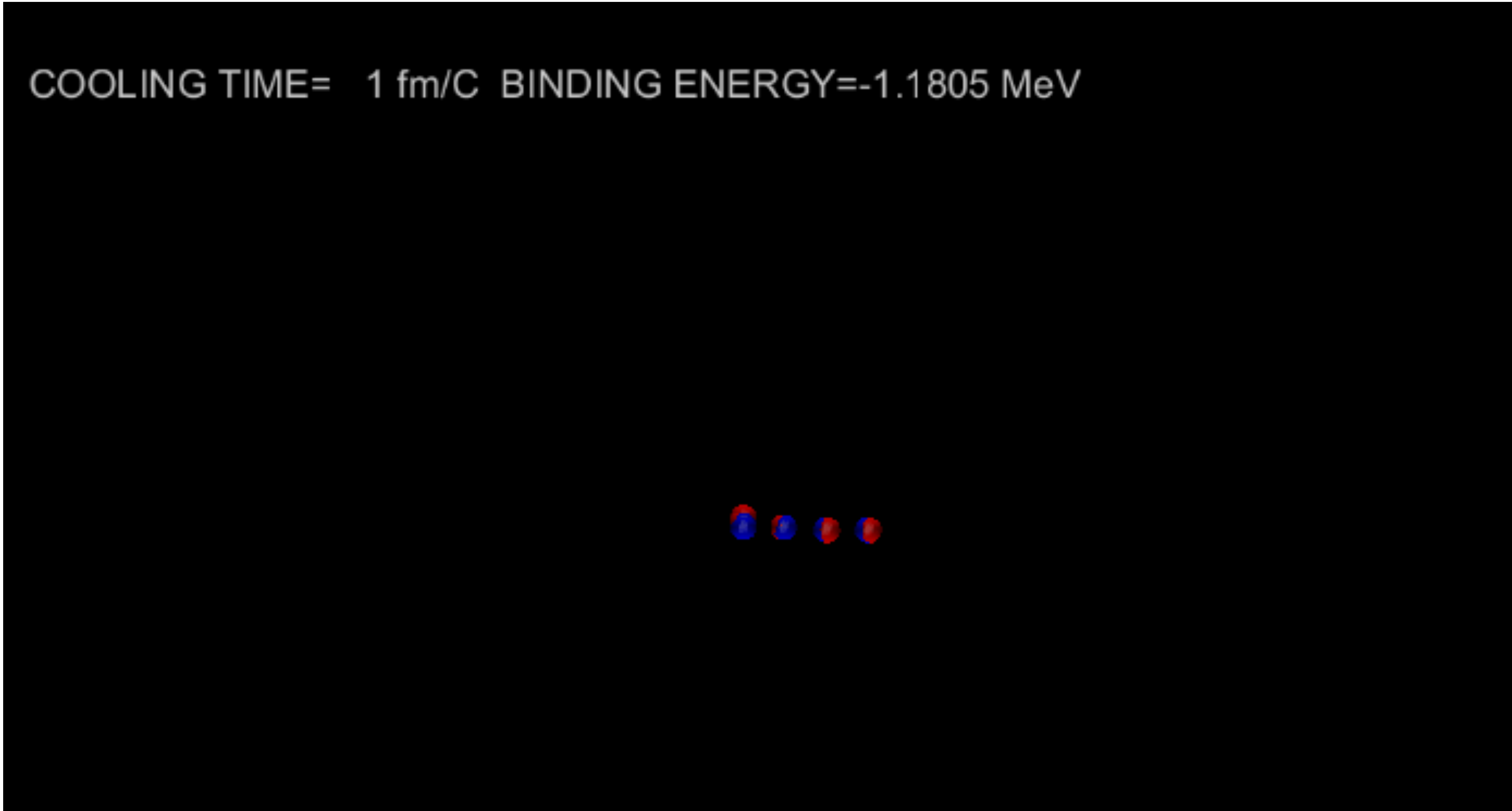

Square 16O

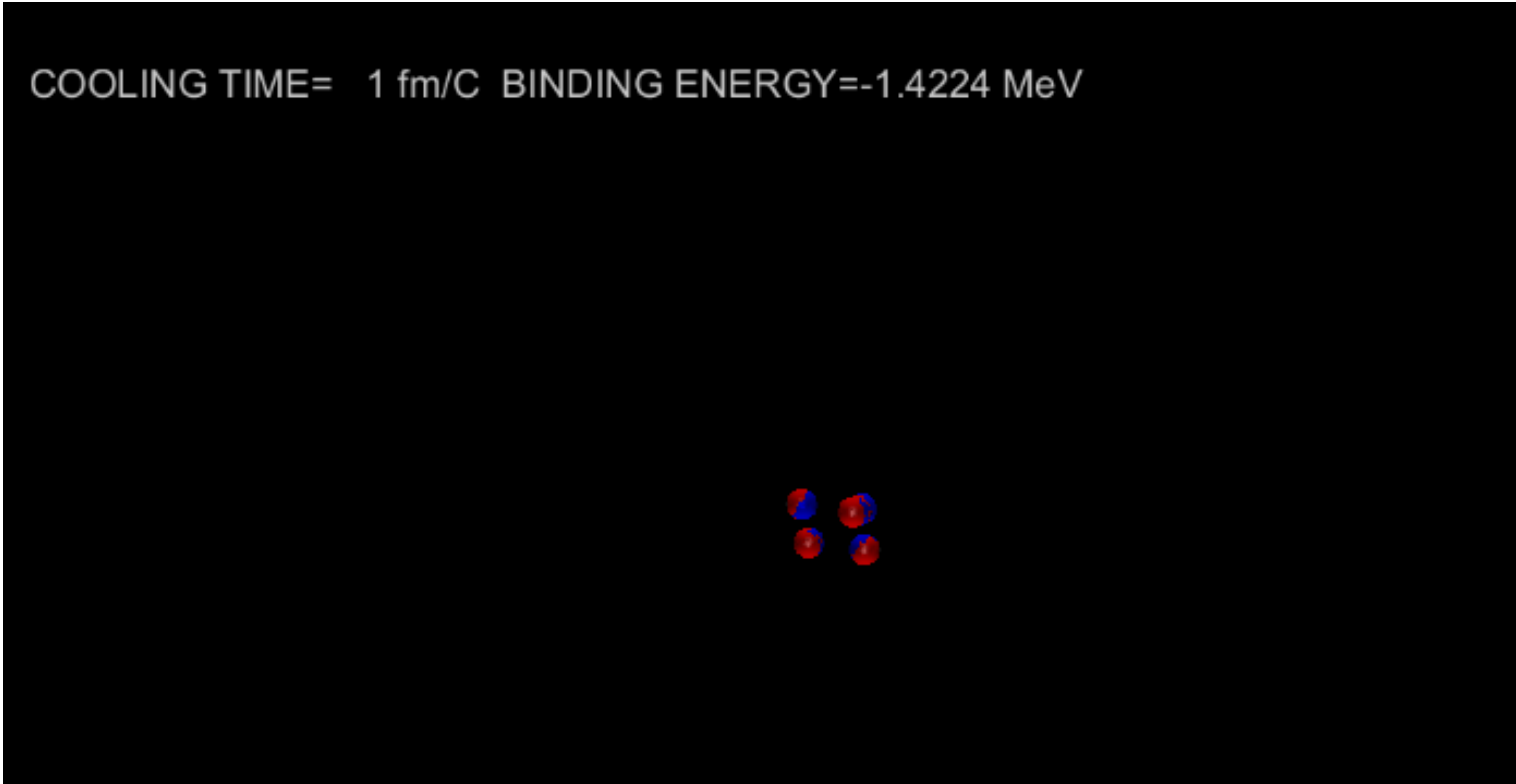

Kite 16O

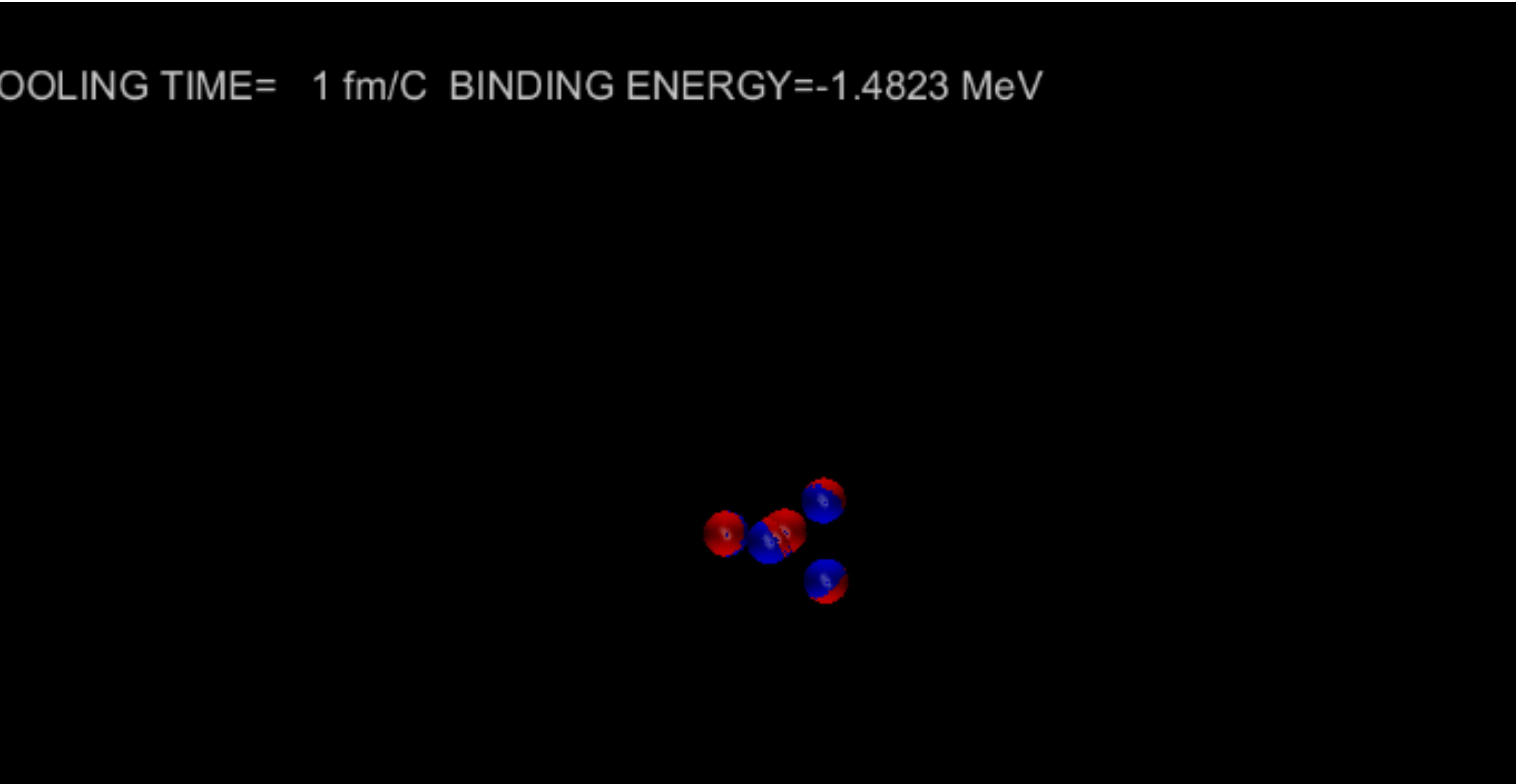

Effects on momentum correlation function @ g(A) 100MeV

质子-质子关联

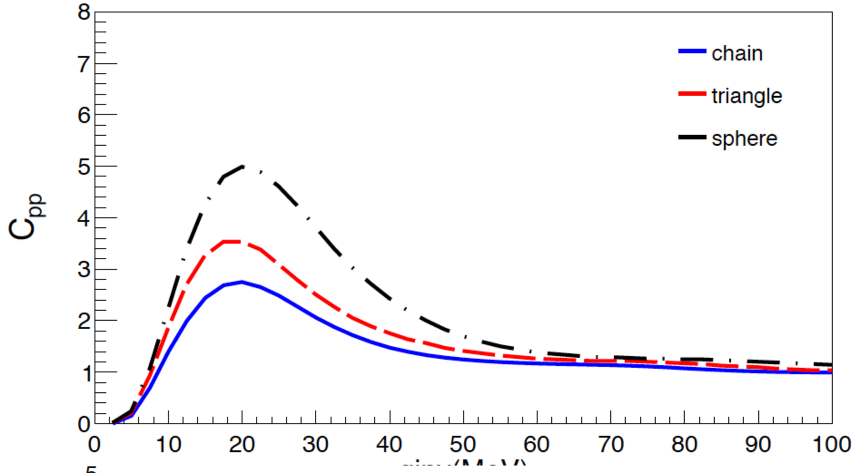

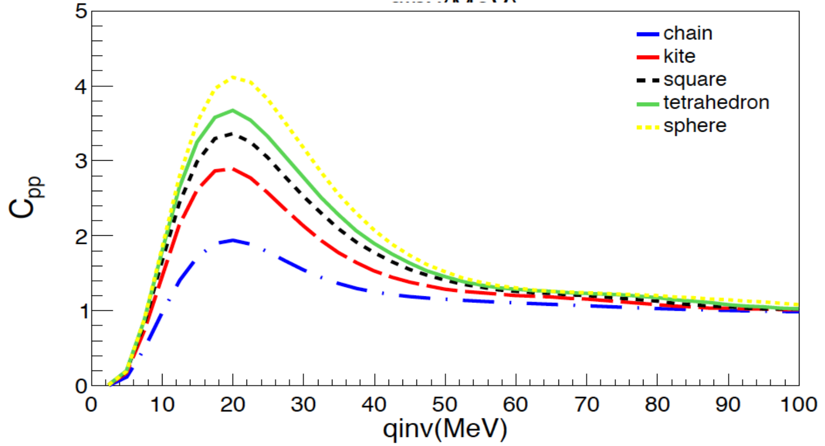

中子-质子关联

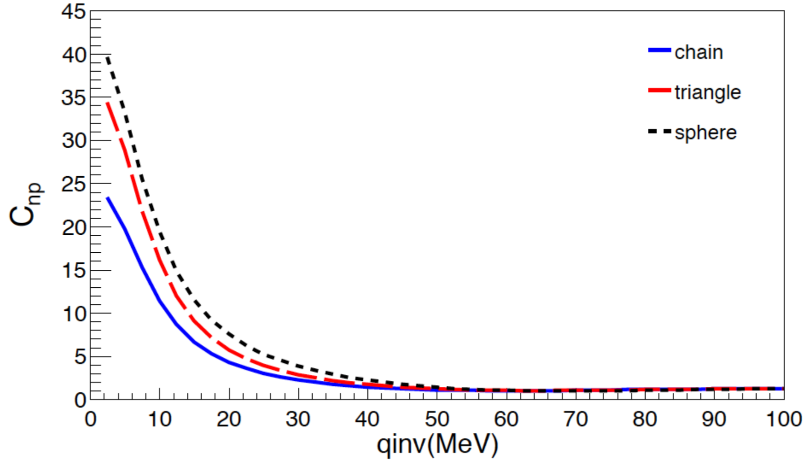

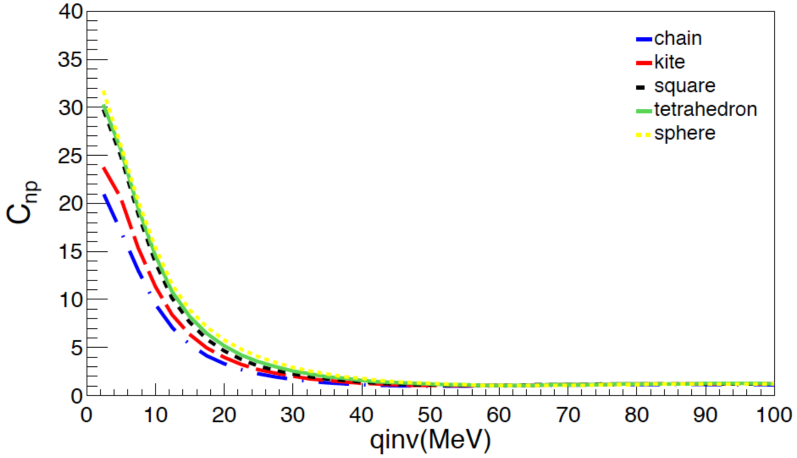

configuration	R_{RMS}	E_{bind}
chain	3.782	7.26
kite	3.254	7.22
square	2.908	7.29
Tetrahedron	2.761	7.20

Np,pp的动量关联函数的强度与alpha-clustering构型依赖敏感

B.S. Huang, YGM et al.

Source size

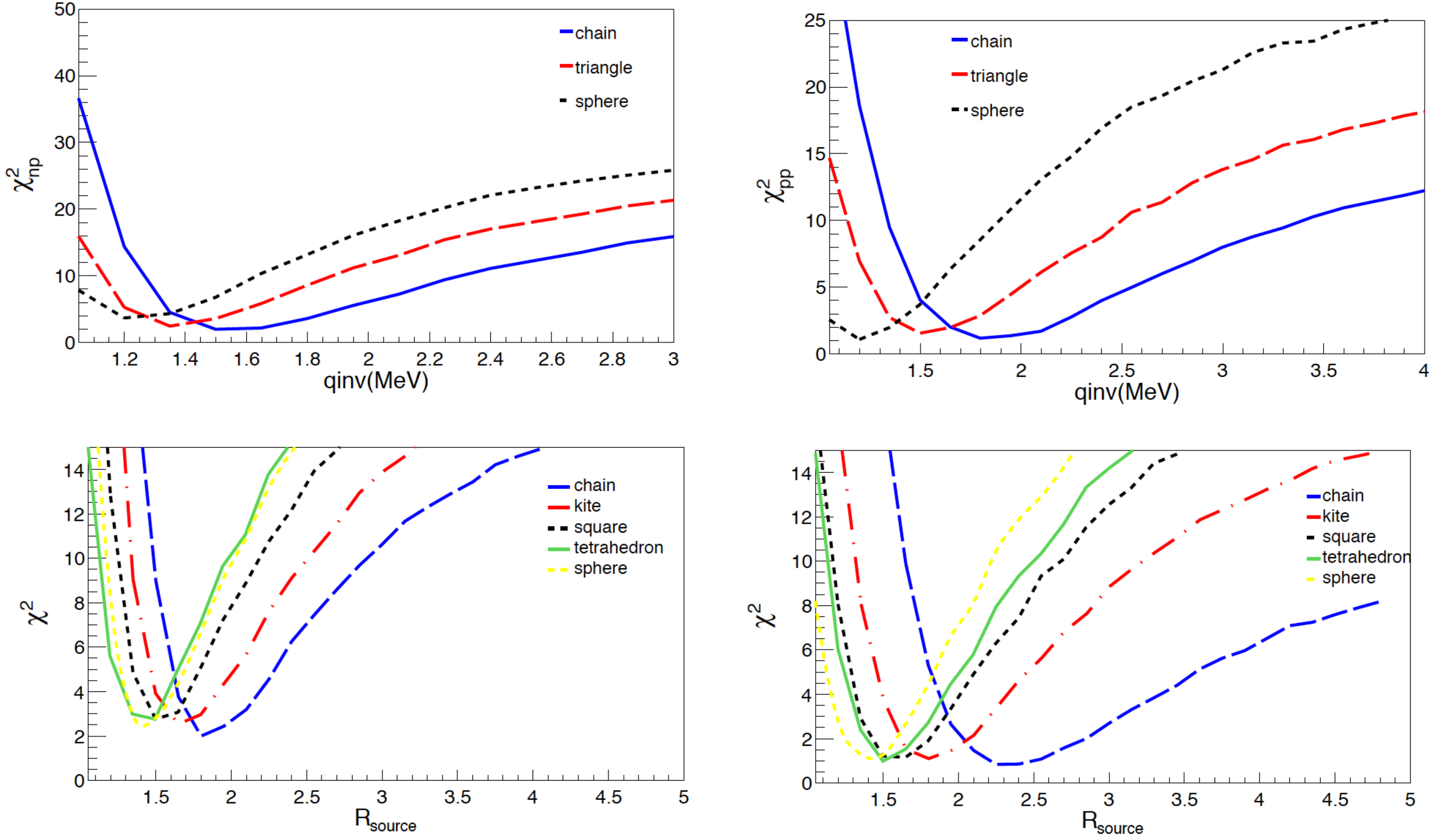

从关联函数提取出发射源的尺寸，其排序与构型的大小自洽

□Alpha-clustering effect on flows in $^{12}C+^{197}Au$@ 10GeV & 200A GeV

□S. Zhang, YGM et al., PHYSICAL REVIEW C 95, 064904 (2017)

alpha集团效应对集体流的影响@低能:C+C,O+O

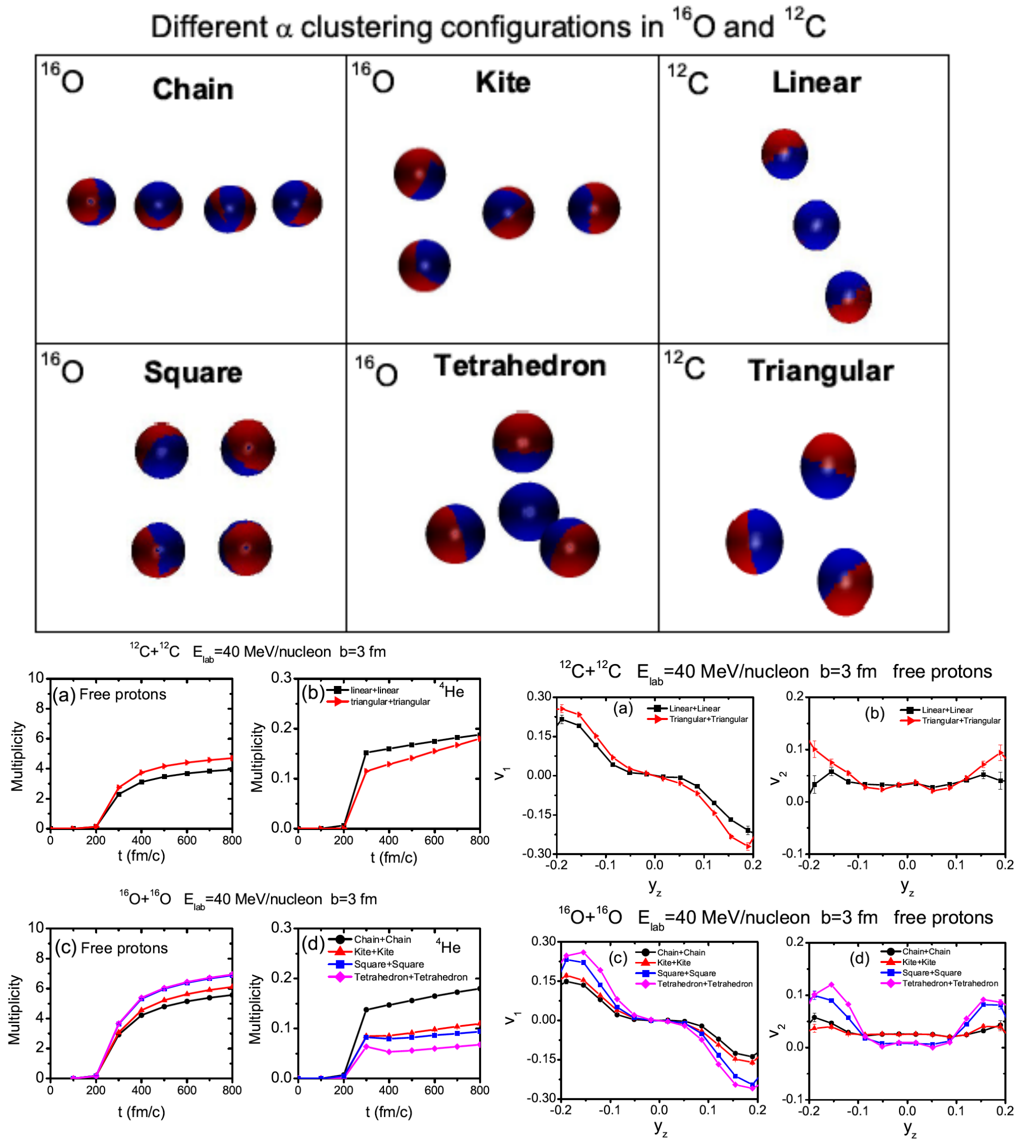

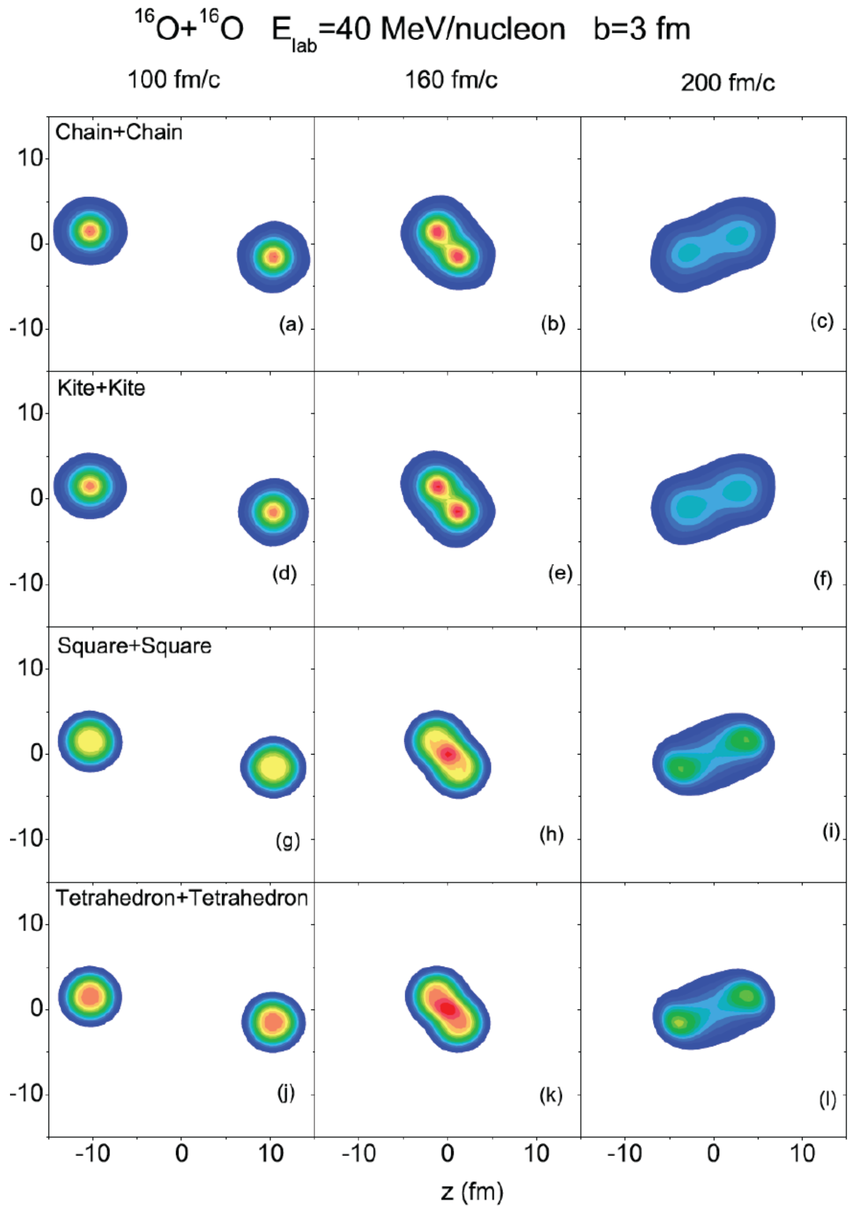

C.C. Guo, YGM et al., PRC 99, 044607 (2019)

AMPT model {Melting version of AMPT}

—————— A Multi-Phase Transport model, Ko & Lin et al.

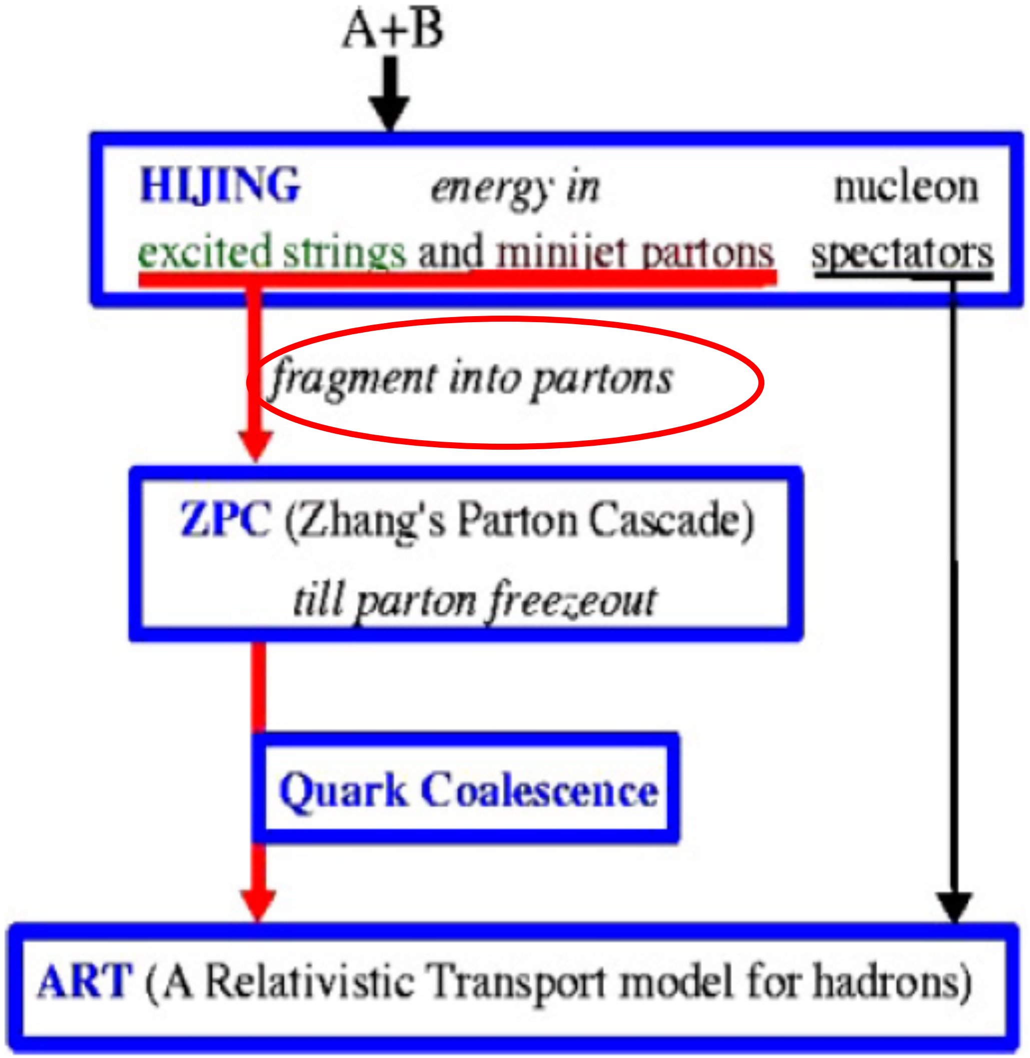

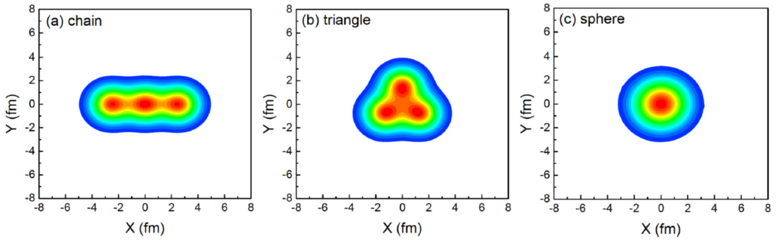

EQMD distri. → AMPT distri.

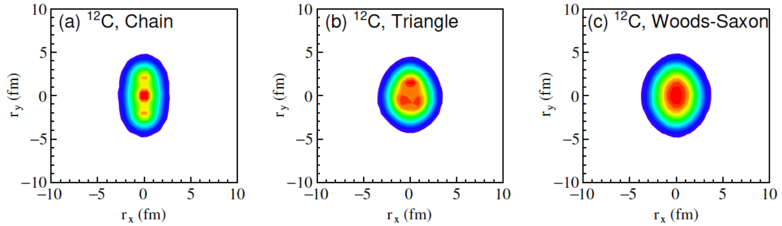

FIG. 1: Participant distributions of ^{12}C + ^{197}Au central collisions with different initial configurations of ^{12}C.

The distribution of the radial center of the α clusters in ^{12}C is assumed to be a Gaussian function, $e^{-0.5(\frac{r-r_c}{\sigma_{r_c}})^2}$, here r_c is the average radial center of an α cluster and σ_{r_c} is the width of the distribution. And the nucleon inside each α cluster will be given by Woods-Saxon distribution. The parameters of r_c and σ_{r_c} can be obtained from the EQMD calculation [41–43]. For the triangle structure, $r_c = 1.8$ fm and $\sigma_{r_c} = 0.1$ fm. For the chain structure, $r_c = 2.5$ fm, $\sigma_{r_c} = 0.1$ fm for two α clusters, and the other one will be at the center in ^{12}C.

→ **Hadron rescattering**

Coordinate distribution

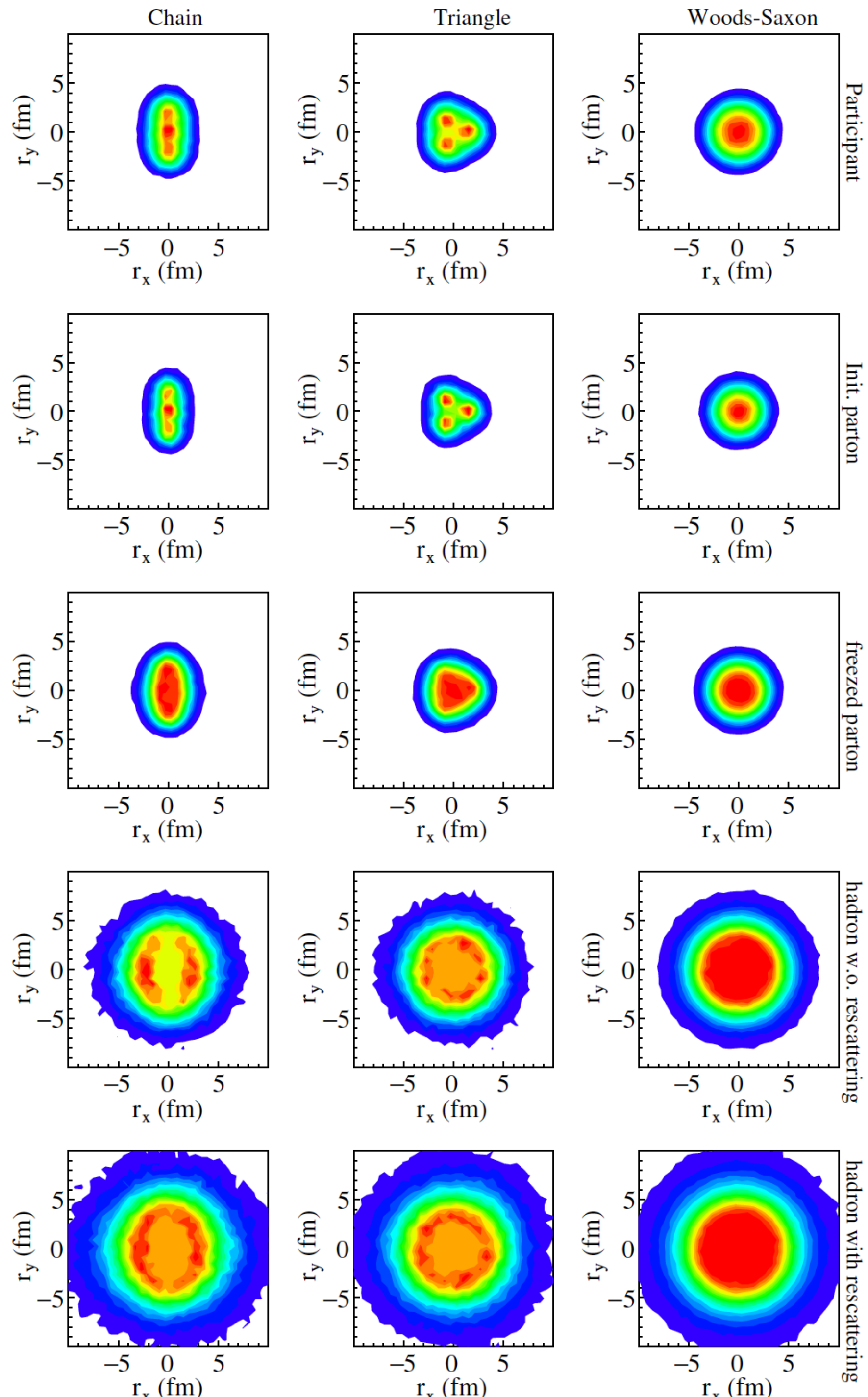

Participant

Initial parton

Freeze-out partons

Hadron w/o rescattering

Hadron w/ rescatering

Px-py distribution

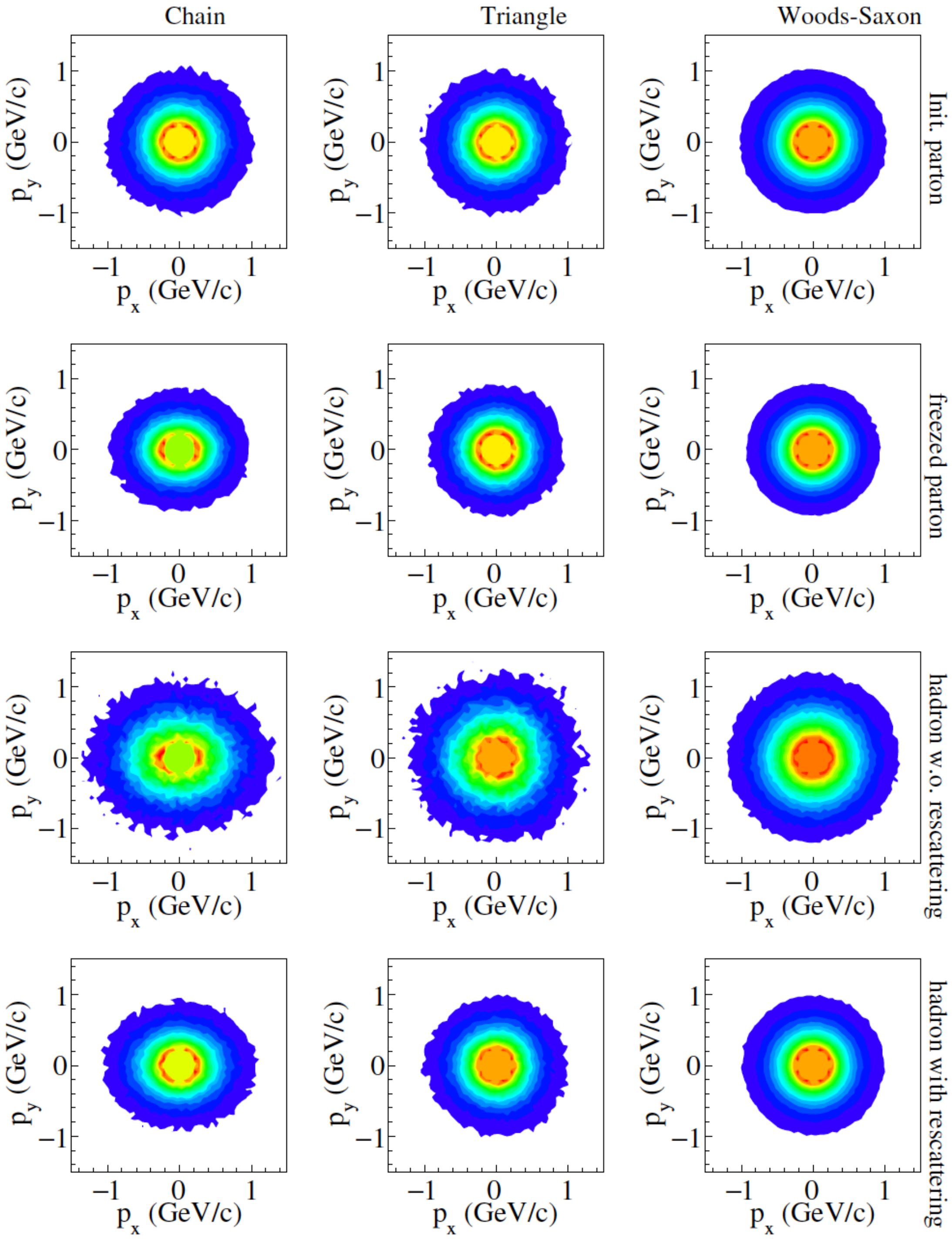

Initial parton

Freeze-out partons

Hadron w/o rescattering

Hadron w/ rescatering

Elliptic flow@12C+Au

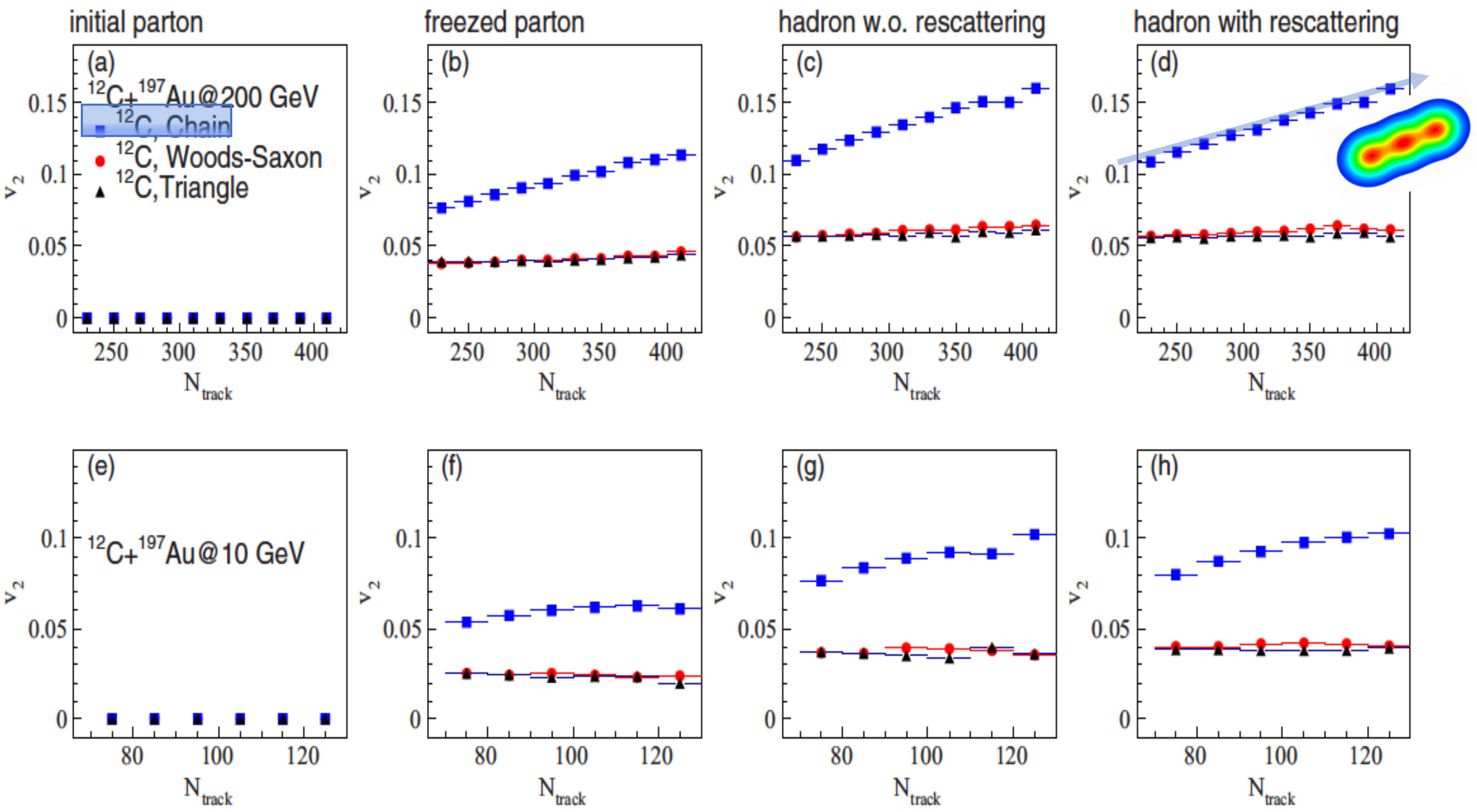

Elliptic flow (v2) is significant for **linear 3-alpha 12C structure**

Triangular flow @12C+Au

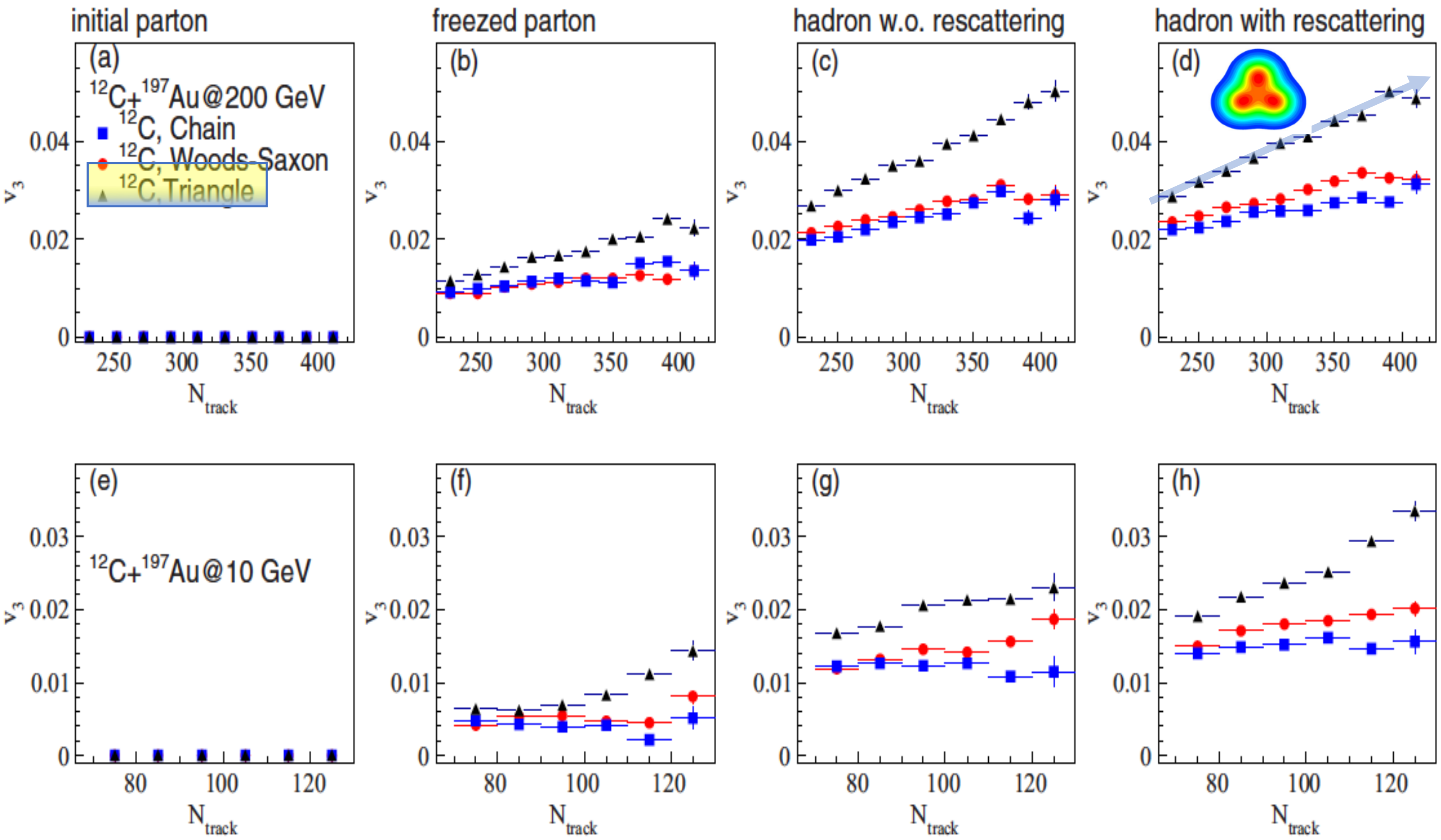

Triangular flow (v3) is significant for triangle 3-alpha 12C structure

A sensitive probe to structure: e3/e2 & v3/v2

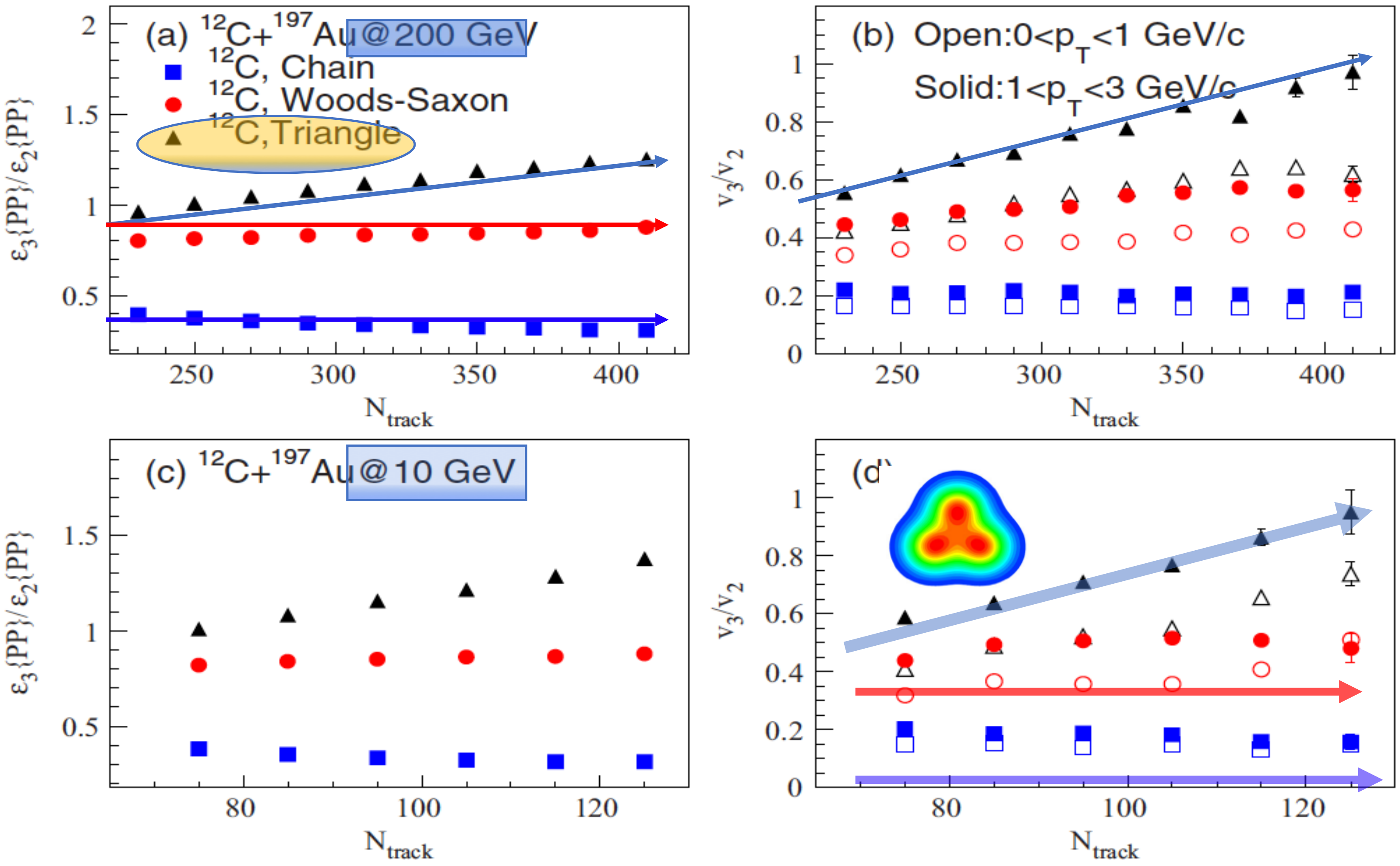

V3/v2 increases with the multiplicity → triangle 3-alpha 12C

S. Zhang, YGM et al., Phys. Rev. C 95, 064904 (2017); Eur. Phys. J. A (2018) 54

α-clustering effect on eccentricity

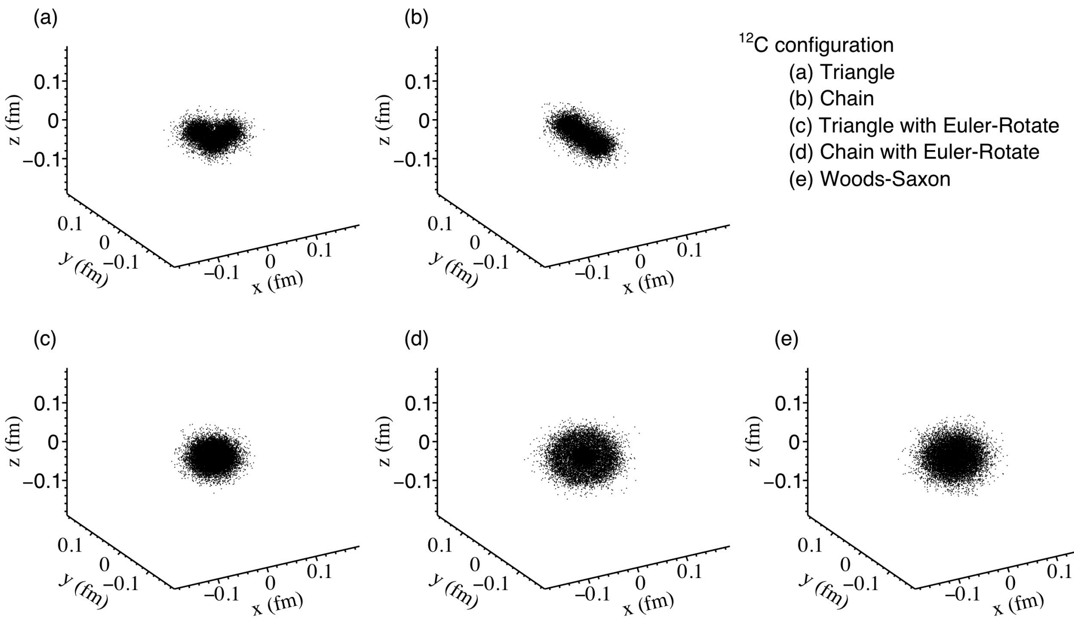

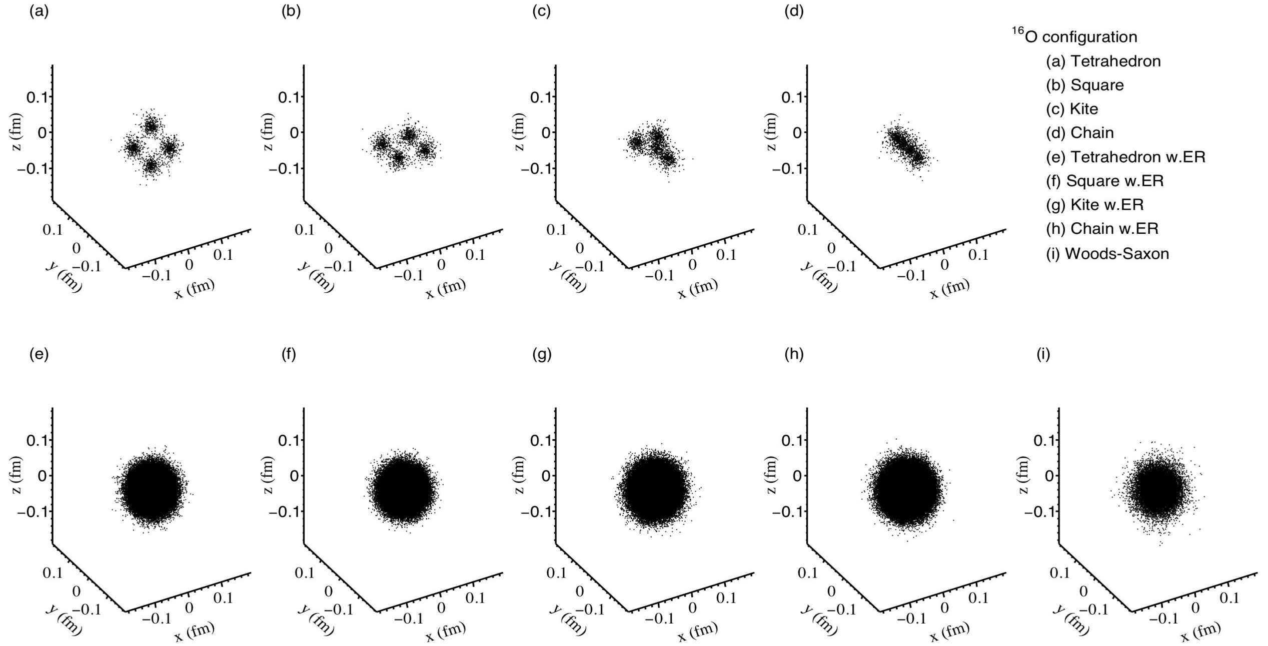

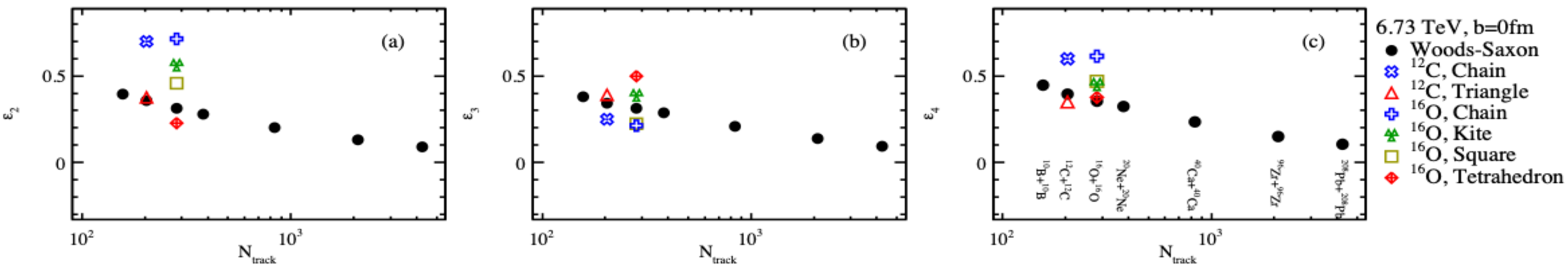

✓Sensitive to fluctuation

✓Also to intrinsic geometry (α-cluster structure)

α-clustering effect on collective flow

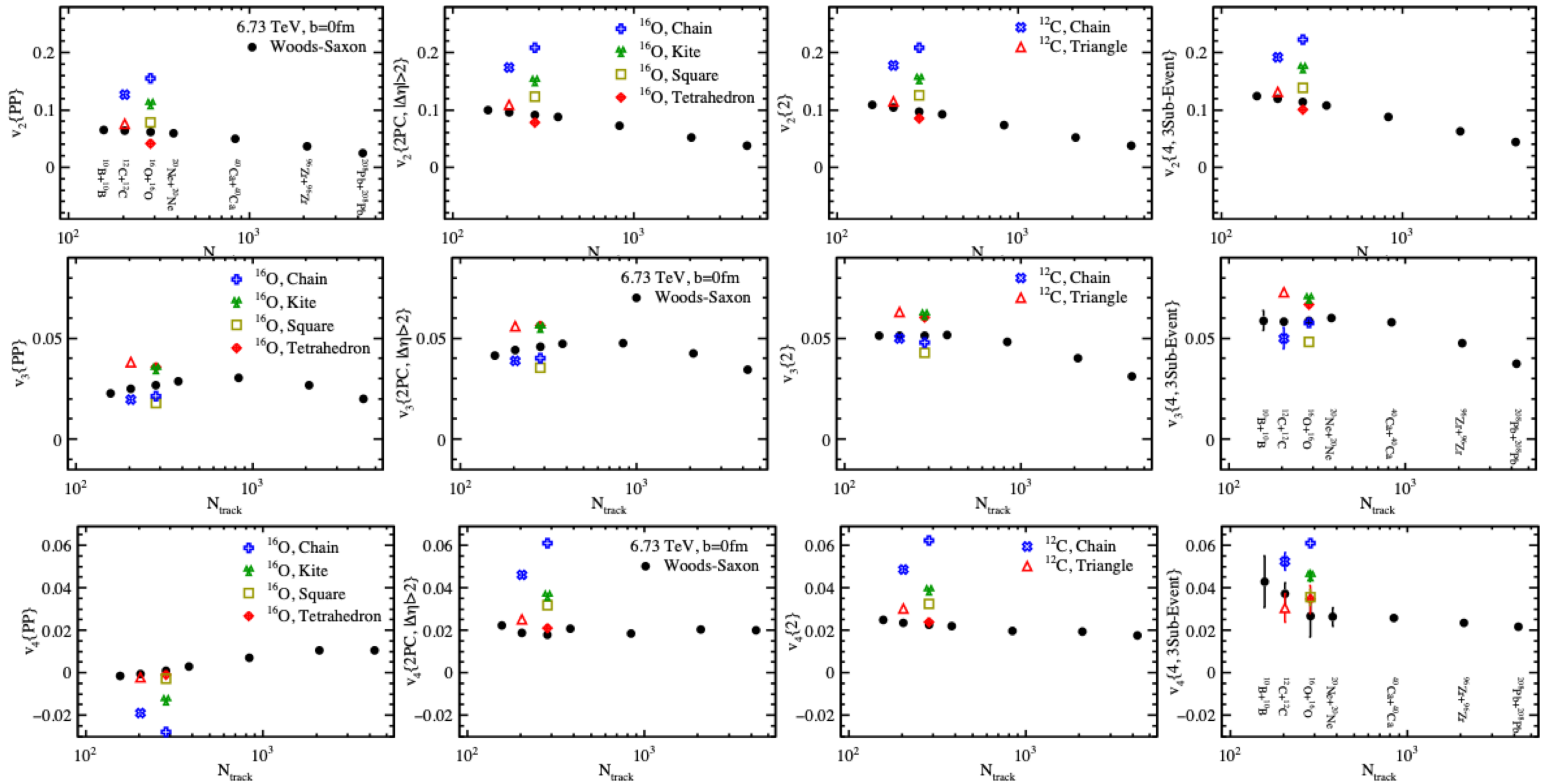

✓ Smoothly changing with increasing size of collision system (most central, Woods-Saxon distribution)

✓ Deviation from Woods-Saxon case for α-clustered initial system

- Alpha-clustering effect on HBT radii in head-on $^{12}C+^{197}Au$@ 200A GeV

Formulation of HBT correlation

$$C(\vec{q},\vec{K}) = 1 \pm \left| \frac{\int d^4x e^{i\vec{q}\cdot(\vec{x}-\vec{\beta}t)} S(x,K)}{\int d^4x S(x,K)} \right|^2, \qquad (1)$$

$$C(\vec{q},\vec{K}) = 1 + \lambda(\vec{K})\exp(-\sum_{i,j=o,s,l} R_{ij}^2(\vec{K})q_i q_j). \qquad (2)$$

$$R_s^2(K_\perp,\Phi,Y) = \langle\tilde{x}^2\rangle \sin^2\Phi + \langle\tilde{y}^2\rangle \cos^2\Phi - \langle\tilde{x}\tilde{y}\rangle \sin 2\Phi, \qquad (3)$$

$$\begin{aligned} R_o^2(K_\perp,\Phi,Y) = &\langle\tilde{x}^2\rangle \cos^2\Phi + \langle\tilde{y}^2\rangle \sin^2\Phi + \beta_\perp^2\langle\tilde{t}^2\rangle \\ &- 2\beta_\perp\langle\tilde{t}\tilde{x}\rangle\cos\Phi - 2\beta_\perp\langle\tilde{t}\tilde{y}\rangle\sin\Phi \qquad (4) \\ &+ \langle\tilde{x}\tilde{y}\rangle \sin 2\Phi, \end{aligned}$$

$$R_l^2(K_\perp,\Phi,Y) = \langle(\tilde{z}-\beta_l\tilde{t})^2\rangle, \qquad (5)$$

where $\tilde{x}_\mu = x_\mu - \langle x_\mu\rangle$, $\beta_\perp = p_T/E$, and $\beta_l = p_z/E$.

$$\Phi' = \Phi - \Psi_{EP}, \qquad (6)$$

$$\Psi_{EP} = \frac{\mathrm{atan2}(\langle r^2\sin(2\phi_{\mathrm{part}})\rangle, \langle r^2\cos(2\phi_{\mathrm{part}})\rangle) + \pi}{2}, \qquad (7)$$

$$dY/d(\Phi-\Psi_{EP}) = a_0 + a_1 cos[2(\Phi-\Psi_{EP})], \qquad (8)$$

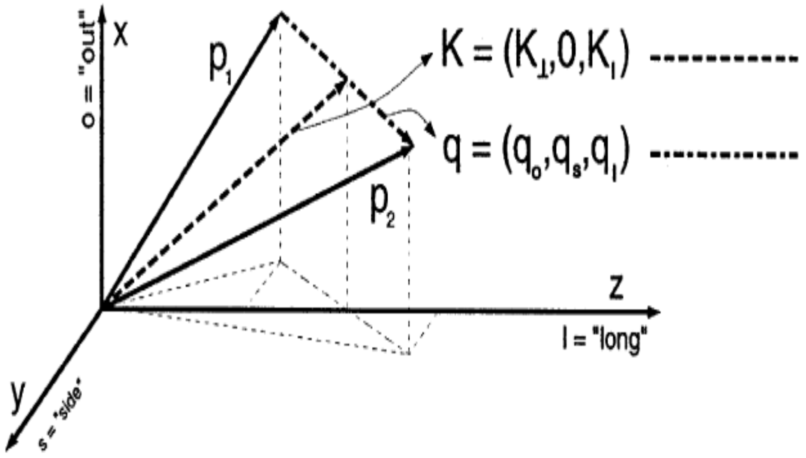

Fig. 3.1. The osl coordinate system takes the longitudinal (long) direction along the beam axis. In the transverse plane, the “out” direction is chosen parallel to the transverse component of the pair momentum $\boldsymbol{K}_\perp$, the remaining Cartesian component denotes the “side” direction.

Azimuthal dependent HBT radii (1)

Hadron rescattering time (AFTER hadronization)

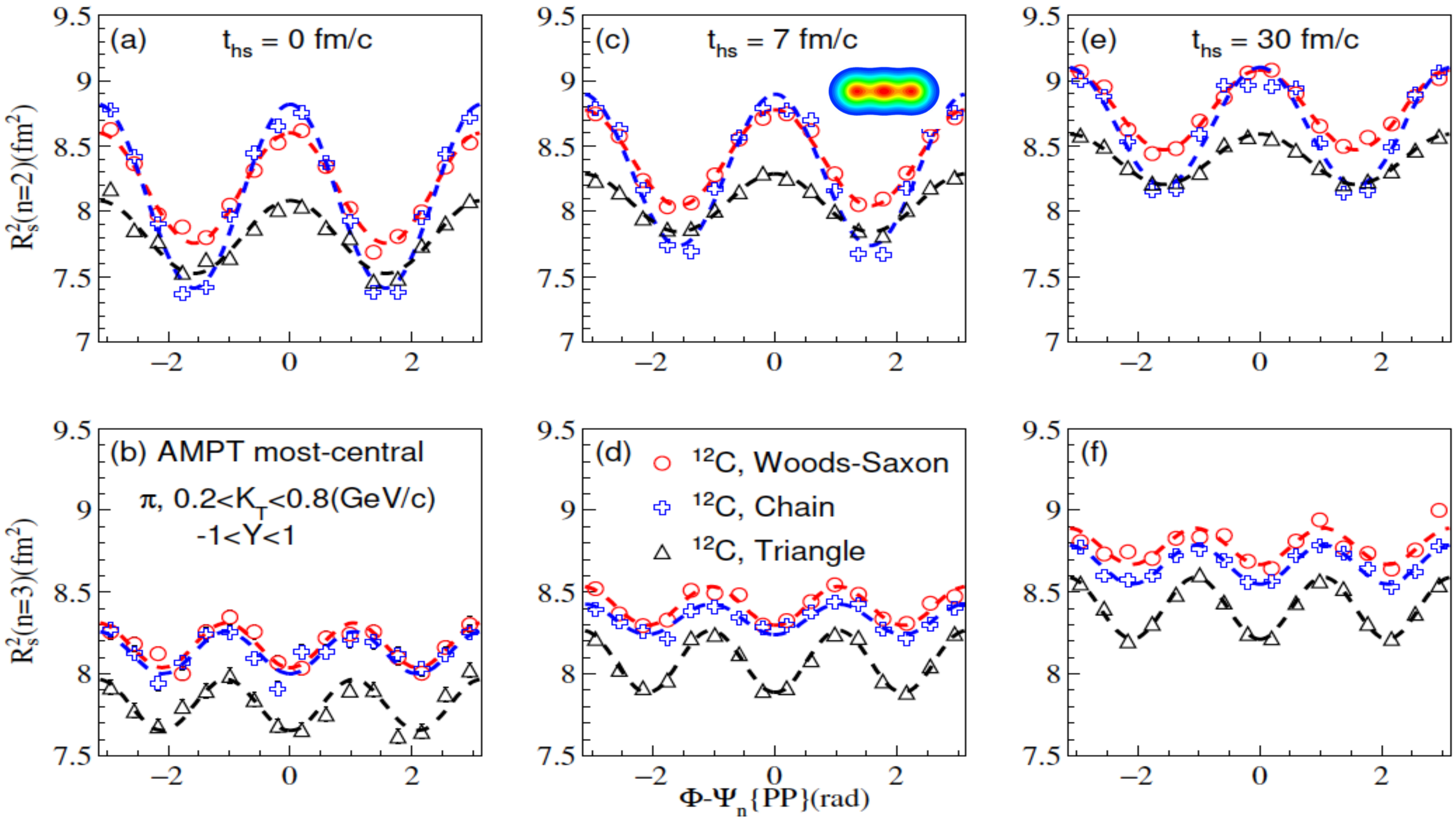

Pion-pion correlation

pion-pion correlation for the Chain structure shows a stronger azimuthal dependence!

Azimuthal dependent HBT radii (2)

Hadron rescattering time

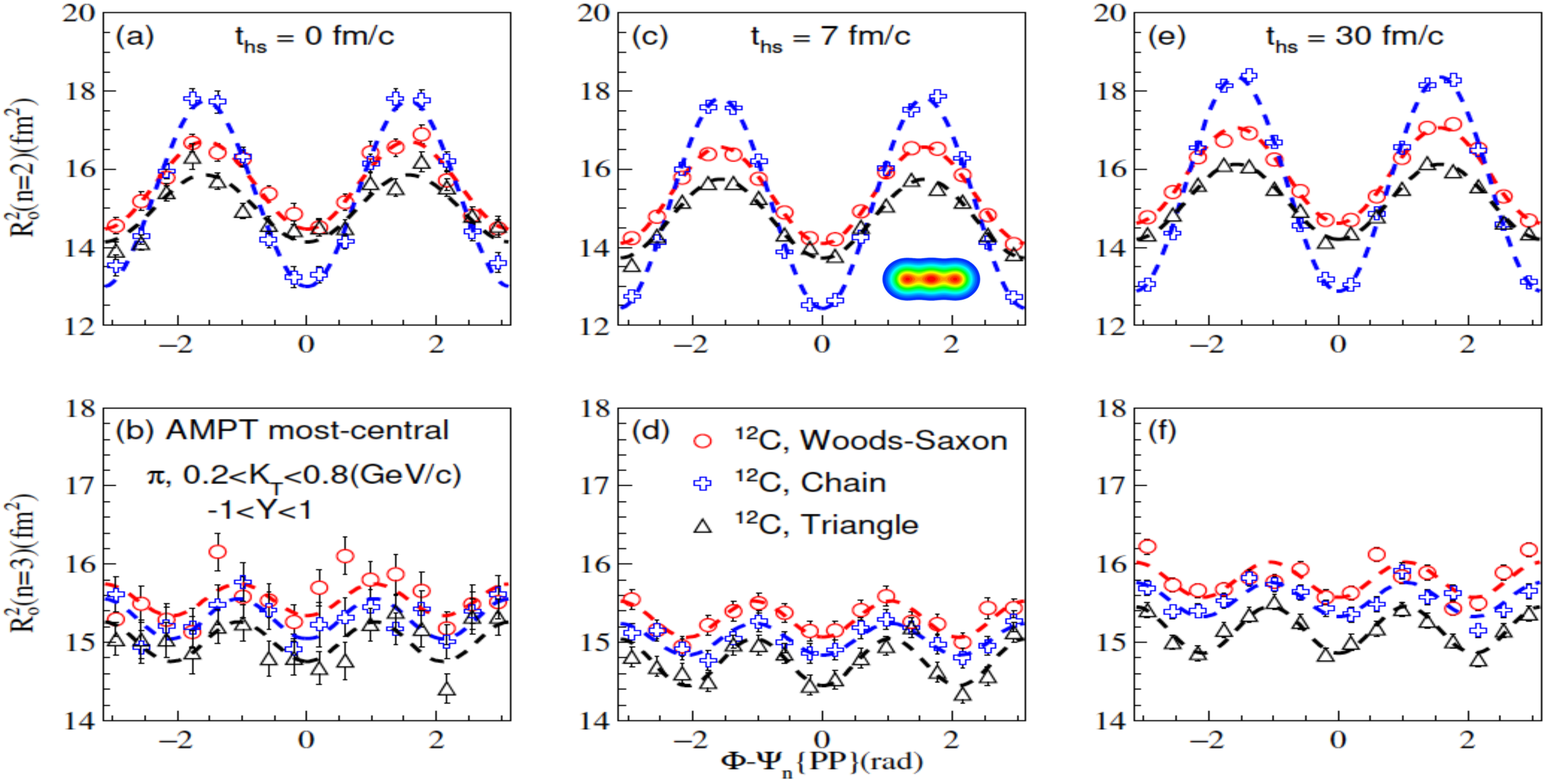

R0^2 of Pi-pi correlation for the chain structure shows a stronger azimuthal dependence!

□Alpha-clustering effect on EM fileds in $^{12}C+^{197}Au$@ 200A GeV

Magnetic field

Rotation of many charged particles

Hydro-dynamics,

Kinetic Theory

Orbital angular momentum

Magnetic fields in heavy ion collision

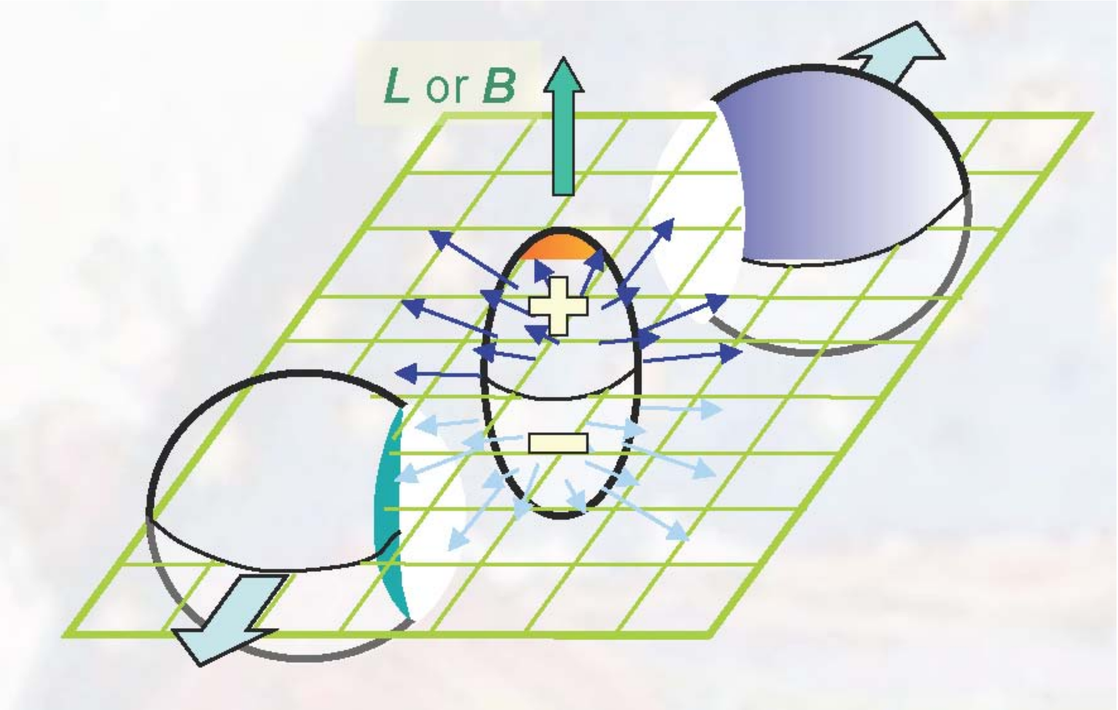

- **High energy HIC**

$$v = \sqrt{(s-m_n^2)/s} \sim 1 - \frac{m_n^2}{2s}$$

$$\gamma = 1/\sqrt{1-v^2/c^2} \sim \frac{\sqrt{s}}{m_n}$$

- **Electric field in cms frame of nucleus,**

$$\mathrm{E} = \frac{Ze}{R^2}\hat{\mathrm{r}}$$

- **Boost to Lab frame (v_z= 0.99995 c for 200GeV),**

Scale of strong interaction

$$\mathrm{B} = -\gamma \mathbf{v}_z \times \mathrm{E} \to eB \to 2\gamma v_z \frac{Ze^2}{R^2} \sim \boxed{1.3 m_\pi^2} \sim 2.6 \times 10^{18}\ \mathrm{Gs}$$

Kharzeev, McLerran, Warringa (2008), Skokov (2009), Deng & Huang (2012), Bloczynski,Huang, Zhang, Liao (2012); many others ……

Electromagnetic calculation A+197Au@200GeV, AMPT model

we used the Lienard-Wiechert potential to calculate the electromagnetic fields

$$e\vec{E}(t,\vec{r}) = \frac{e^2}{4\pi}\sum_n Z_n \frac{\vec{R}_n - R_n\vec{v}_n}{(R_n - \vec{R}_n\cdot\vec{v}_n)^3}(1-v_n^2),$$

$$e\vec{B}(t,\vec{r}) = \frac{e^2}{4\pi}\sum_n Z_n \frac{\vec{V}_n \times \vec{R}_n}{(R_n - \vec{R}_n\cdot\vec{v}_n)^3}(1-v_n^2),$$

Magnetic filed

Y. L. Cheng, S. Zhang, Y. G. Ma, et al., Phys Rev C 99, 054906 (2019)

Chain structure shows a little stronger magnetic field

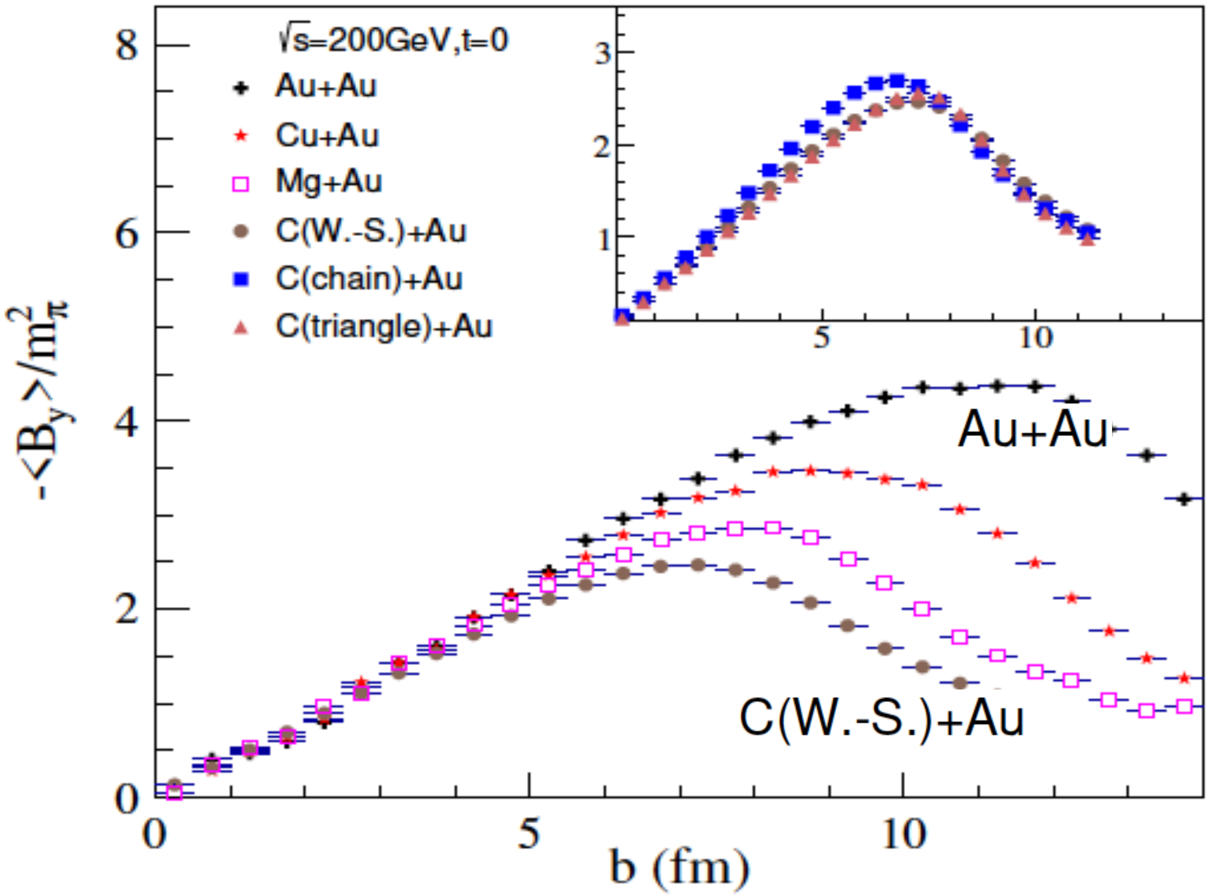

The larger (the more asy. N/Z) the projectile, the stronger the <-By>

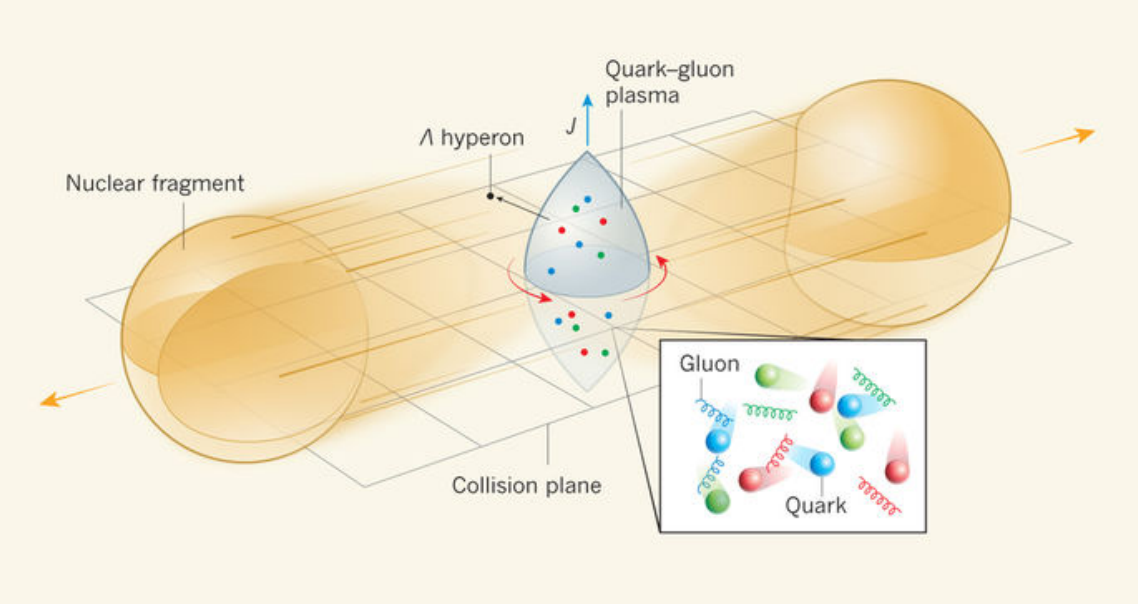

Projectile-side

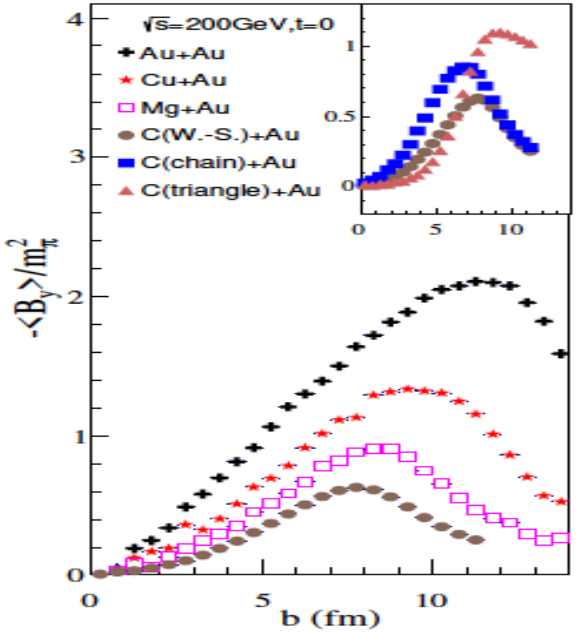

Target (Au)-side

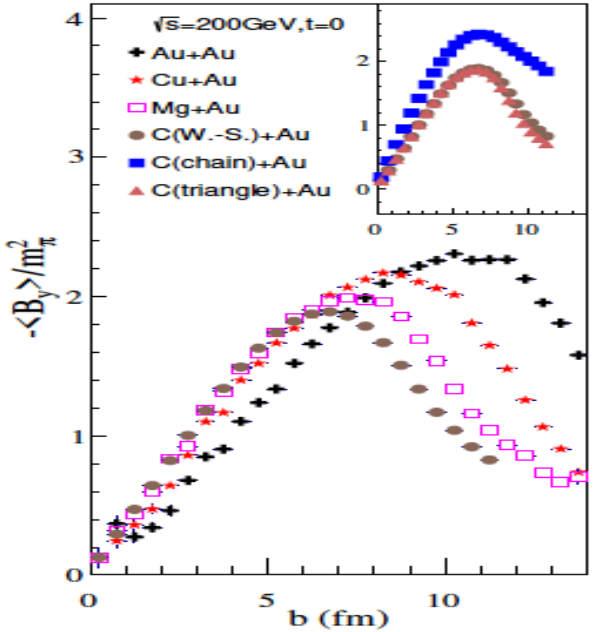

Electric filed

Chain structure shows weaker electric field

Projectile-side   Target (Au)-side

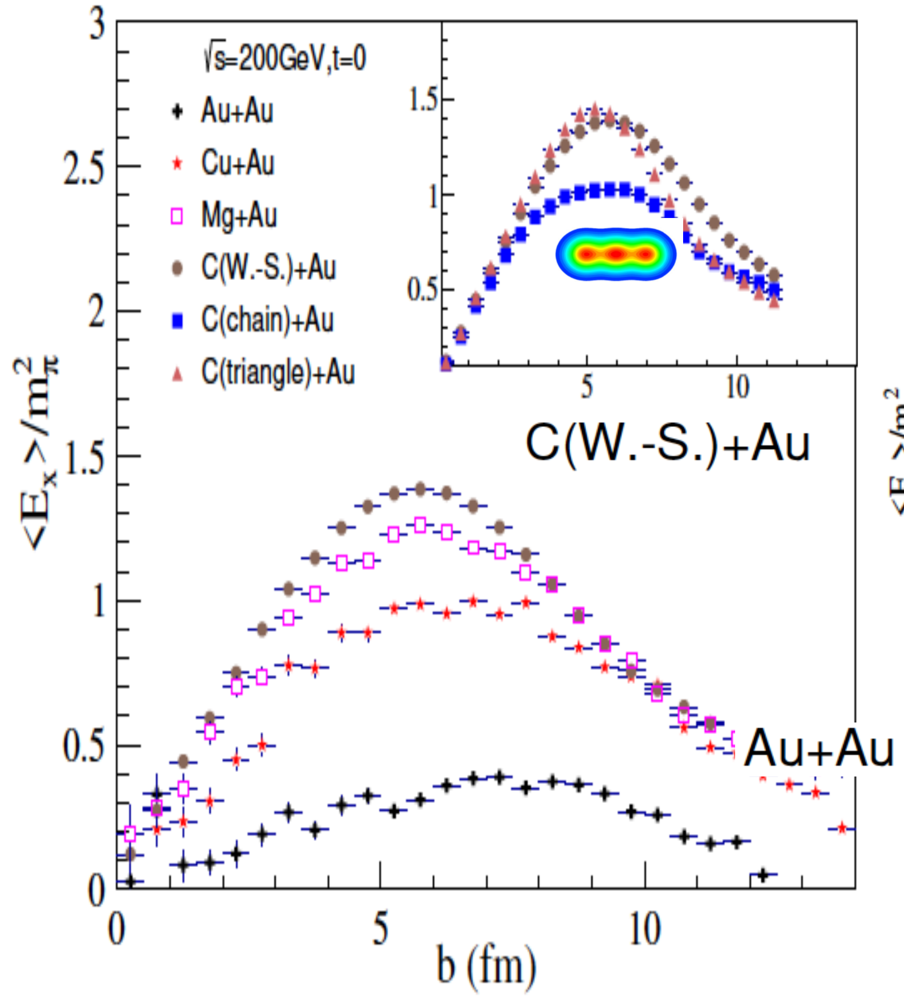

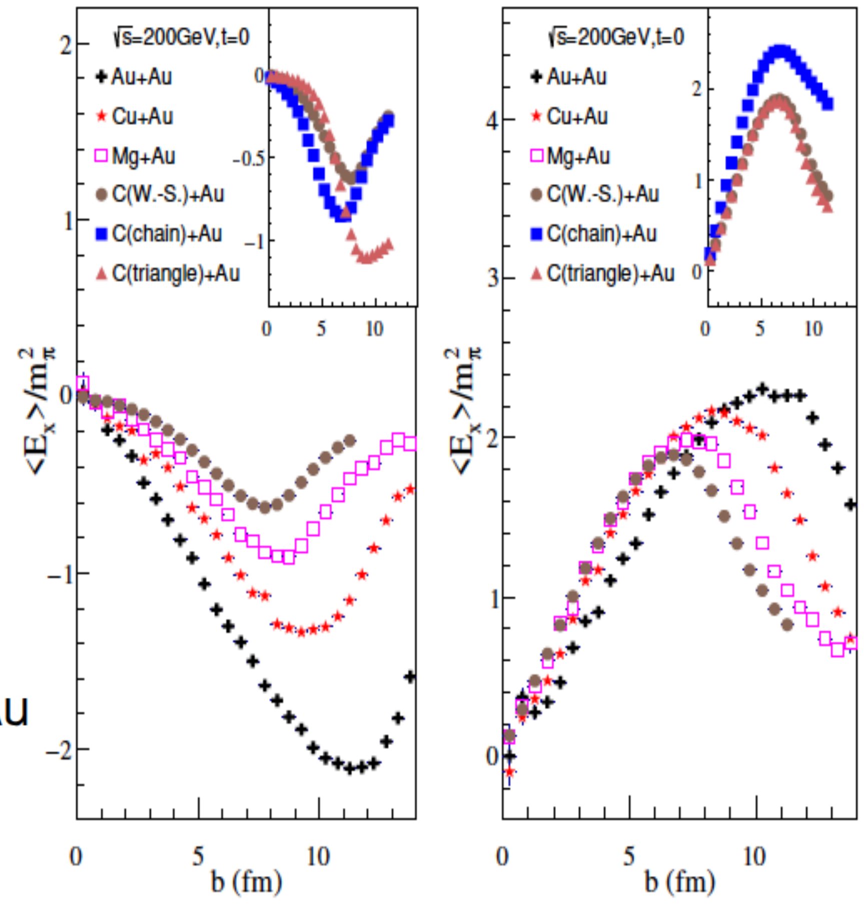

- ✓ <Ex>: the asymmetric projectile and target nuclear collisions produce stronger electric field than symmetrical collision system
- ✓ -<By>: the magnetic field will be in the reverse trend
- ✓ α-cluster effect at semi-central collisions for chain structure

The larger (more asym. N/Z) the projectile, the weaker the <Ex>

Conclusion

- Heavy ion collisions provide a wide range to learn nucleon dynamics to partonic dynamics.
- Many common observables and features emerge in nucleonic degree of freedom as well as in partonic degree of freedom.
- In this talk, I just show examples for collective flows and alpha-clustering effects. In fact, much more can be explored. eg. viscosity, phase transition, fluctuations…
- Heavy ion collisions provide a rich mine for understanding nucleonic matter, quark matter, even for astrophysics process and neutron star etc.

Thanks for your attentions